Title

A three-dimensional quantitative investigation of frontal sinus morphology and function in mammalian carnivores

Author

Curtis, Abigail Ann

Publication Date

2014

Peer reviewed|Thesis/dissertation

UNIVERSITY OF CALIFORNIA

Los Angeles

A three-dimensional quantitative investigation of frontal sinus morphology and function in mammalian carnivores

A dissertation submitted in partial satisfaction of the

Requirements for the degree Doctor of Philosophy

in Biology

by

Abigail Ann Curtis

2014

ABSTRACT OF THE DISSERTATION

A three-dimensional quantitative investigation of frontal sinus morphology and function in mammalian carnivores

by

Abigail Ann Curtis

Doctor of Philosophy in Biology

University of California, Los Angeles, 2014

Professor Blaire Van Valkenburgh, Chair

Mammal skulls contain up to four mucosal-lined, air-filled cavities called paranasal sinuses within the bones surrounding the nasal chamber, including the maxilla, ethmoid, sphenoid, and frontal. Paranasal sinuses are highly variable in presence and morphology among mammals, and their function is not well understood due to the fact that they are hidden within the skull and inaccessible without use of destructive methods. The leading hypothesis to explain sinus function is that they opportunistically form where bone is mechanically unnecessary. Sinuses may also help dissipate stress more evenly across the skull during feeding and other behaviors. To test these hypotheses, I conducted the first quantitative and comparative investigation of how frontal sinus morphological disparity relates to skull morphology, ecology and diet in mammalian carnivores. To do so, I used non-destructive CT scans and applied a novel technique to quantify the three-dimensional shape of sinuses. Cranial shape, body size, diet, and

ecology vary markedly within Carnivora, with many examples of convergence, making them an ideal framework within which to examine sinus function. I quantified frontal sinus morphology for fifty-six carnivore species, including a large intraspecific sample of coyotes (*Canis latrans*) with associated age and diet information. Results support the hypothesis that frontal sinuses from where bone is mechanically unnecessary, but several taxa lacked frontal sinuses, suggesting that there may be phylogenetic constraints on which taxa can develop frontal sinuses. Among Carnivora with frontal sinuses, sinus morphology was strongly correlated with the size and shape of the frontal bone, and was also correlated with allometric differences in skull shape between families that relate to biomechanical function. Skull shape disparity related to ecology also appears to affect frontal sinus morphology. Dorsal flattening of the skull roof in aquatic and fossorial carnivores was associated with reduced or absent frontal sinuses. Large, anteriorly oriented eyes and foreshortened snouts of arboreal species also appear to limit space where a sinus can form. Intraspecific variation in sinus shape suggests frontal sinus morphology is affected by diet-related skull utility, and that frontal sinus morphology can vary throughout an organism's life and be modified to improve skull performance.

The dissertation of Abigail Ann Curtis is approved.

Michael Edward Alfaro

Sotirios Tetradis

Blaire Van Valkenburgh, Committee Chair

University of California, Los Angeles

2014

TABLE OF CONTENTS

ACKNOWLEDGEMENTS

I thank Dr. Blaire Van Valkenburgh for providing invaluable mentoring that has helped me become a more independent and skilled scientist. I also thank the rest of my dissertaion committee, Drs. Michael Alfaro, Sotirios Tetradis, Robert Wayne, and Andrew Farke, for all of their valuable guidance that greatly improved my dissertation and skills as a researcher.

Dr. Graham Slater, Deborah Bird, Dr. Anthony Friscia, Jeffrey Wolf, and other past and present graduate students and postdocs in Dr. Blaire Van Valkenburgh's and Dr. Michael Alfaro's lab have all generously given their time to offer advice, discussions, and technical expertise, for which I am greatly appreciative.

I am grateful to my family, especially my parents, Daniel Curtis, Sr. and Kathleen Curtis, siblings, nieces, and nephews, friends, and mentors who have always supported and encouraged my love of learning and science.

Chapter 1 is a version of Curtis A, Van Valkenburgh B. In press. Beyond the sniffer: frontal sinuses in Carnivora. Anat Rec. A. Curtis was the primary author of this article, and developed the study concept and design, data analysis, and interpretation. A. Curtis collected all frontal sinus and skull morphometric data and conducted all data analyses. B. Van Valkenburgh was the secondary author and involved in study design, data analysis, interpretation, and contributed to the writing of this article.

Chapter 2 is a reprint of Curtis AA, Lai G, Wei F, Van Valkenburgh B. 2014. Repeated loss of frontal sinuses in arctoid carnivorans. J Morphol DOI:10.1002/jmor.20313, and is reprinted with permission from the *Journal of Morphology* granted to A. Curtis (License Number: 3464400629058). A. Curtis was the primary author of this article. A. Curtis developed the study concept and design, as well as data analysis, and interpretation. G. Lai and A. Curtis

collected all frontal sinus volume and skull morphometric data and conducted all data analyses. F. Wei provided the CT scans of the giant panda. B. Van Valkenburgh was the secondary author, and involved in study design, data analysis and interpretation. All authors contributed to the writing of this article.

Chapter 3 is a version of Curtis A, Orke M, Tetradis S, Van Valkenburgh B. In prep. Intraspecific disparity in frontal sinus and cranial morphology in relation to diet-related skull use and age in coyotes (Canis latrans). A. Curtis was the primary author of this manuscript. A. Curtis developed the study concept and design, as well as data analysis and interpretation. A. Curtis and M. Orke collected all frontal sinus and skull morphometric data and conducted all data analyses. S. Tetradis collected and processed all CT data, and was involved in study design, data analysis, and interpretation. B. Van Valkenburgh was the secondary author and was involved in study design, data analysis, and interpretation. All authors contributed to the writing of this manuscript. Chapter 3 was additionally made possible by the help of J. Dines at the Los Angeles County Museum of Natural History and L. Abraczinskas at the Michigan State University Museum of Natural History for their help with museum speciemns, and L. Parker in the UCLA School of Dentistry for her help with compiling CT scans.

Funding for Chapters 1-3 were provided by NSF IOB-0517748 and IOS-1119768 to B. Van Valkenburgh, and the Department of Ecology and Evolutionary Biology to A. Curtis, and for Chapters 1 and 2 by U.S. Department of Education P200A120027 to A. Curtis.

VITA

EDUCATION

B.S. 2008 State University of New York at Albany (Biological Sciences), Minor in Spanish

AWARDS AND HONORS

2011 First Place in Graduate Poster category, 14th Annual Biology Research Symposium, Dept. of Ecology and Evolutionary Biology, UCLA, $150

2010 A.M. Schechtman Award for distinguished teaching, Dept. of Ecology and Evolutionary Biology, UCLA, $100

2008 Department of Biological Sciences Excellence in Research Award, SUNY at Albany, $200

FELLOWSHIPS

2012 – 2013 UCLA Science and Engineering of the Environment of Los Angeles Gratuate Teaching Fellows in K-12 Education (SEE-LA GK-12) Fellowship, $45,000

2011 – 2012 Graduate Assistance in Areas of National Need (GAANN) Fellowship, UCLA, $27,000

2014 UCLA Department of Ecology and Evolutionary Biology, $6,500

RESEARCH GRANTS

2013 UCLA Office of Instructional Development Grant, $14000

2012 UCLA Departmental Research Grant, $1000

2011 GAANN Fellowship Research Stipend, $7500

2011 UCLA Departmental Research Grant, $1000

2011 Sigma Xi Grant-in-Aid of Research, $400

2010 UCLA Departmental Research Grant, $1500

2010 UCLA Travel Award, $500

ACADEMIC EMPLOYMENT

Research

2008 – 2012 Graduate Research Assistant, University of California, Los Angeles

2007 – 2008 Research Assistant, New York State Museum, Albany, NY

2007 – 2008 Research Assistant, New York State Museum, Albany, NY

2006 – 2008 Museum Collections Intern, New York State Museum, Albany, NY

Teaching

2009 – 2014 Teaching Assistant, Dept. of Ecology and Evolutionary Biology, University of California, Los Angeles

2013 Curriculum Development, Dept. of Ecology and Evolutionary Biology, University of California, Los Angeles

2011 – 2012 Instructor, Dept. of Humanities and Sciences, UCLA Extension

PEER-REVIEWED PUBLICATIONS

Curtis A, Van Valkenburgh B. in press. Beyond the sniffer: frontal sinus disparity in Carnivora. Anat Rec.

Van Valkenburgh B, Pang B, Bird D, **Curtis A**, Yee K, Wysocki C, Craven B. In press. Respiratory and olfactory turbinals in feliform and caniform carnivorans: the influence of snout length. Anat Rec.

Curtis A, Lai G, Wei F, Van Valkenburgh B. 2014. Repeated loss of frontal sinuses in arctoid carnivorans. J Morphol DOI: 10.1002/jmor.20313

Green PA, Van Valkenburgh B, Pang B, Bird D, Rowe T, **Curtis A**. 2012. Respiratory and olfactory turbinal size in canid and arctoid carnivorans. J Anat 221:609-621.

Van Valkenburgh B, **Curtis A**, Samuels JX, Bird D, Fulkerson B, Meachen-Samuels J, Slater GJ. 2011. Aquatic adaptations in the nose of carnivorans: evidence from the turbinates. J Anat 218:298-310.

Kays R, **Curtis A**, and Kirchman JJ. 2010. Reply to Wheeldon et al. 'Colonization history and ancestry of northeastern coyotes.' Biol lett 6:248-249.

Kays R, **Curtis A**, and Kirchman JJ. 2010. Rapid adaptive evolution of northeastern coyotes via hybridization with wolves. Biol lett 6:89-93.

PUBLISHED ABSTRACTS

Curtis A, Van Valkenburgh B. 2013. Frontal sinus disparity in Carnivora. 73rd Annual Meeting of the Society of Vertebrate Paleontology, Los Angeles, CA

Curtis A, Van Valkenburgh B. 2013. Beyond the sniffer: frontal sinus disparity in Carnivora.10th International Congress of Vertebrate Morphology. Barcelona, Spain.

Curtis A, Farke AA. 2012. Strut your stuff: frontal sinus complexity in Bovidae and Carnivora. Society for Integrative and Comparative Biology Meeting, Charleston, North Carolina.

Curtis A, Lai G, Van Valkenburgh B. 2012. Frontal sinus morphology in arctoid carnivorans. Society for Integrative and Comparative Biology Meeting, Charleston, North Carolina.

Curtis A, Van Valkenburgh B. 2011. A quantitative study of frontal sinus morphology in Carnivora. American Society of Mammalogists Meeting, Portland, Oregon.

Lai G, **Curtis A**, Van Valkenburgh B. 2011. Frontal sinus size and shape in aquatic and terrestrial carnivores. American Society of Mammalogists Meeting, Portland, Oregon.

McNutt A, Slater GJ, **Curtis A**, Van Valkenburgh B. 2011. Humeral shape and locomotor behavior in carnivores. American Society of Mammalogists Meeting, Portland, Oregon.

Eckert K, **Curtis A**, & Van Valkenburgh B. 2011. Getting inside a weasel's head: frontal sinus size and shape in Mustelidae. Society for Integrative and Comparative Biology Meeting, Salt Lake City, Utah.

Curtis A, Van Valkenburgh B. 2011. Cats and dogs in 3D: a quantitative study of canid and felid frontal sinuses using CT technology. Society for Integrative and Comparative Biology Meeting, Salt Lake City, Utah.

Curtis A, Van Valkenburgh B. 2010. Frontal sinus size and shape in felids. American Society of Mammalogists Meeting, Laramie, Wyoming.

Curtis A, Kays RW, Ferenec R. 2008. The morphological variation in eastern coyote skulls. Northeast Natural History Conference, Albany, New York.

CHAPTER 1:

BEYOND THE SNIFFER: FRONTAL SINUSES IN CARNIVORA

ABSTRACT

Paranasal sinuses are some of the most poorly understood features of mammalian cranial anatomy. They are highly variable in presence and form among species, but their function is not well understood. The best-supported explanations for the function of sinuses is that they opportunistically fill mechanically unnecessary space, but that in some cases, sinuses in combination with the configuration of the frontal bone may improve skull performance by increasing skull strength and dissipating stresses more evenly. We used CT technology to investigate patterns in frontal sinus size and shape disparity among three families of carnivores: Canidae, Felidae, and Hyaenidae. We provide some of the first quantitative data on sinus morphology for these three families, and employ a novel method to quantify the relationship between 3-dimensional sinus shape and skull shape. As expected, frontal sinus size and shape were more strongly correlated with frontal bone size and shape than with the morphology of the skull as a whole. However, sinus morphology was also related to allometric differences among families that are linked to biomechanical function. Our results support the hypothesis that frontal sinuses most often opportunistically fill space that is mechanically unnecessary, and they can facilitate cranial shape changes that reduce stress during feeding. Moreover, we suggest that the ability to form frontal sinuses allows species to modify skull function without compromising the performance of more functionally constrained regions such as the nasal chamber (heat/water conservation, olfaction), and braincase (housing the brain and sensory structures).

KEY WORDS: Paranasal sinuses; Carnivora; CT scans; Spherical Harmonics; Geometric Morphometrics

INTRODUCTION

The external shape of a mammal skull is largely determined by feeding adaptations as well as the need to house the brain and sensory organs. While much has been published on how differences in external shape reflect these functions, the internal anatomy of the skull has received less attention. Here we use computed tomography (CT) scans and 3D visualization software to examine the position, shape and size of frontal sinuses within three families of Carnivora: felids, hyaenids, and canids. Frontal sinuses are one of several pneumatic, mucosa-lined spaces called paranasal sinuses that are located in the bones surrounding the nasal chamber. All these sinuses develop when the cartilage composing the developing nasal capsule breaks down, allowing a vascular, osteoclastic lamina propria and the nasal epithelium to escape the nasal chamber and invade the bones surrounding the nasal chamber including the frontal, maxilla, ethmoid, and sphenoid (Wang et al., 1994; Witmer, 1999; Maier, 2000; Smith et al., 2008).

Previous work on paranasal sinuses has largely focused on maxillary sinuses of primates (e.g., Rae et al., 2002; Márquez and Laitman, 2008; Rae and Koppe, 2008). Maxillary sinuses are present in all placental mammals, with the exception of most aquatic species and extremely small species, and their presence is considered to be plesiomorphic for placentals (Paulli 1900a,b). The frontal sinuses, on the other hand, are much more variable in their presence among species (Paulli, 1900 a,b; Edinger, 1950; Witmer, 1999). Edinger (1950) suggested that these structures have evolved and/or been lost at least once in each mammalian order. Within the artiodactyl family Bovidae, frontal sinuses have arisen and/or degenerated at least six times (Farke, 2010). A few studies have focused on the frontal sinuses, but, with the exception of Farke (2010), most are limited in their taxonomic breadth, and/or are only qualitative. Sphenoid and ethmoid sinuses

also appear to vary in their presence among species, but very little attention has been paid to these sinuses as well.

The function of frontal sinuses is not well understood. It has been suggested that sinuses serve minimal function and develop opportunistically in areas of the skull where bone is biomechanically unnecessary (Witmer, 1997, 1999). Alternatively, by altering skull shape and because they can have internal struts, frontal sinuses might aid in the absorption of shock and/or dissipation of stress during feeding and combat. In a large survey of bovids with frontal sinuses, Farke (2010) found that sinus size and amount of internal struts were not related to head-butting behavior. Instead, frontal sinus size was well correlated with frontal bone size and he suggested that this is consistent with an opportunistic rather than biomechanical model of development. This is also supported by studies of fossil and modern hominins, in which interspecific variation in frontal sinus morphology is correlated with changes in skull shape (Witmer, 1997, 1999; Zollikofer and Weissmann, 2008; Zollikofer et al., 2008). However, Tanner et al. (2008) found support for the biomechanical role of frontal sinuses in their finite element analysis of spotted hyena skulls. Based on their observation that presence of frontal sinuses in addition to the dome-shaped profile results in more even dissipation of stress across the skull during feeding, they argued that the extensive frontal sinus in this species could play a role in stress dissipation during forceful biting. Farke (2008) also used finite element methods to test how frontal sinus morphology and frontal bone shape affected stress distribution and shock absorption during head-butting behavior in a domestic goat skull. Results showed support for a vaulted and pneumatized frontal bone aiding in even dissipation of stress across the skull during head-butting behavior in the domestic goat, but showed limited support for sinuses acting to absorb shock during head-butting.

Given that frontal sinuses evolved multiple times among mammals, there may not be a single factor driving their evolution and sampling a broad assortment of taxa might reveal a range of sinus function. Here, we provide the first quantitative study of frontal sinuses in three families from the order Carnivora: Felidae, Hyaenidae, and Canidae. Frontal sinuses originated one or more times within each of these families (Fig. 1-1). They form an excellent framework within which to study sinus morphological variation because they exhibit much of the diversity in body size, as well as skull size and shape disparity within Carnivora. Moreover, the functional morphology of their skulls has been well studied (e.g., Radinsky, 1981a,b; Van Valkenburgh and Koepfli, 1993; Covey and Greaves, 1994; Tanner et al. 2008; Slater et al., 2009; Slater and Van Valkenburgh, 2009; Tseng and Wang, 2011). This allowed us to explore the influence of skull size and shape, as well as feeding behavior on sinus presence, size and shape. Among these three families, there are species with short broad snouts, long narrow snouts, relatively flat profiles to highly domed skulls, all of which are functionally linked to prey size and feeding behavior, making them ideal for a study of how sinuses contribute to skull function (Ewer, 1973; Van Valkenburgh and Koepfli, 1993; Covey and Greaves, 1994; Tanner et al., 2008; Slater et al., 2009; Slater and Van Valkenburgh, 2009).

Previous work on Carnivoran Frontal Sinuses

Paulli (1900b) provided some of the first detailed descriptions of frontal sinuses for various representatives from Carnivora including members of Canidae, Felidae, and Hyaenidae among others. Frontal sinuses can be composed of multiple chambers with ostia that open behind different frontoturbinals, or ectoturbinals to some. Paulli systematically named the different sinus chambers based on which frontoturbinal they formed behind. Despite contention over the

homology among different sinuses and chambers within, Paulli's classification system does provide an excellent framework for comparative studies because the different chambers form in similar regions of the skull among even distantly related species. In Carnivora, the largest of these chambers, and also often the only chamber present, is sinus 2', which opens posterior to frontoturbinal 2 and pneumatizes the space between the postorbital processes and toward the fronto-parietal suture.

The veterinary literature has also paid extensive attention to the frontal sinuses of domestic dogs and cats with respect to their normal anatomy and descriptions of pathologies (e.g., Sharp et al. 1991).

Felidae

Salles (1992) described three general morphologies for felid frontal sinuses based on their position relative to the postorbital processes. The first, and most common, is to have the sinuses centralized in the region of the postorbital processes. The second is to have sinuses that lie posterior to the postorbital region, which is seen in pantherines. The third is to have sinuses located anterior to the postorbital processes, as seen in the black-footed cat (*Felis nigripes*) and Scottish wildcat (*F. silvestris*). The largest sinuses relative to skull size were observed in the cheetah (*Acinonyx jubatus*), followed by Pallas cat (*Otocolobus manul*), and the snow leopard (*Panthera unica*) (Salles, 1992).

Hyaenidae

Hyaenid frontal sinuses have received the most attention due to an extreme morphology that is linked to their ability to crack open bones using specialized premolars. All four extant

members of Hyaenidae: the spotted hyena (*Crocuta crocuta*), brown hyena (*Parahyaena brunnea*), striped hyena (*Hyaena hyaena*) and the aardwolf (*Proteles cristata*) have frontal sinuses (Joeckel, 1998; Ferretti, 2007). In the predominantly insectivorous aardwolf, the frontal sinuses do not pneumatize posterior to the fronto-parietal suture. However, this is not the case for the other three bone-cracking species, all of which share a domed cranial roof that houses large, caudally extended frontal sinuses. Unlike the plate-like sagittal crest seen in most carnivorans, the sagittal crests of these hyenas are triangular in cross section and contain large sinuses with numerous bony struts that completely overlie the braincase (Joeckel, 1998; Tannner et al., 2008). The association between a domed frontal bone, pneumatized sagittal crest, and dependence on bone-cracking suggests that they are adaptations for a durophagous diet. The appearance of caudally elongated frontal sinuses in hyaenine hyaenas correlates with a shift in the Late Miocene from a generalist diet to a more durophageous diet as suggested by heavier tooth wear, more robust skulls, and premolars (Joeckel, 1998; Ferretti, 2007; Tseng, 2011; Tseng and Wang, 2011).

These unique frontal sinuses were hypothesized to function as a structural arch to produce a stronger skull shape that could dissipate stresses imposed upon the skull while feeding on bone and other hard foods (Werdelin, 1989; Joeckel, 1998). Tanner et al. (2008) tested this hypothesis in a spotted hyena skull using finite element analysis to compare the performance of a skull with a normal pneumatized sagittal crest, a bone-filled sagittal crest, and a plate-like crest during bone- cracking. Results showed that models with caudally elongated frontal sinuses inside a domed frontal were better at dissipating stresses than models with a bone-filled sagittal crest or those with a plate-like sagittal crest (Tanner et al., 2008). Based on their results, the authors concluded that the enlarged frontal sinuses and triangular shape of the sagittal crest in spotted

hyenas evolved to dissipate stress during hard-object feeding, while maintaining a minimal mass of the skull (Tanner et al., 2008).

In addition to hyaenids, caudally elongated frontal sinuses have evolved within ursids and extinct borophagine canids. Among ursids, they are present in the giant panda (*Ailuropoda melanoleuca*) (Davis, 1964), a species that subsists on an herbivorous durophagous diet consisting mainly of tough bamboo shoots (Schaller et al., 1985; Schaller et al., 1989). Several species of extinct bone-cracking borophagine canids exhibit a vaulted frontal bone, with two of the most highly derived members (*Borophagus dudleyi*, *B. diversidens*) having sinuses that extend far caudally and pneumatize the sagittal crest (Werdelin, 1989, Wang et al., 1999, Tseng and Wang, 2010). Tseng and Wang (2010) showed that the vaulted frontal bone of derived borophagine canids helped dissipate stress more evenly across the skull, and strengthened the skull to resist bending and tension during biting.

Canidae

The prevalence of frontal sinuses within Canidae is well documented, and is considered a useful phylogenetic character (Huxley, 1880; Wang, 1994; Tedford et al., 1995, 2009; Wang et al., 1999). The ancestral condition of Canidae is a lack of frontal sinuses and there are extant species without them, but sinuses evolved independently at least seven times among the three major canid subfamilies, Hesperocyoninae, Borophaginae, and Caninae. Within Caninae (the lineage to which all extant canids belong), frontal sinuses evolved at least three times, within an extinct vulpine fox (*Vulpes stegnognathus*), the raccoon dog (*Nyctereutes procyonoides*), and within the tribe Canini that includes the South American canids (Cerdocyonina) and their sister taxon Canina (e.g. *Canis*, *Lycaon*, and *Cuon*) (Tedford et al., 1995, 2009).

Tedford et al. (1995, 2009) described three general sinus morphologies among canids. The first is seen in *Vulpes stegognathus*, raccoon dogs and South American canids (Cerdocyonina), all of which have small frontal sinuses that do not penetrate the postorbital processes (Tedford et al., 1995, 2009). Most members of Canini show the second morphology in which the frontal sinuses extend into the postorbital processes but do not pneumatize all the way to the fronto-parietal suture. The third morphology, in which sinuses pneumatize up to the fronto-parietal sutures, is seen in *Canis lupus* and other extinct large hypercarnivorous Canini, with some highly derived extinct canids showing sinuses that pneumatized beyond the fronto-parietal suture into the parietal (Tedford et al., 1995, 2009).

Aims of this study

We explore frontal sinus morphology in Carnivora to further investigate various hypotheses for the function and structure of paranasal sinuses. The "epithelial hypothesis" predicts that sinuses form opportunistically via osteoclastic fronts in areas where bone is not mechanically necessary. This hypothesis was first put forth explicitly by Witmer (1997) and is supported by histological studies of sinus development (e.g., Smith et al., 2005; Smith et al., 2011). A second hypothesis, which is not mutually exclusive from the first, predicts that in some species, sinuses may play a more active biomechanical role, such as aiding in even dissipation of stress across the skull and/or absorbing shock (Tanner et al., 2008; Farke, 2008). Tangential to these hypotheses are predictions that frontal sinus size and the number of internal struts will be a function of frontal bone size and/or skull size (e.g., Farke, 2007, 2010) and that frontal sinus size relates to durophagy or head-butting behavior (e.g., Tanner et al. 2008; Farke, 2008). Whereas

the latter prediction clearly supports a biomechanical role for the frontal sinus, the former is not so easily interpreted.

Here, we use CT scans of museum skulls to test the generality of these predictions in a group of mammals that display a variety of diets, including durophagy, a range of skull sizes and shapes, and vary in frontal sinus dimensions: felids, canids and hyaenids. In addition, we quantify the shape of the frontal sinus and explore its relationship to skull shape and phylogeny. If sinuses opportunistically fill space where bone is not mechanically necessary, we expect to find that sinus volume increases with frontal bone size in all groups, but that the scaling of frontal size to skull size in each family might differ due to differences in skull shape allometry. If sinuses play a biomechanical role, we expect to see similar sinus morphology among species with similar diets. For example, large canids tend to have proportionally shorter snouts and somewhat more domed skulls than smaller canids due to selection for higher bite forces associated with hypercarnivory (Covey and Greaves, 1994; Slater et al. 2009). Doming of the frontal bone is associated with expanded sinuses, especially in durophagous species such as spotted hyenas and giant pandas. Consequently, large canids with higher bite forces and more domed skulls are expected to have relatively larger frontal sinuses. Among the hyaenids, we expect to see similarly enlarged frontal sinuses among all three bone-cracking species based on the conclusions of Tanner et al. (2008) and observations by Joeckel (1998). However, the fourth species, *Proteles cristata*, feeds primarily on termites and has a relatively flat dorsal skull profile. Consequently, aardwolves are expected to exhibit sinuses similar to those of other carnivorans, unless phylogeny prevails over function.

By contrast, felids are expected to show a different pattern of frontal sinus allometry. Unlike canids, larger felids have proportionally longer snouts with flatter skull profiles while

smaller felids have short snouts and rounded skulls (Slater and Van Valkenburgh, 2008, 2009). The longer snouts of large cats, such as lions, reflect the need to increase gape to accommodate larger prey (Covey and Greaves, 1994; Slater and Van Valkenburgh, 2009). Because of their flattened dorsal profiles, we expect to see lower allometric coefficients in the scaling of felid frontal sinuses with frontal bone size compared with Canidae and Hyaenidae. Due to their shorter snouts, smaller felids have relatively curved frontal bones that connect the rostrum to the braincase and produce a rounded dorsal profile somewhat similar to that of the large hyaenids. Consequently, smaller felids may have proportionally bigger frontal sinuses than larger felids.

MATERIALS AND METHODS

Specimens

Our comparative sample consisted of 59 skulls representing 33 species of Carnivora from the families Canidae, Felidae, and Hyaenidae (Table 1-1, Table S1). Whenever possible, we included two adult wild-caught individuals per species, one male and one female. Adult age was determined by full eruption of adult dentition and closure of the basioccipital-basisphenoid suture. Two difficult to obtain species were represented by zoo animals (*Panthera uncia* and *Speothos venaticus*).

CT Scanning and Segmentation of Frontal Sinuses

Skulls were CT scanned at the University of Texas High-Resolution CT (UTHRCT) scanning facilities (http://www.ctlab.geo.utexas.edu/), the UCLA Crump Preclinical Imaging Technology Center (http://www.crump.ucla.edu/tech.aspx), or the UCLA School of Dentistry. Slice numbers range from 292-1200 slices per skull. All scans done at the UTHRCT facilities are

freely available at www.digimorph.org along with scan parameters, and the remaining scans will be deposited on Digimorph upon publication.

We used Mimics (http://biomedical.materialise.com/mimics) and Aviso (http://www.vsg3d.com/) advanced imaging software to visualize CT data and segment frontal sinuses from skulls (Fig. 1-2). Scans of skulls were examined for presence of frontal sinuses, defined as a cavity lying between the outer and inner tables of the frontal bone with an ostium connecting it to the nasal cavity (Cave, 1967). The literature suggests that felids, hyaenids, and canids independently evolved the ability to develop frontal sinuses (Huxley, 1880; Joeckel, 1998; Ferretti, 2007; Tedford et al., 2009). Thus, we do not assume that frontal sinuses are homologous among these three clades, or within Canidae, where frontal sinuses appear to have evolved multiple times (Tedford et al., 2009).

Frontal sinuses can consist of several separate chambers as numbered by Paulli (1900a,b) based on the frontoturbinal to which they are posterior. We focused on the 2' frontal sinuses (defined by Paulli (1900a,b) as the sinus extending posteriorly from the second frontoturbinal, or ectoturbinal to some) because they are the largest and often the only chamber in carnivorans. We manually thresholded CT scans to segment bone (skulls) from air, and then segmented left and right 2' frontal sinuses from each reconstructed skull and used to generate three-dimensional digital endocasts on which were measured total surface area (mm^2) and volume (mm^3) (Fig. 1-2). The epithelium lining the frontal sinuses is extremely thin; underlying bone can be seen through the tissue, even on the struts (A. Curtis, personal observation on a domestic dog cadaver). Therefore, surface area and volume measurements taken from dry skulls should be nearly identical to those taken with the epithelium present. Volumetric models of skulls with sinus endocasts were created in lieu of detailed anatomical descriptions. All models were constructed

and measured by A. Curtis, and there was negligible measurement error (< 0.35%) between both visualization software packages.

Quantifying Sinus Shape

Homology of the paranasal sinuses among species is poorly understood, and because they are highly irregular in size and shape, there are few landmarks that are consistently identifiable among species. To quantify frontal sinus shape, we used SPHARM spherical harmonic analysis software (http://www.enallagma.com/SPHARM.php; Shen and Makedon, 2006; Shen et al., 2009). SPHARM performs 3-dimensional spherical harmonic analyses of triangular mesh surfaces and was successfully used to quantify the shape of insect reproductive organs (McPeek et al., 2009, 2011). Spherical harmonic analysis is a 3-dimensional extension of elliptical Fourier analyses that generate a 3D mathematical model of an object's surface. SPHARM better captures details of curvature than geometric morphometrics, and requires fewer landmarks for scaling, rotating, and aligning specimens for analysis (Shen and Makedon, 2006; Shen et al., 2009).

In preparation for spherical harmonic analysis, frontal sinus endocasts were edited to remove any holes that completely punctured sinus surfaces (Fig. 1-2). For sinuses with extremely complex surfaces due to the presence of bony struts subdividing the sinuses (e.g. spotted hyena), we used the wrap tool in Mimics to reduce the depth of furrows in sinus endocasts. We exported volumetric models of right frontal sinuses as binary STL files from Mimics and Amira, and imported them into Geomagic Studio (www.geomagic.com) for editing. In Geomagic Studio, we removed holes from all sinus endocasts and reduced each endocast mesh to 10,000 triangles. For species that had damaged right frontal sinuses, we mirrored the left sinus to allow for comparison to other species. Four landmarks that we could consistently identify on all sinuses among all

three families were placed on each sinus using the Landmarks tool in Amira. These landmarks are used in SPHARM to scale, rotate and align sinuses before performing a spherical harmonic analysis. Each sinus had a triangular-shaped near-flat surface on the medial surface where it is bounded by the septum between the frontals (Fig. 1-2). Landmark 1 was placed on the antero-dorsal point, landmark 2 on the ventral point, and landmark 3 on the postero-dorsal point of this triangle. Landmark 4 was placed on the lateral-most point on the sinus that extends laterally into the postorbital process.

Edited sinus endocasts and associated landmark data were uploaded to SPHARM, and sinuses were scaled to a common centroid size to remove the effects of size differences (Zelditch et al., 2004). To rotate and align surfaces in SPHARM, it is necessary to select a template surface against which all other surfaces are rotated and aligned. Although McPeek et al. (2009) did not specify a criterion for template selection, we selected the right sinus from the female *Acinonyx jubatus* to act as the template because its sinuses are centered at the postorbital processes, in a position intermediate to that of the two extreme positions of frontal sinuses. Spherical harmonic coefficients were calculated to the 18th degree for each specimen (the default setting in the program that captures the desired shape details for frontal sinuses), and spherical harmonic representations of original sinuses were generated from the coefficients for comparison with the actual shapes (Fig. 1-2).

The variation in frontal sinus shape among Felidae, Canidae, and Hyaenidae, was explored with a Principal Components Analysis on sinus SPHARM coefficients. This should reveal if there is phylogenetic clustering in sinus shape, as well as the variance in sinus shape within each family.

Quantifying Skull Size and Shape

To quantify skull size and shape, we identified a series of 23 landmarks that captured skull shape variation among carnivores and could be consistently identified from CT data (Fig. 1-2, Table 1-2). Landmarks were placed on 3-dimensional renderings of skulls using either the Landmarks tool in Amira (http://www.vsg3d.com/) or the Points tool in the MedCAD module in Mimics (http://biomedical.materialise.com/mimics). We used MorphoJ geometric morphometrics software (http://www.flywings.org.uk/) to divide landmarks into two datasets (Table 1-2), skull and frontal bone, on which we performed a Procrustes fit on all specimens to scale, rotate and align specimens and extract centroid sizes. We were interested in capturing how sinus morphology varies with size and shape across the entire skull because it might illuminate the relationship between sinus size and allometry of the feeding apparatus. We were also interested in the specific relationship between frontal sinus morphology and frontal bone morphology due to the fact that the frontal sinus is confined to the frontal bone in most species, and the two should therefore be strongly correlated with one another relative to the rest of the skull.

Relationships among the Variables

Sinus Size and Skull Size. To examine the relationship between sinus size and skull size (entire skull and frontal bone), we regressed log-transformed species means for total sinus volume against skull centroid size and frontal bone centroid size, respectively, using traditional ordinary least squares (OLS) and reduced major axis (RMA) regressions using the smatr package (Warton et al., 2012) in R (R Core Team, 2012). RMA regression analysis is preferred over OLS when both variables are measured with error, and the allometric relationship between two

variables is the desired outcome rather than the ability to predict one variable from another (Warton et al., 2006; Smith, 2009). Consequently, we present the results of the RMA regressions here. The OLS regressions were performed because phylogenetic least squares analysis requires them for comparison rather than RMA.

To account for non-independence among species due to common ancestry, we calculated phylogenetic generalized least squares (PGLS) analyses (Martins and Hansen, 1997) using the caper package in R (Orme, 2012; R Core Team, 2012). We used a phylogenetic tree for the Carnivora based on that published by Slater et al. (2012) that we pruned to include only our sampled species (Fig. 1-1). PGLS estimates the relationship between two variables similarly to OLS, but adds an error term based on the covariance among the branches in the phylogeny (Martins and Hansen, 1997). If the regression statistics between the OLS and PGLS are largely similar, it suggests that phylogeny plays a limited role in the scaling of two variables. We conducted a pooled analysis including all species to examine overarching patterns in the scaling of carnivoran frontal sinuses, as well as separate regression analyses for each family to test for patterns relating to the different allometric patterns shown in Canidae versus Felidae. We present data on regressions for Hyaenidae but caution that their significance is marginal at best because there are only four species, three of which are relatively large and similar in morphology, while the fourth is much smaller, thus providing us with effectively two points for regression analysis.

Sinus Size vs. Skull Shape. To test for covariation between sinus size and skull and frontal shape, we $\log_{10}$-transformed values of total sinus volume and conducted a two-block partial least squares (2B-PLS) analysis (Rohlf and Corti, 2000) of sinus volume against Procrustes coordinates obtained from skull and frontal bone landmark configurations using functions in MorphoJ (Klingenberg, 2011). We expected to see the largest sinuses in species with

domed frontal bones and large jaw muscle attachment sites, and expected that sinus size would be more strongly related to frontal bone size than to the entire skull due to the fact that the frontal sinus is confined to the frontal bone in most species.

Two-block partial least squares (2B-PLS) analysis provides a measure of covariation between multivariate datasets (Rohlf and Corti, 2000). A 2B-PLS maximizes covariation between two multivariate datasets and provides an RV coefficient, which is a measure of the strength of covariation between the two blocks of data, and is analogous to r^2 in linear regression (Rohlf and Corti, 2000). Statistical significance of the covariation between two blocks is evaluated using permutation tests that test against a null expectation of no covariation between the blocks (Rohlf and Corti, 2000). We ran analyses on our pooled dataset, as well as separate analyses for individual families, again interpreting results for Hyaenidae with caution. All permutation tests were set to run 10,000 rounds. We exported coordinates for skull and frontal shape variation at the extremes along PLS axes and used the rgl package (Adler and Murdoch, 2013) in R (R Core Team, 2012) to visualize shape differences in a three-dimensional manipulative environment.

Sinus Shape vs. Skull Size and Skull Shape. We conducted a 2B-PLS analysis of sinus SPHARM coefficients (i.e. sinus shape) against skull and frontal bone centroid sizes to explore how sinus shape covaries with the size of the entire skull and frontal bone. To test for covariation between frontal sinus shape and skull and frontal shape, we did a 2B-PLS analysis using SPHARM coefficients against Procrustes coordinates for the entire skull and frontal bone. We again used rgl (Adler and Murdoch, 2013) to visualize differences in shape along each PLS axis.

Sinus Surface Complexity. Farke (2010) observed that larger sinuses have a greater number of struts than smaller sinuses in members of Bovidae. Because it is difficult to count the

total number of struts due to their complex and variable form (they split, can be complete or incomplete), Farke (2007) developed a sinus complexity index that is similar to that used to quantify trabecular bone (e.g. Hildebrand and Rüegsegger, 1997; Hildebrand et al., 1999). To quantify sinus complexity in Carnivora, we instead chose to use the relationship between sinus surface area against volume. Carnivore frontal sinuses are much less complex than bovid frontal sinuses, with many species having struts that do not completely cross the sinus, and, thus, the methods used by Farke (2007) are not appropriate for quantifying complexity in carnivoran sinuses. Given two sinuses of equivalent volume, and assuming that struts are generally plate-like structures (confirmed by qualitative observations) (Hildebrand et al., 1999), a sinus with greater surface area will have a more furrowed appearance because the folds or grooves on the surface of a sinus endocast reflect the location of internal struts of bone that partially or completely subdivide the sinus (Fig. 1-3). Thus, the relationship between surface area and volume should serve as a proxy for the number of bony struts that are present within a sinus. In addition, the surface area is a direct estimate of the amount of bone surface covered by the pneumatic epithelium, and will allow us to test the scaling relationship between the volume of pneumatized space versus the amount of epithelial tissue present. If larger sinuses have proportionally larger surface area than smaller sinuses, and thus more struts, it would suggest that larger sinuses have struts for structural support and/or that struts are byproducts of rapid pneumatization (i.e., large sinuses are a result of rapid pneumatization), as suggested by Zollikoffer and Weissmann (2008). However, because sinuses appeared to be so variable in shape, size, and complexity we did not expect to observe a strong relationship between sinus surface area and volume. It is possible that dramatic differences in sinus shape could bias our results (i.e., a nearly spherical sinus would have a proportionally smaller surface area than a disc

or tube-shaped sinus of the same volume). Qualitative observations of the variability in size and shape of sinuses suggested that this is not a problem.

Raw data including sinus surface area and volume, as well as centroid sizes for the skull, SPHARM coefficients, and skull Procrustes coordinates are provided as a supplemental file associated with this paper. See Supplemental Information for an explanation of the variables listed in this file. All other data including STL files of sinuses, accompanying landmarks, and skull landmarks are available upon request from the corresponding author.

RESULTS

Qualitative observations

In general, left and right frontal sinuses were relatively symmetrical within individual skulls, and intraspecific variation was similar in our limited sample (Fig. 4). Species that deviated from this general pattern are discussed further below.

Felidae. Frontal sinuses were present in all sampled felid species. We observed four general frontal sinus morphologies among our sampled felids (Fig. 4), as opposed to three observed by Salles (1992) despite his larger sample. The first was characteristic of most of the smallest felids in our sample, (*Lynx rufus*, *Puma yaguarundi*, *Leopardus wiedii*, *Prionalilurus bengalensis*, and the female *Felis libyca*), in which the frontal sinuses are positioned anterior to the postorbital processes due to the relatively large size of the brain and lack of dorsal displacement of the outer table of the frontal bone and strutting. The frontal sinuses of the male *F. libyca* pneumatized further posteriorly than in the female and showed longitudinal struts posteriorly (Fig. 1-5). The second morphology is exhibited by *Acinonyx jubatus*, *F. chaus*, *Panthera uncia*, and *Pardofelis marmorata*, in which the sinuses are centered at the postorbital

processes and are dorsally inflated with extensive strutting. *Lynx canadensis*, *Leopardus pardalis*, *Puma concolor*, *P. pardus*, and *Neofelis nebulosa* have sinuses that are located mostly posterior to the postorbital processes, with most of the pneumatization anterior to the postorbital processes occurring laterally, and less dramatic doming and struts compared to the previous group. Lastly, *Panthera leo* and the male *N. nebulosa* showed proportionally small sinuses positioned far posterior to the postorbital processes with no struts, a morphology not described by Salles (1992).

Canidae. Canids showed three frontal sinus morphologies (Fig. 4), the first of which is complete absence as seen in *Urocyon cinereoargenteus*, all of the sampled vulpine foxes, (*Vulpes vulpes*, *V. macrotis*, *V. lagopus*, and *Otocyon megalotis*), the female *Nyctereutes procyonoides,* and *Speothos venaticus*. Huxley (1880) stated that *S. venaticus* had small frontal sinuses, and because our single specimen was from a zoo, it would be important to look at additional specimens before concluding what is typical of the species. The second morphology, observed in the male *N. procyonoides* is the presence of small frontal sinuses that do not pneumatize into the postorbital processes or far posterior to the postorbital processes. The frontal sinuses of the remainder of our canid sample are generally located largely posterior to the postorbital processes but do not extend beyond the fronto-parietal suture. This includes the South American canids *Cerdocyon thous* and *Chrysocyon brachyurus* as well as all the members of the Canini, *Canis latrans*, *C. mesomelas*, *C. lupus* and *Lycaon pictus*. Among these, the *Chrysocyon brachyurus* and the *C. lupus* are the only species in which the frontal sinus extends all the way to the fronto-parietal suture, and the gray wolf differs from all of them in having dorsoventrally domed frontal sinuses with many struts,

Hyaenidae. *Proteles cristata* had relatively small frontal sinuses for its skull size that were located between the postorbital processes (Fig. 4). *Crocuta crocuta*, *Parahyaena brunnea*, and *Hyaena hyaena* all had sinuses with extensive struts that pneumatized posterior to the fronto-parietal suture and into the parietal, creating a hollow sagittal crest with a triangular cross-section (Fig. 4). The space pneumatized by the sinuses in bone-cracking species was relatively symmetrical in shape, but in all specimens from all three species, the left sinus was larger and pneumatized farther posteriorly than the right sinus.

Quantitative Results

Sinus Shape Variation. A principal components analysis on SPHARM coefficients representing frontal sinus shape revealed that sinuses were highly variable among species (Fig. 1-6), and that there is a weak relationship between sinus shape and phylogeny. Principal Component 1 (PC1) explained 34.08% of shape variation and contrasted species with negative values and dorsoventrally shallow sinuses with flat dorsal profiles that appear somewhat trapezoidal when looked at in dorsal view (e.g. *Lynx rufus*) with those that had positive PC1 values and caudally elongated dorsoventrally deep sinuses and domed dorsal profiles (e.g. bone-cracking hyaenids). The differences in sinus depth reflect the position of the sinuses relative to the postorbital processes; sinuses that lie mostly in front of these processes are shallow while those that lie mostly behind are deeper.

Principle Component 2 (PC2) explained 14.18% of total shape variation among frontal sinuses, and separated species that differed in the amount of doming of the frontal sinuses. Species that loaded positively on PC2 have sinuses that are relatively flat dorsally and shallow with a rather amorphous shape, and are confined to the space between the postorbital processes,

such as *Proteles cristata* and *Leopardus wiedii*, whereas species that loaded negatively have sinuses that show the greatest dorsal doming, and consequentially deeper sinuses that expand much farther anteroposteriorly to the postorbital processes as well as laterally into the postorbital processes such as *Pardofelis marmorata* and *Acinonyx jubatus*.

Felids exhibited the most variation in sinus shape across both PC1 and PC2, which is surprising given their relatively uniform skull shape compared with the other two groups. Canid sinuses shared similar shape morphospace with the sinuses of larger bodied felids, and hyaenids were distinguished from both former groups, plotting with the most extreme positive values along PC1, except for the insectivorous *Proteles cristata*, which shared shape morphospace with small-bodied felids.

Sinus Volume and Skull Size. Regression statistics from OLS and PGLS regressions were largely similar, which suggests that sinus size variation in our sample is largely independent of phylogeny (Supplementary information, Tables S2, S3). Thus, we only present regression statistics from RMA regression analyses. Sinus volume scaled with positive allometry to overall skull size across all species ($r^2 = 0.69$, $p < 0.01$, Table 1-3). The three bone-cracking hyaenids (Fig. 1-7A) exhibit exceptionally large sinuses that exceed those of similar sized canids and felids, but the insectivorous *Proteles cristata* is more similar to canids in relative sinus size (Fig. 1-7A). In canids, sinus volume scaled with positive allometry (slope > 3, $r^2 = 0.81$, $p < 0.01$, Fig. 1-7A, Table 1-3) and thus larger canids have proportionally larger sinuses than smaller species (Fig. 1-7A, Table 1-3). In contrast, the relationship between frontal sinus size and skull size in felids did not differ significantly from isometry (Table 1-3, $r^2 = 0.77$, $p < 0.01$, Fig. 1-7A). Instead, larger felids tend to have reduced sinuses relative to smaller species, with the exception of *Acinonyx jubatus* and *Panthera uncia* (Fig. 1-7A).

Sinus size scaled with positive allometry to frontal bone size across all species ($r^2 = 0.82$, $p < 0.01$, Fig. 1-7B, Table 1-3). Bone cracking hyaenids have extremely large sinuses relative to frontal bone size due to the fact that the sinuses pneumatize posteriorly beyond the fronto-parietal suture, whereas *Proteles cristata* is similar in frontal sinus size to the canids (Fig. 1-7B). Canids showed strong positive allometry ($r^2 = 0.82$, $p < 0.0001$, Fig. 1-7B, Table 1-3) in the scaling of sinus size to frontal bone size, but felids were isometric for this relationship with proportionally smaller sinuses than canids or hyaenids.

Sinus Volume and Skull Shape. A 2B-PLS of $\log_{10}$ total sinus volume against Procrustes coordinates from the entire skull revealed that there is not a significant relationship between frontal sinus size and skull shape among our inclusive sample, nor was there a significant relationship seen in Canidae. However, there was strong and significant covariation between frontal sinus size and skull shape in Felidae (RV = 0.74, $p < 0.0001$). In the cats, the absolutely largest sinuses belonged to the largest species, all of which are characterized by dorsoventrally deep frontal bones and snouts, anteriorly shifted premaxillae, large mastoids and sagittal crests, and proportionally smaller braincases. Smaller felids with less deep frontal bones, proportionally large braincases and orbits, and less pronounced muscle attachment sites for the feeding apparatus had the smallest sinuses.

Sinus size was weakly correlated with frontal bone shape across all species (RV = 0.23, $p = 0.01$), but among 2B-PLS analyses on individual families we observed a significant correlation between sinus size and frontal bone shape only in Felidae (RV = 0.61, $p < 0.001$). In our inclusive sample and also among felids, the largest sinuses were associated with frontals with domed dorsal profiles and inflated postorbital processes, and with more posterior and ventral expansion of the frontal bone posterior to the postorbital processes. Smaller sinuses were

associated with a relatively flat cranial roof, postorbital processes that form a greater portion of the orbit, a more anteriorly positioned fronto-parietal suture, and less ventral extension of the frontal bone.

Sinus Shape and Skull Size. We observed significant covariance between sinus shape and skull size in 2B-PLS analyses in the pooled sample (RV = 0.56, $p < 0.0001$, Fig. 1-8A) and within individual families (Canidae: RV = 0.61, $p < 0.05$, Felidae: RV = 0.57, $p = 0.0001$). Species with the largest skulls had sinuses that were dorsoventrally deep and positioned mostly posterior to the postorbital processes, whereas species with the smallest skulls showed dorsoventrally shallow sinuses positioned mostly anterior to the postorbital processes.

We also observed significant covariance between sinus shape and frontal size in 2B-PLS analyses of sinus shape versus frontal size for all species (RV = 0.49, $p < 0.0001$, Fig. 1-8B) and within individual families (Canidae: RV = 0.61, $p < 0.01$, Felidae: RV = 0.52, $p < 0.01$). Interestingly, we did not observe appreciably larger RV coefficients for the relationship between sinus shape and frontal size than for sinus shape versus skull size.

Sinus Shape and Skull Shape. Among all species, sinus shape was weakly, but significantly, correlated with skull shape (RV = 0.32, $p < 0.01$). The first PLS (PLS 1) explained 77.0% of the covariation between both blocks in the pooled sample, and thus is representative of the relationship between sinus shape and skull shape. Species with shallow sinuses positioned anterior to the postorbital processes had relatively flat skull roofs, proportionally short snouts and proportionally large braincases and orbits. Species with dorsoventrally deep sinuses positioned posteriorly to the postorbital processes showed proportionally longer snouts and proportionally smaller braincases. Sinus shape showed a strong correlation with skull shape in Felidae (RV =

0.61, $p < 0.001$), with PLS 1 explaining 84.9% of covariation between blocks, but was not significantly correlated with skull shape in Canidae.

Sinus shape significantly correlated with frontal bone shape among all species in our sample (RV = 0.54, $p < 0.0001$), and in Felidae (RV = 0.66, $p < 0.01$) but not Canidae. The first PLS explained 83.3% and 88.3% of the covariation between both blocks in the pooled sample and Felidae, respectively, and thus is representative of the relationship between sinus shape and skull shape. Sinus shape largely reflected the shape of the frontal bone in that domed frontal bones that expanded behind and below the postorbital processes contained sinuses that were dorsally convex, dorso-ventrally deep, and pneumatized farther back toward, or even beyond the fronto-parietal suture in the case of bone cracking hyenas.

Sinus Surface Complexity. Despite large differences in the size and shape of sinuses and area of the frontal bone that they occupy, sinus surface area and sinus volume were strongly correlated ($r^2 = 0.98$, $p < 0.0001$, Fig. 1-9, Table 1-5). All three families showed similar scaling of sinus complexity in individual regression analyses (Fig. 1-9, Table 1-5). Sinus surface area scaled with positive allometry to sinus volume, meaning that species with larger sinuses had proportionally greater than expected surface area given a null expectation of isometry (slope = 0.66). This relationship appears to reflect the relative degree of strutting, because species with the largest sinuses had more extensive strutting (Fig. 1-10), with the exception of the lion, which plotted below the regression line (Fig. 1-9). Thus, as is true within Bovidae (Farke, 2010), larger sinuses are more complex than smaller sinuses in carnivores.

DISCUSSION

Our qualitative descriptions of frontal sinus morphology were largely similar to those by Paulli (1900b, Carnivora), Salles (1992, Felidae), Huxley (1880, Canidae), Tedford et al. (1995, 2009, Canidae), and Ferretti (2007, Hyaenidae). We observed the three general morphologies described by Salles (1992) for Felidae, but they were not as strongly tied to phylogeny as Salles' descriptions suggested. We additionally described differences in the relative amount of strutting and doming of the frontal, which were associated with the position of the sinuses with respect to the frontal bone.

Huxley (1880) described frontal sinuses in *Speothos venaticus*, but we did not observe any pneumatization in the single specimen we examined. The skull in our study was from a zoo animal, and its skull was probably not subjected to the typical biomechanical loading experienced by the skulls of wild *Speothos venaticus* during prey apprehension and feeding, and thus may not reflect the typical cranial anatomy of *Speothos venaticus*. We observed that the sinuses of *Cerdocyon thous* and *Chrysocyon brachyurus*, both from the South American lineage of canids, showed sinuses that were similar to species within the genus *Canis*, rather than being similar to *N. procyonoides*, as described by Tedford et al. (1995, 2009). The small, oddly-shaped sinuses of the male raccoon dog and absent sinuses in the female suggest that this species may be at the cusp at which skull size and shape allow a sinus to form. This species is similar in size to several canids without frontal sinuses, *Urocyon*, *Vulpes*, and *Otocyon*, but *N. procyonoides* has a proportionally shorter, broader snout, greater development of the sagittal crest, and a slightly more convex frontal, all of which are traits typical of canids that produce relatively large bite forces and have stronger skulls (Slater et al., 2009; Tseng and Wang, 2010). It may be that this shape difference allows the occasional development of sinuses in this relatively small canid.

As expected, we observed large, posteriorly elongated sinuses that pneumatize beyond the fronto-parietal suture into the parietal bone in bone-cracking hyaenids, and relatively small sinuses in *Proteles cristata*. We made the additional discovery that all specimens from the three bone cracking hyena species in our study had asymmetrical sinuses, with the left sinus always larger than the right. It is unclear if this asymmetry is conserved across the lineage leading to modern bone cracking hyenas, or if it is a result of behavior. Joeckel (1998) mentioned that hyaenas have asymmetrical sinuses, and that *Ictitherium viverrinum*, a Late Miocene jackal-sized hyaenid, showed a larger left frontal sinus. Habitually asymmetric behavior such as a side preference in chewing can result in asymmetries between bilaterally symmetrical structures (Hallgrímsson, 1998), so perhaps asymmetrical sinuses result from greater loading on one side of the skull affecting the extent of pneumatization. Examining sinus asymmetry in association with tooth wear among a larger sample of hyenas might reveal a functional relationship.

Our quantitative results supported our predictions about the relationship between sinus morphology and cranial morphology, and were largely similar to our qualitative observations. As expected, frontal sinus size increases with the size of the skull and frontal bone in Carnivora with sinuses. In Canidae and Hyaenidae, larger species had proportionally larger sinuses with a greater amount of strutting than smaller species. The extreme allometry in hyaenids was driven by the extremely large frontal sinuses that pneumatize beyond the fronto-parietal suture in bone-cracking hyaenids versus the relatively reduced sinuses in the insectivorous aardwolf, *P. cristata*. Felids showed proportionally smaller frontal sinuses compared to canids and hyaenids, as predicted due to the positive allometry of snout length in Felidae. Sinus size and shape appear to be limited by the size and shape of the frontal bone, as well as the size and shape of the surrounding skull. Smaller species have proportionally larger braincases than larger species,

which limits how far the sinuses can pneumatize posteriorly. This is evident in small felids versus large felids, except when the frontal bone is domed and allows larger sinuses to form, as seen in the cheetah, *A. jubatus* and Bengal cat, *Prionailurus bengalensis*. Sinus shape largely conforms to the shape of the frontal bone, with domed frontals containing convex sinuses, and flat frontals containing sinuses that are flat dorsally. This pattern suggests that sinuses fill space that is not mechanically necessary within a pre-existing configuration of bone, and that they do not act to inflate the frontal bone.

These results were further supported by observations made on a scan of a domestic cat skull in which we observed incomplete pneumatization of the left frontal bone. The external shape of the frontal bone was not observably affected, however, and non-pneumatized space within the frontal was filled with cancellous bone. This suggests that, for some species, the external shape of the skull can develop normally even if pneumatization does not occur. This, in turn, suggests that pneumatic epithelia are not pushing the bones apart, but are able to pneumatize once the incipient outer table has been displaced, creating space for the epithelium to pneumatize. An exploration of sinus ontogeny would be useful in further understanding the interaction between growing bone and the pneumatic epithelium.

All bone-cracking hyaenids had domed frontals filled with large posteriorly elongated frontal sinuses, thus supporting the findings of Tanner et al. (2008). We also observed that large canids that take large prey (and also produce relatively high bite forces), also showed doming and consequent larger sinuses. This association supports the hypothesis that a domed frontal and expanded sinus is an adaptation for durophagy and production of large bite forces. Tanner et al. (2008) showed that in hyenas, the vaulted frontal bone with an expanded sinus aids in the dissipation of stress more evenly across the skull. Skulls with vaulted frontal bones are stronger

than skulls with unvaulted frontal bones (Tseng and Wang, 2010), which may explain why species with domed frontals have proportionally larger frontal sinuses (i.e. a stronger external shape results in a lesser amount of bone necessary to maintain skull function). Felidae present an interesting contrast to this pattern, with larger felids having proportionally smaller sinuses than canids and hyaenids. Like canids and hyaenids, larger felids produce absolutely larger bite forces, but it appears that felid skull shape is a tradeoff between the demands of increasing gape to accommodate large prey versus the need for a strong bite (Slater and Van Valkenburgh, 2009). The longer jaws required for increased gape result in greater torsional loads on the skull during forceful biting and it appears that this is resolved by increased bone volume in the skull, which results in proportionally smaller sinuses. Smaller felids have intrinsically strong skulls due to their extremely foreshortened snouts, which allows them to produce relatively high bite forces with proportionally smaller jaw muscles, and consequently the frontal bone does not show doming.

The strong relationship between sinus surface area and sinus volume despite appreciable differences in size and shape showed that patterns in sinus complexity are conserved across multiple families. Our results appear consistent with previous work by Farke (2010) who showed that larger sinuses are more complex (i.e. contain more bony struts) than smaller sinuses in Bovidae. Because we employed different methods to quantify sinus complexity, it would be of interest to compare our results to those of Farke (2010). Theoretical work that modeled sinus development (Zollikofer and Weissmann, 2008) suggested that varying rates of growth and/or ossification could determine how complex a sinus is, with respect to the number of struts. A larger frontal bone may allow rapid pneumatization, with struts being a byproduct of the rapid erosion of bone. In smaller frontal bones, there is less room for rapid expansion and

consequently the removal of bone is more complete, resulting in fewer struts. Additionally, if the struts served as structural supports, we would expect them to be organized such that they align with principal stresses, as seen in the trabeculae within the spinous processes of thoracic vertebrae of horses, for example (Currey, 2002:162). Qualitative observations suggest that the struts in frontal sinuses are not aligned with predominant stresses, and quantitative data on bighorn sheep (*Ovis canadensis*) also suggest that this is true (A.A. Farke, pers. comm.).

Although we observed that phylogeny plays a limited role in determining sinus morphology, vulpine foxes, such as those from the genera *Urocyon*, *Vulpes*, and *Otocyon* appear to lack the ability to form frontal sinuses. Huxley (1880) mentioned that despite having a similar skull size and shape to the red fox, *V. vulpes*, the South American crab-eating fox, *C. thous,* has sinuses while the former does not. In several bovid species that lack frontal sinuses, Farke (2008, e.g. Fig. 1-3E) observed an indentation in the anterior margin of the frontal bone, which may be evidence of primary pneumatization, a process that involves folding of the nasal capsular cartilage and appears to be a necessary step in the development of a sinus within bone (secondary pneumatization) (Wang et al., 1994; Witmer, 1997; Smith et al., 2008). *Urocyon*, *Vulpes*, and *Otocyon* showed no evidence of primary pneumatization. However, there was a significant amount of cancellous bone in these canids in the region of the frontal bone where sinuses typically form, suggesting that there may be selection for mass reduction. The frontal bones of the bush dog, *S. venaticus*, and the female raccoon dog, *N. procyonoides* did exhibit an indentation or frontal recess, suggesting that sinuses can form in these species. This is consistent with Huxley's (1880) observation of sinuses in wild *S. venaticus* and our observation of sinuses in the male *N. procyonoides*.

Many questions about the distribution of paranasal pneumaticity and the function of sinuses still remain. Given that the frontal sinuses of durophagous species, such as hyenas, pandas, and extinct borophagine canids, appear to play a role in the even dissipation of stress across the skull, it would be interesting to investigate whether the frontal sinuses of less derived species are playing a similar role in skull function. If the presence of frontal sinuses always or usually results in some selective advantage, such as a more even distribution of stresses during feeding or simply a lighter skull, then this may explain why frontal sinuses are present in small-bodied South American canids that overlap in skull size and shape with vulpine foxes. A similar pattern was described in the fossil record of horses in which horses reached a relatively large body size before the first appearance of frontal sinuses, but species that later reverted to much smaller body sizes retained sinuses, suggesting that they either conferred some functional advantage or are retained simply because they descend from species with sinuses (Edinger, 1950). In addition, histological investigation of the development of the nasal chamber in a broad array of species with differing cranial morphologies may reveal factors that limit and facilitate development of sinuses, such as timing of capsular cartilage breakdown (Wang et al., 1994; Smith et al., 2008). It also appears that struts within a sinus are byproducts of rapid pneumatization and/or large sinus volume, rather than structural supports. However, struts may still play a secondary role in the biomechanical function of the skull, and it is possible that they may be reoriented over the organism's lifetime to improve skull function due to the plastic nature of bone. If and how sinus morphology changes throughout an organism's ontogeny remains largely unexplored. Sorting this out will also require biomechanical analyses that model the impact of loading on skulls with sinuses of different size and shape, as in Farke (2008).

With this study, we showed that sinus size and shape are related to cranial size and shape disparity, and provided support for the hypothesis that sinuses opportunistically fill space where bone is not mechanically necessary. We hypothesize that the ability to modify the shape of the frontal bone and develop an internal sinus allows some mammals to modify skull performance while maintaining minimal mass. In addition, because of its location, modifications to frontal bone shape can occur with minimal impact on the configuration of regions that are constrained by the demands of multiple functions, such as the rostrum (feeding apparatus, heat and water conservation, olfaction) and the braincase (houses the brain, sensory structures, and the feeding musculature). In the future, we hope to investigate the relationship between the ability to form sinuses and the evolution of skull shape variation within clades, as well as the ontogeny of the frontal sinus within species.

ACKNOWLEDGEMENTS

We thank the University of Texas HRCT Digital Morphology group, W Ladno at the UCLA Crump Preclinical Imaging Technology Center, and S Tetradis in the UCLA School of Dentistry for their skill and care in producing CT scans, as well as curators and collection managers who lent us skulls for scanning. P Yang helped with data collection, and we are grateful to A Friscia and G Slater for assistance with the phylogeny. A Friscia, D Bird, G Slater, and J Wolf provided useful discussions and the paper was greatly improved by the insightful suggestions of AA Farke and TD Smith. Funding was provided by NSF IOB-0517748 and IOS-1119768 to B. Van Valkenburgh and by U.S. Department of Education P200A120027 to A Curtis.

TABLES

Table 1-1. Species sampled, sample size, and measurement data.

Species	CODE	N	SK	FR	TSV	TSA
Felidae						
Cheetah (*Acinonyx jubatus*)	AJU	2	280.99	99.17	31215.45	11079.79
Jungle Cat (*Felis chaus*)	FCH	1	179.52	65.66	5819.34	3188.85
African Wild Cat (*Felis libyca*)	FLI	2	134.91	51.84	1444.53	1342.39
Jaguarundi (*Puma yagouaroundi*)	HYA	2	148.74	54.90	2115.38	1418.20
Canadian Lynx (*Lynx canadensis*)	LCA	2	193.15	72.59	5503.36	3374.17
Ocelot (*Leopardus pardalis*)	LPA	2	200.51	68.21	4218.42	2740.44
Bobcat (*Lynx rufus*)	LRU	3	164.89	63.88	2099.88	1594.02
Margay (*Leopardus wiedii*)	LWI	2	138.92	54.23	2539.59	1828.06
Clouded Leopard (*Neofelis nebulosa*)	NNE	2	229.55	74.53	6222.63	3194.88
Leopard Cat (*Prionailurus bengalensis*)	PBE	1	143.96	52.92	685.53	621.88
Puma (*Puma concolor*)	PCO	2	294.53	101.80	16555.16	6400.68
African Lion (*Panthera leo*)	PLE	3	498.17	152.70	28469.56	6996.53
Marbled Cat (*Pardofelis marmorata*)	PMA	1	144.68	58.64	4344.19	2774.84
Leopard (*Panthera pardus*)	PPA	1	341.72	110.25	14123.20	5595.88
Snow Leopard (*Panthera uncia*)	UUN	1	284.51	103.29	24661.11	8267.07
Hyaenidae						
Spotted Hyena (*Crocuta crocuta*)	CCR	2	360.38	122.44	62117.80	19525.50
Striped Hyena (*Hyaena hyaena*)	HHY	1	323.24	108.59	51195.99	16231.81
Brown Hyena (*Parahyaena brunnea*)	PBR	2	363.24	119.41	78144.10	21158.00
Aardwolf (*Proteles cristata*)	PCR	1	195.40	64.21	927.30	897.72
Canidae						
Maned Wolf (*Chrysocyon brachyurus*)	CBR	1	331.91	87.04	16586.81	6347.59
Coyote (*Canis latrans*)	CLA	2	259.93	76.34	4272.22	2172.40
Gray Wolf (*Canis lupus*)	CLU	4	326.21	97.73	16165.85	6640.38
Black-Backed Jackal (*Canis mesomelas*)	CME	1	233.21	67.51	6036.08	2919.31
Ethiopian Wolf (*Canis simensis*)	CSI	1	286.82	78.29	4923.70	2745.66
Crab-Eating Fox (*Cerdocyon thous*)	CTH	1	186.57	60.24	3080.15	1906.28
African Wild Dog (*Lycaon pictus*)	LPI	2	296.85	93.72	8736.20	3929.81
Raccoon Dog (*Nyctereutes*	NPR	2	164.28	50.14	385.89	652.58

procyonoides)						
Bat-Eared Fox (*Otocyon megalotis*)	OME	2	172.23	52.20	0	0
Bush Dog (*Speothos venaticus*)	SVE	1	196.88	56.16	0	0
Gray Fox (*Urocyon cinereoargenteus*)	UCI	2	162.42	51.58	0	0
Arctic Fox (*Vulpes lagopus*)	VLA	2	184.00	59.45	0	0
Kit Fox (*Vulpes macrotis*)	VMA	2	154.45	51.97	0	0
Red Fox (*Vulpes vulpes*)	VVU	2	203.56	64.72	0	0

CODE: labels for species used in figures. All data are species means. N, sample size; SK, skull centroid size; FR, frontal centroid size; TSV, total frontal sinus volume and TSA, total frontal sinus surface area.

Table 1-2. Descriptions of landmarks used for geometric morphometric analysis of skull shape.

Landmark	Region	Description
1	SK	Posteromedial most point on the palatine
2	SK	Anteromedial most point on the incisive
3	SK	Anterior border of the C1 alveolus
4	SK	Posterior border of the C1 alveolus
5	SK	Anterior border of the P4 alveolus
6	SK	Posterior border of the alveolus of the last upper cheek tooth
7	FR	Intersection of the frontal, maxilla, and lacrimal
8	FR	Post-orbital process of the frontal
9	SK	Anterior extension of the squamosal on the zygomatic arch
10	SK	Posterior extension of the jugal on the zygomatic arch
11	SK	Superior border of the external auditory meatus
12	SK	Ventral most point on the mastoid process
13	SK	Medial point on the ventral border of the foramen magnum
14	SK	Posterior most point on the sagittal crest
15	FR	Midsagittal point of the frontoparietal suture
16	FR	Mid-point between landmarks 15 and 17
17	FR	Midsagittal point of the frontonasal suture.
18	SK	Intersection of the incisive, maxilla, and nasal
19	SK	Anteromedial most point on the nasal
20	FR	Midpoint between landmarks 16 and 8
21	FR	Intersection of the parietal, frontal, and alisphenoid
22	FR	Intersection of the frontal, lacrimal, and palatine
23	FR	Intersection of the frontal, nasal, and maxilla

SK, skull, FR, frontal bone (also included in SK). See Figure 1-2 for illustration of landmarks on a skull.

Table 1-3. Summary statistics for RMA regressions of frontal sinus volume against skull and frontal bone size.

Log_{10} TSV vs.	Group	N	a	b	95% C.I.	r^2
Log_{10} FR	All	27	-4.65	4.48*	3.76 - 5.34	0.82
	Canidae	8	-6.10	5.23*	3.46 - 7.91	0.82
	Hyaenidae	4	-9.64	6.98*	4.80 - 10.15	0.98
	Felidae	15	-2.87	3.53	2.76 - 4.52	0.83
Log_{10} SK	All	27	-5.19	3.81*	3.03 - 4.78	0.69
	Canidae	8	-7.43	4.63*	3.04 - 7.04	0.81
	Hyaenidae	4	-13.49	7.19*	5.07 - 10.21	0.99
	Felidae	15	-3.11	2.96	2.24 - 3.92	0.77

Regressions used log_{10} transformed data. TSV, total sinus volume; FR, frontal bone centroid size; SK, skull centroid size. N= sample size, a = y-intercept, b = slope, 95% C.I. = 95% confidence intervals for the slope, r^2 = correlation coefficient. Asterisks indicate slopes that differed significantly from isometry, all of which were positively allometric.

Table 1-4. Summary statistics for partial least squares analyses.

	Log_{10} TSV vs.	Group	RV coefficient	p
Skull Shape	SK Procrustes	All families	0.13	NS
		Canidae	0.38	NS
		Felidae	0.74	< 0.0001
		Hyaenidae	0.95	<0.05
	FR Procrustes	All families	0.23	0.01
		Canidae	0.39	NS
		Felidae	0.61	<0.001
		Hyaenidae	0.89	<0.05
	Sinus SPHARM coeffs vs.			
Skull Size	Log_{10} SK	All Families	0.56	< 0.0001
		Canidae	0.61	<0.05
		Felidae	0.57	0.0001
		Hyaenidae	0.98	<0.05
	Log_{10} FR	All Families	0.49	< 0.0001
		Canidae	0.68	<0.01
		Felidae	0.52	< 0.01
		Hyaenidae	0.98	NS
Skull Shape	SK Procrustes	All families	0.32	<0.01
		Canidae	0.55	NS
		Felidae	0.61	<0.001
		Hyaenidae	0.96	<0.05
	FR Procrustes	All families	0.54	< 0.0001
		Canidae	0.54	NS
		Felidae	0.66	<0.001
		Hyaenidae	0.92	<0.05

TSV: total sinus volume; SK: skull centroid size; FR: frontal centroid size; SK Procrustes: skull procrustes coordinates; FR Procrustes: frontal procrustes coordinates.

Table 1-5. Summary statistics for RMA regressions of frontal sinus surface area against frontal sinus volume.

	N	a	b	95% C.I.	r^2
All	27	0.88	0.70*	0.67-0.73	0.98
Canidae	8	1.15	0.62	0.54-0.72	0.98
Hyaenidae	4	0.82	0.72*	0.67-0.77	1.00
Felidae	15	0.92	0.68	0.63-0.74	0.98

Abbreviations as in Table 1-3. Asterisks indicate slopes that differed significantly from isometry, all of which were positively allometric.

FIGURE LEGENDS

Figure 1-1. Time-calibrated phylogeny used in this study using a modified topology from Slater et al. (2012) and pruned to include the species in this study. Species with sinuses shown in bold. Yellow stars indicate hypothesized independent appearances of frontal sinuses based on the literature.

Figure 1-2. Schematic showing how CT scan data (steps 1, 2) were used to visualize (step 3) and quantify sinus size and morphology (steps 6, 7, 8) as well as skull size and shape (steps 4, 5) using SPHARM and MorphoJ Software.

Figure 1-3. Transverse section of frontal sinus in *Acinonyx jubatus* (top) taken at the position indicated below by the dashed line in the dorsal view of the sinus within the skull (bottom) to show how an internal bony strut (arrow in top figure) is expressed as a furrow on the external surface of the model of the frontal sinus.

Figure 1-4. Volumetric models of frontal sinuses in skulls highlighting disparity in sinus morphology among Canidae, Felidae and Hyaenidae. Scale bars = 5cm.

Figure 1-5. Sexual dimorphism in frontal sinus morphology in *Felis lybica*. Scale bar = 5cm

Figure 1-6. PCA on SPHARM coefficients. PC 1 accounted for 34.1% of total shape variation, and PC 2 accounted for 14.2% of total shape variation. Dorsal and medial views of skulls showing sinus shapes at the extremes for each PC along each axis, with representative species identified with an asterisk in the plot. Species coded as in Table 1-1.

Figure 1-7. Log_{10}/Log_{10} RMA regressions of total sinus volume against A: skull centroid size and B: frontal bone centroid size. Species codes as in Table 1-1. Regression statistics given in Table 1-3.

Figure 1-8. Partial least squares plot of sinus shape against A) Log_{10} skull centroid size and B) frontal bone centroid size. Species representing the extremes in shape (*Parahyaena brunnea*, negative, *Lynx rufus*, positive) shown along the vertical axis. Statistics summarized in Table 1-4.

Figure 1-9. Log_{10}/Log_{10} RMA regression of total sinus surface area against total sinus volume. Species codes as in Table 1-1. Regression statistics given in Table 1-5.

Figure 1-10. Increasing sinus complexity with size. Sinuses displayed from smallest (left) to largest (right) A, *Nyctereutes procyonoides*; B, *Canis mesomelas*; C, *Canis lupus*; D, *Panthera uncia*; E, *Parahyaena brunnea*. Sinuses not drawn to scale, but are sized to illustrate differences in amount of strutting. Volumes for sinuses can be found in Table 1-1.

FIGURE 1-1

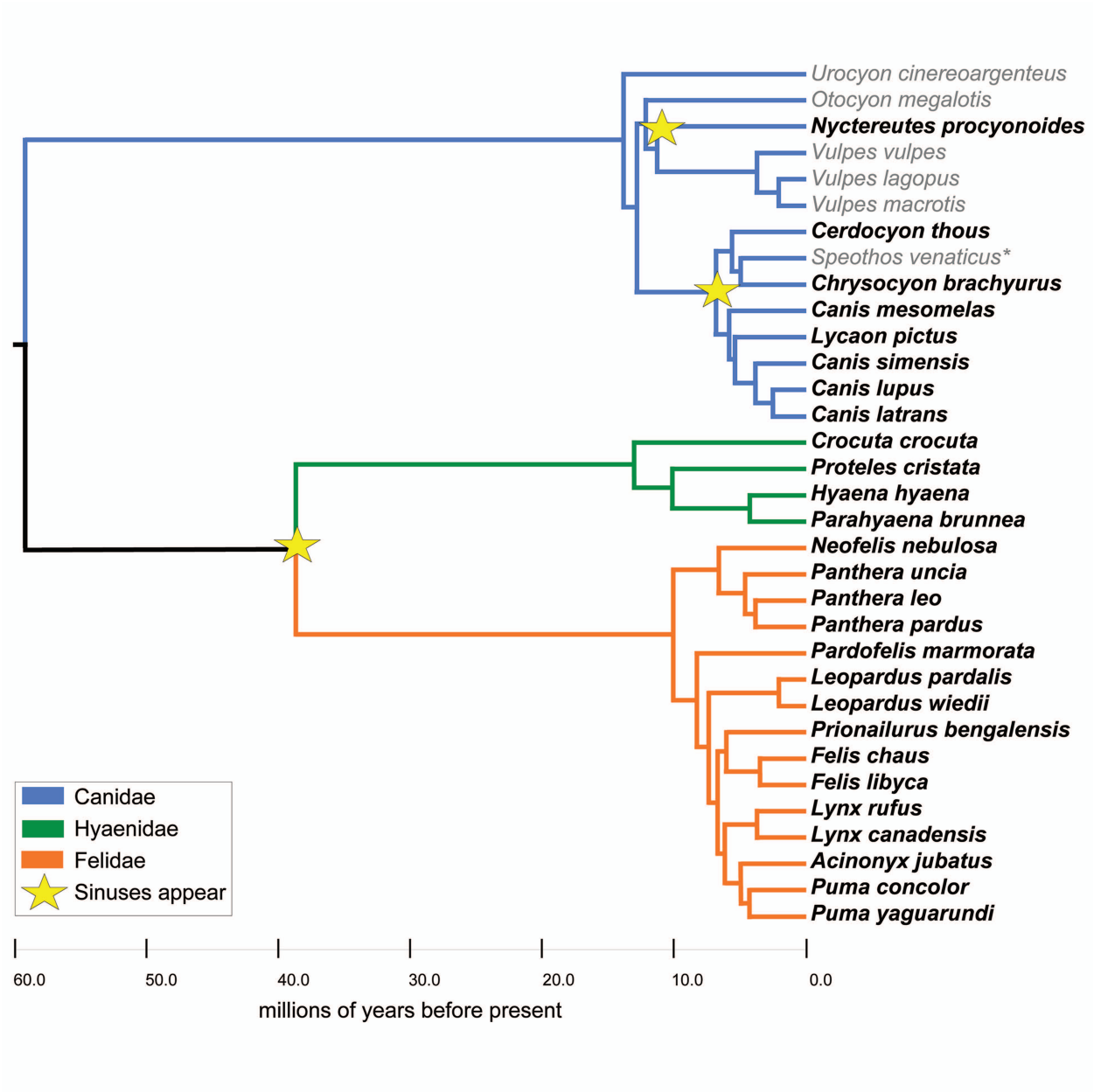
Urocyon cinereoargenteus
Otocyon megalotis
Nyctereutes procyonoides
Vulpes vulpes
Vulpes lagopus
Vulpes macrotis
Cerdocyon thous
Speothos venaticus*
Chrysocyon brachyurus
Canis mesomelas
Lycaon pictus
Canis simensis
Canis lupus
Canis latrans
Crocuta crocuta
Proteles cristata
Hyaena hyaena
Parahyaena brunnea
Neofelis nebulosa
Panthera uncia
Panthera leo
Panthera pardus
Pardofelis marmorata
Leopardus pardalis
Leopardus wiedii
Prionailurus bengalensis
Felis chaus
Felis libyca
Lynx rufus
Lynx canadensis
Acinonyx jubatus
Puma concolor
Puma yaguarundi
Canidae
Hyaenidae
Felidae
Sinuses appear
60.0
50.0
40.0
30.0
20.0
10.0
0.0
millions of years before present

FIGURE 1-2

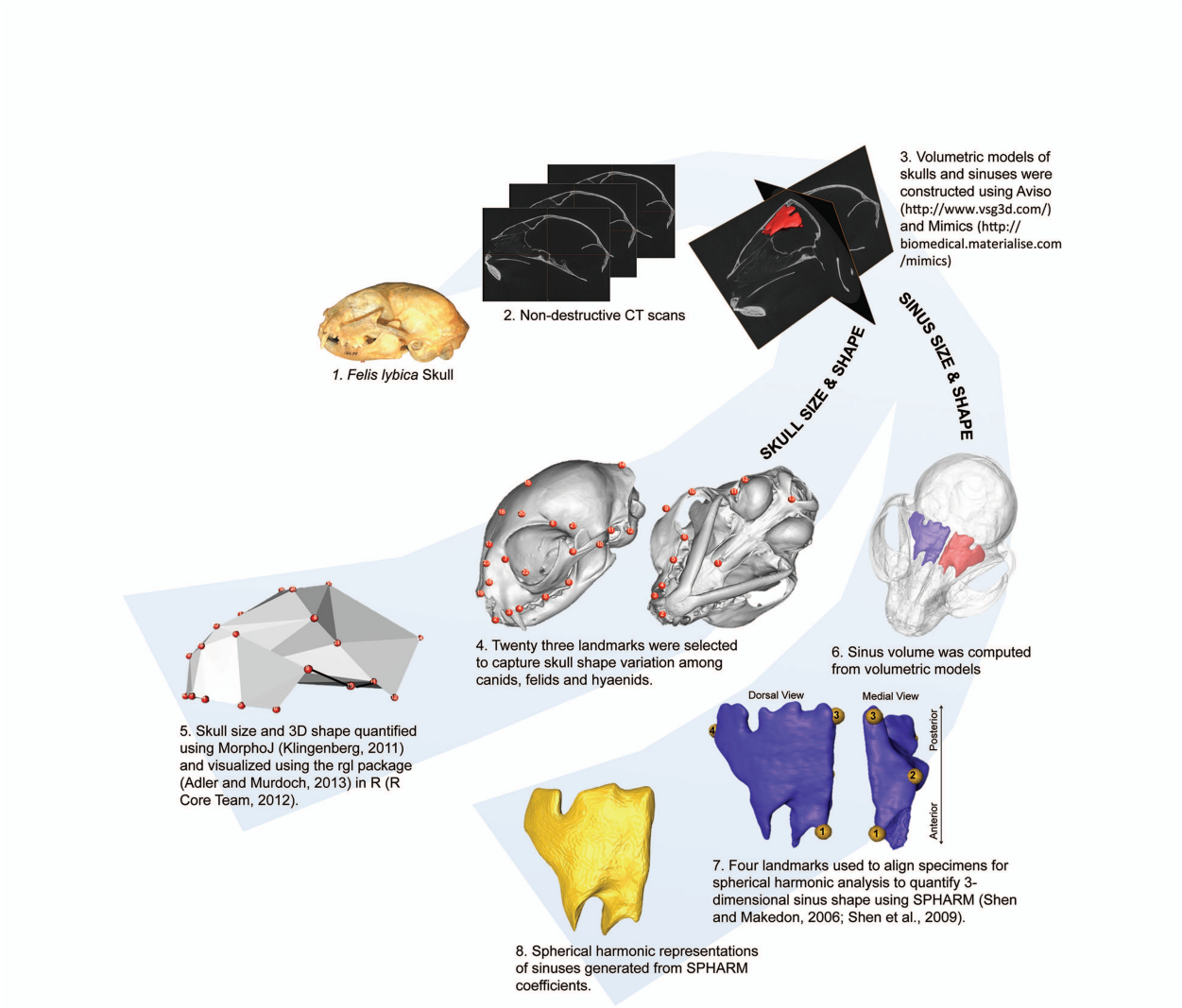
1. Felis lybica Skull
2. Non-destructive CT scans
3. Volumetric models of skulls and sinuses were constructed using Aviso (http://www.vsg3d.com/) and Mimics (http://biomedical.materialise.com/mimics)
SKULL SIZE & SHAPE
SINUS SIZE & SHAPE
4. Twenty three landmarks were selected to capture skull shape variation among canids, felids and hyaenids.
5. Skull size and 3D shape quantified using MorphoJ (Klingenberg, 2011) and visualized using the rgl package (Adler and Murdoch, 2013) in R (R Core Team, 2012).
6. Sinus volume was computed from volumetric models
Dorsal View
Medial View
Posterior
Anterior
7. Four landmarks used to align specimens for spherical harmonic analysis to quantify 3-dimensional sinus shape using SPHARM (Shen and Makedon, 2006; Shen et al., 2009).
8. Spherical harmonic representations of sinuses generated from SPHARM coefficients.

FIGURE 1-3

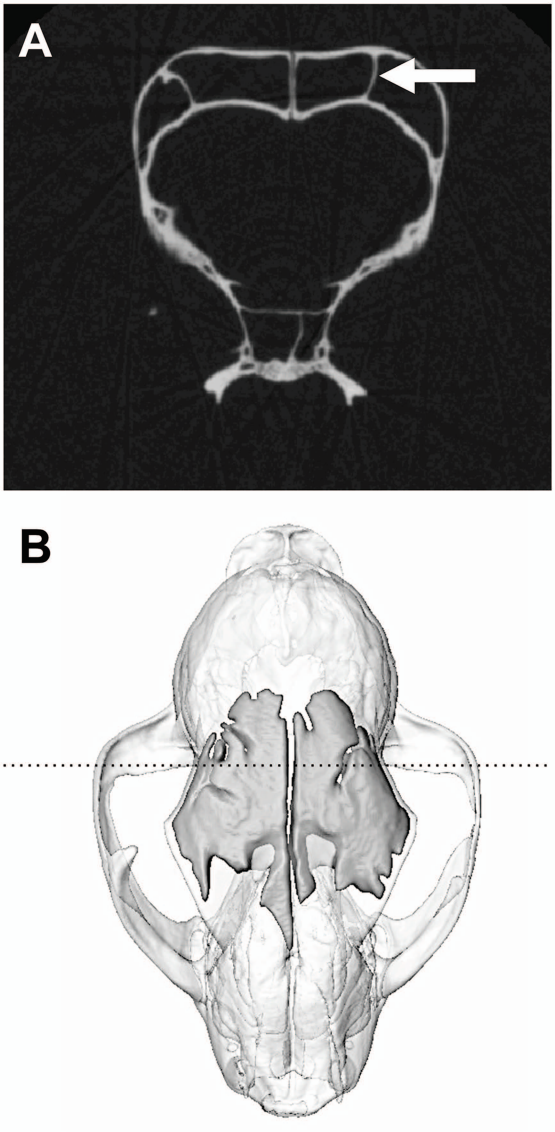

FIGURE 1-4

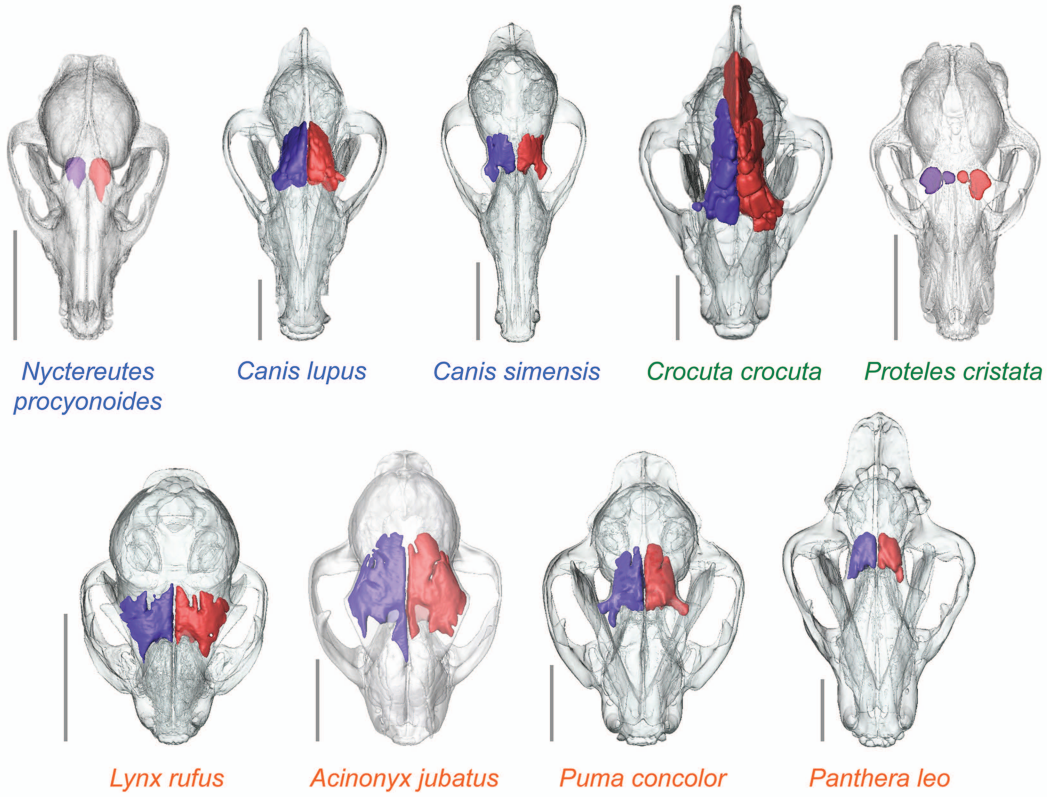
Nyctereutes procyonoides
Canis lupus
Canis simensis
Crocuta crocuta
Proteles cristata
Lynx rufus
Acinonyx jubatus
Puma concolor
Panthera leo

FIGURE 1-5

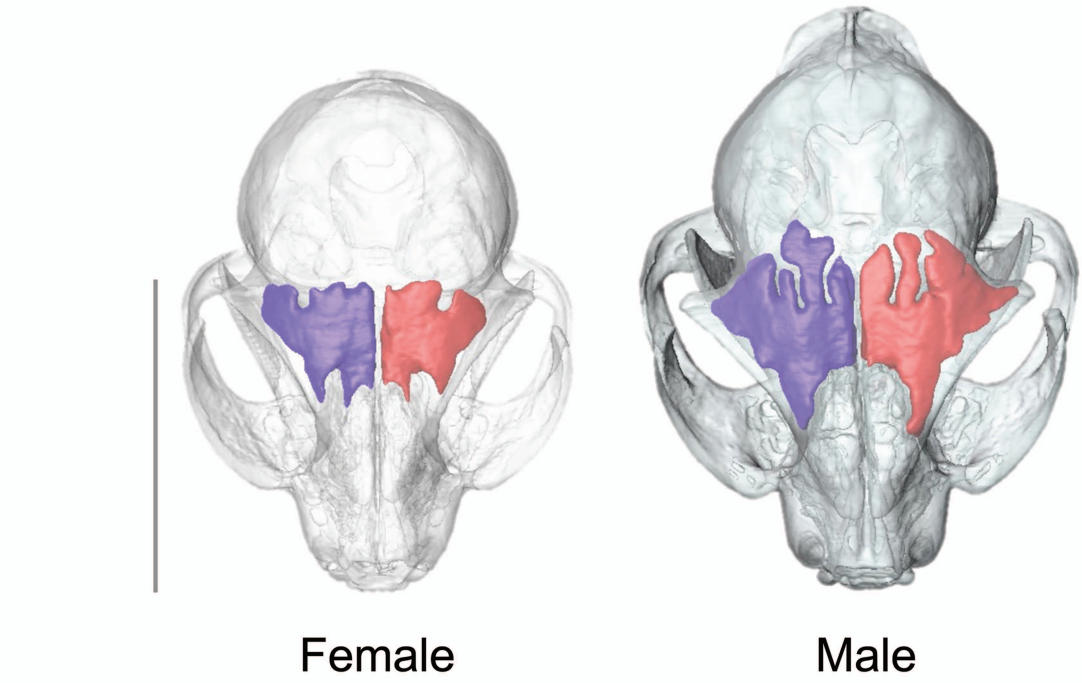

FIGURE 1-6

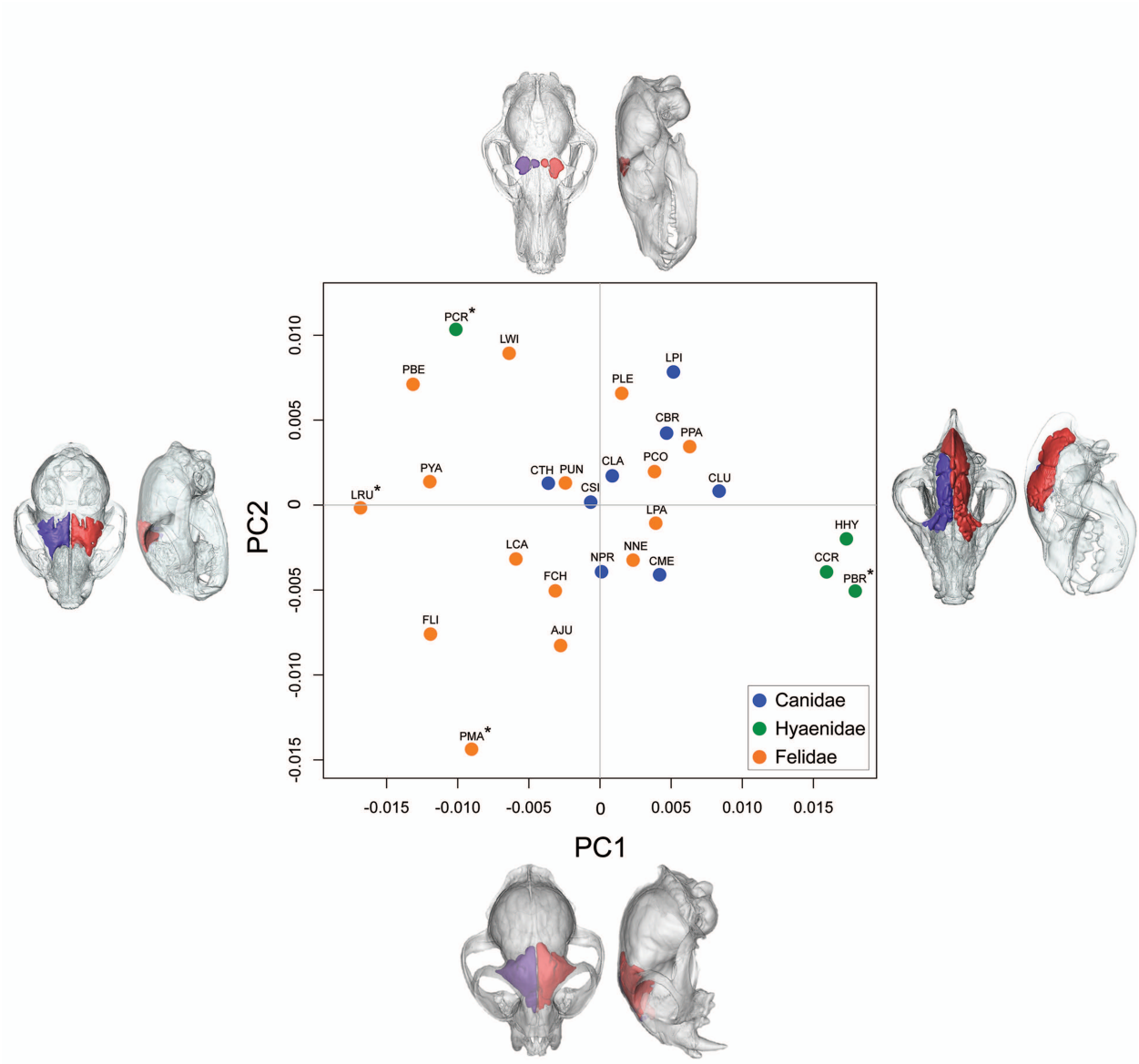
PCR*
LWI
PBE
LPI
PLE
CBR
PPA
PYA
CTH
PUN
CLA
PCO
CLU
LRU*
CSI
LPA
HHY
LCA
NPR
NNE
CME
CCR
PBR*
FCH
FLI
AJU
PMA*
Canidae
Hyaenidae
Felidae
PC2
PC1
0.010
0.005
0
-0.005
-0.010
-0.015
-0.015
-0.010
-0.005
0
0.005
0.010
0.015

FIGURE 1-7

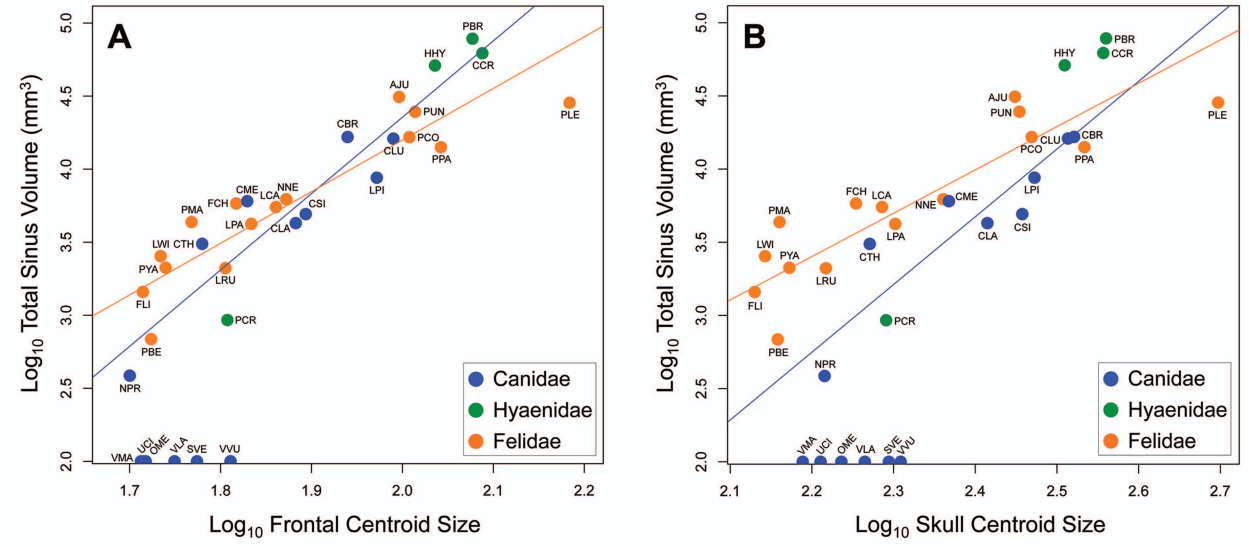
A
B
Log10 Total Sinus Volume (mm3)
Log10 Frontal Centroid Size
Log10 Skull Centroid Size
Canidae
Hyaenidae
Felidae
PBR
HHY
CCR
AJU
PUN
PLE
CBR
CLU
PCO
PPA
LPI
CME
NNE
LCA
FCH
PMA
CSI
CLA
LPA
LWI
CTH
PYA
LRU
FLI
PCR
PBE
NPR
VMA
UCI
OME
VLA
SVE
VVU

FIGURE 1-8

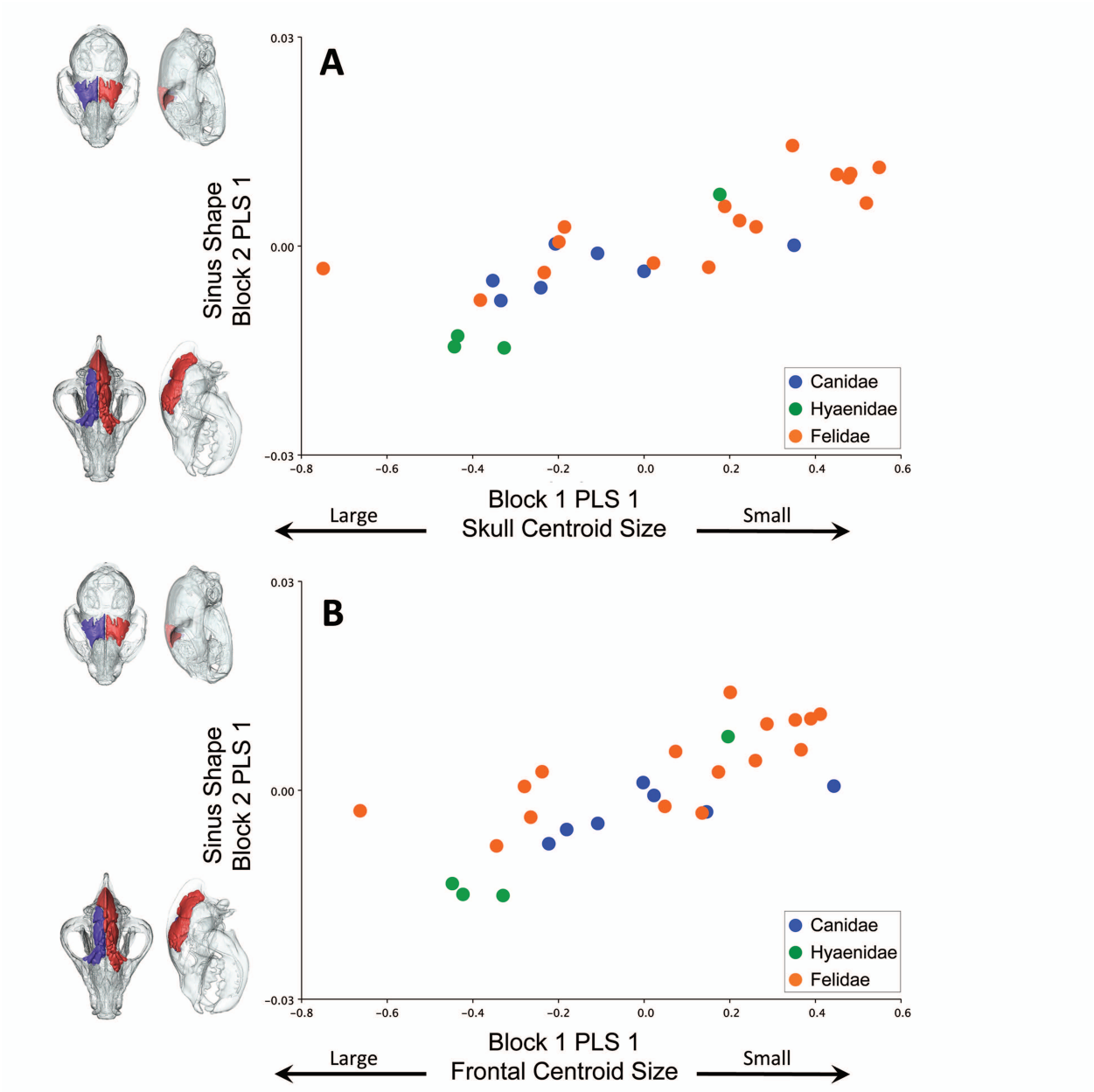
A
B
Sinus Shape
Block 2 PLS 1
0.03
0.00
-0.03
-0.8
-0.6
-0.4
-0.2
0.0
0.2
0.4
0.6
Canidae
Hyaenidae
Felidae
Large
Small
Block 1 PLS 1
Skull Centroid Size
Block 1 PLS 1
Frontal Centroid Size

FIGURE 1-9

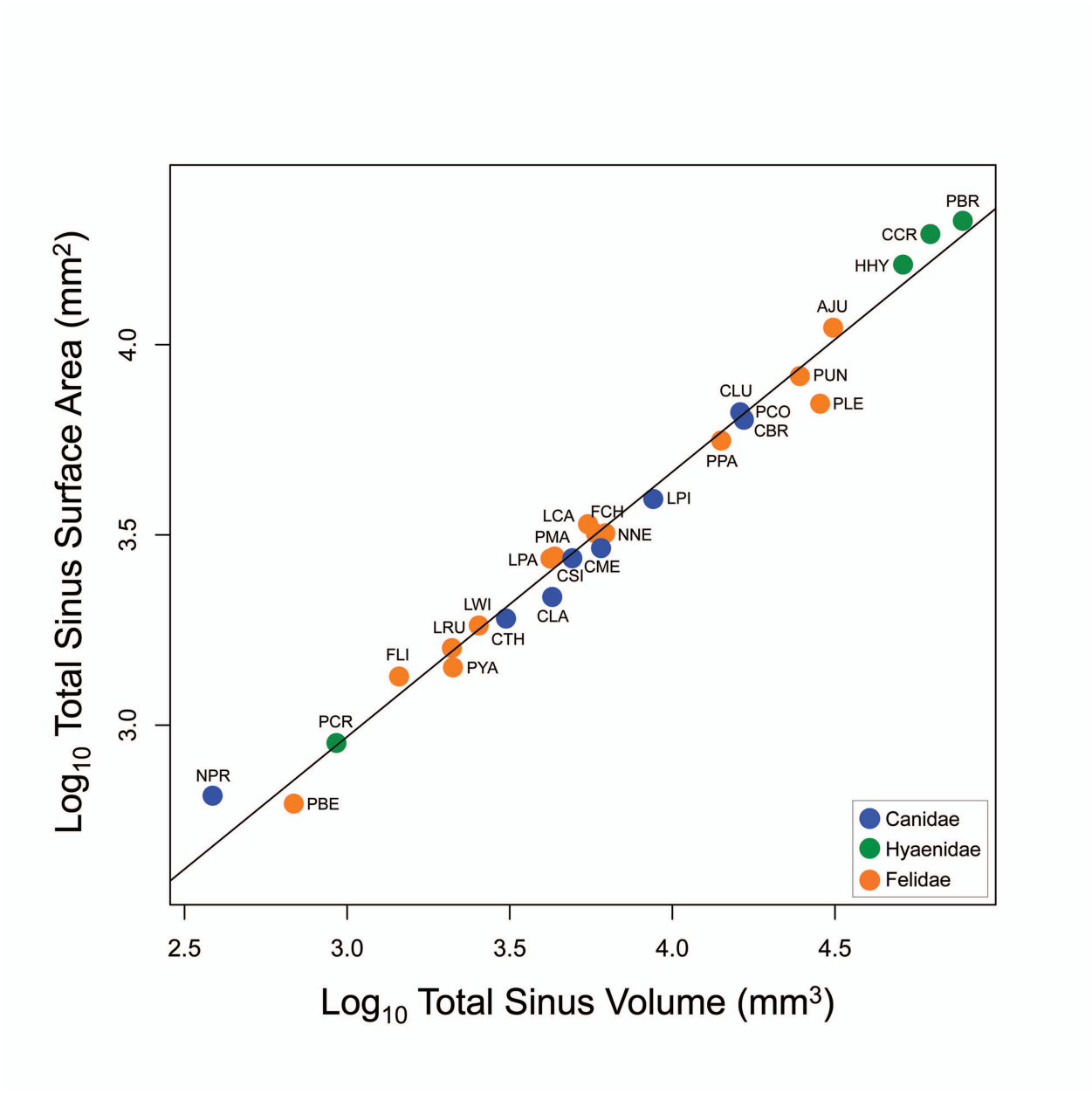
PBR
CCR
HHY
AJU
PUN
PLE
CLU
PCO
CBR
PPA
LPI
LCA
FCH
NNE
PMA
LPA
CME
CSI
CLA
LWI
LRU
CTH
PYA
FLI
PCR
NPR
PBE
Canidae
Hyaenidae
Felidae
3.0
3.5
4.0
2.5
3.0
3.5
4.0
4.5
Log10 Total Sinus Surface Area (mm2)
Log10 Total Sinus Volume (mm3)

FIGURE 1-10

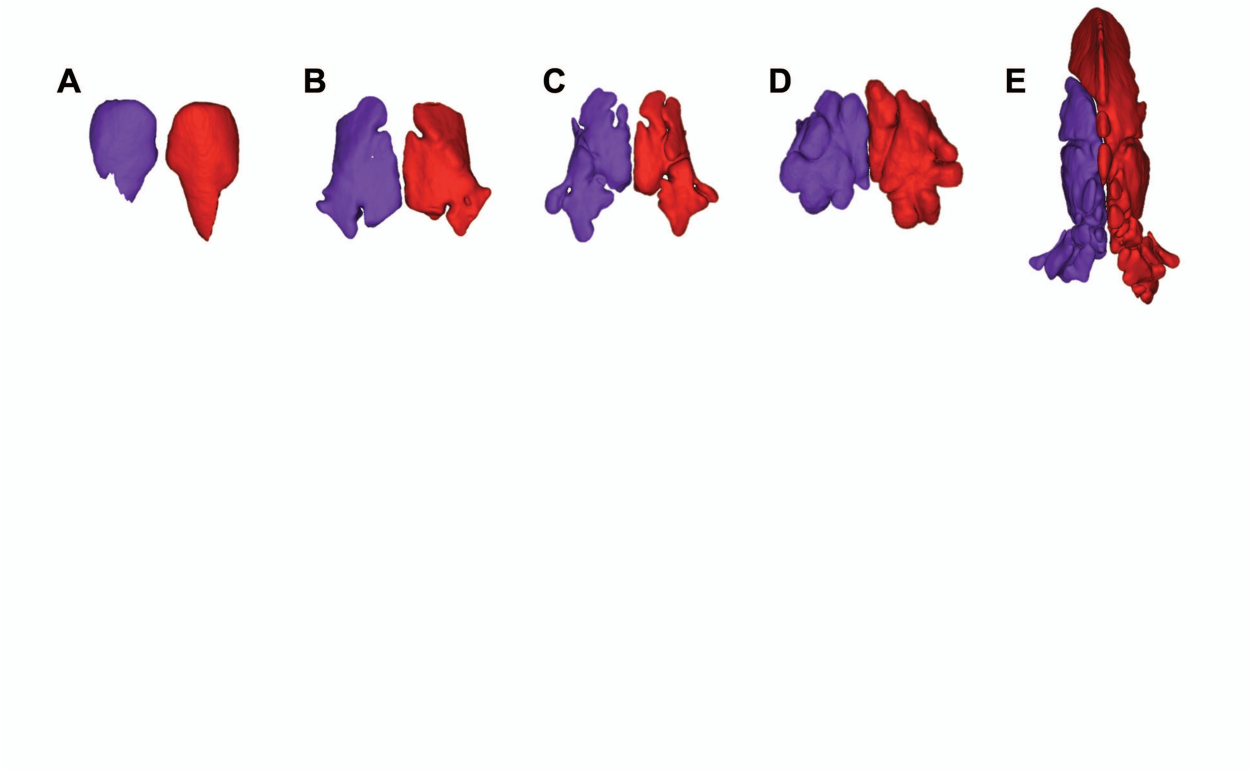

SUPPLEMENTAL INFORMATION

Table S1-1. Specimens included in this study.

Species	Specimen Numbers
Felidae	
African Wildcat (*Felis libyca*)	LACM14474 (f), LACM14480 (m)
Bobcat (*Lynx rufus*)	UCLA10118 (f), UCLA15254 (f), UCLA10115 (m)
Ocelot (*Leopardus pardalis*)	LACM26789 (f), FMNH34339 (m)
Puma (*Puma concolor*)	LACM85440 (f), LACM85440 (m)
Clouded leopard (*Neofelis nebulosa*)	USNM282124 (m), LACM31155 (u)
Lion (*Panthera leo*)	MMNH17533 (f), MMNH17537 (m), MVZ117849 (u)
Cheetah (*Acinonyx jubatus*)	FMNH127834 (f), FMNH29635 (m)
Leopard (*Panthera pardus*)	LACM11704 (m)
Snow Leopard (*Panthera uncia*)	LACM54708 (m)
Canadian Lynx (*Lynx canadensis*)	LACM92581 (f), LACM92582 (m)
Jungle cat (*Felis chaus*)	LACM8224 (m)
Jaguarundi (*Puma yaguarundi*)	LACM33299 (m), LACM61144 (f)
Marbled Cat (*Pardofelis marmorata*)	LACM469 (m)
Margay (*Leopardus wiedii*)	LACM29326 (f), LACM59449 (m)
Leopard cat (*Prionailurus bengalensis*)	LACM8223 (m)
Canidae	
Gray Wolf (*Canis lupus*)	USNM507338 (f), USNM98311 (f), USNM291012 (m), USNM98307 (m)
Black Backed Jackal (*Canis mesomelas*)	UCLA3000 (u)
Arctic Fox (*Vulpes lagopus*)	UCLA15163 (f), UCLA15161 (m)
Kit Fox (*Vulpes macrotis*)	UCLAHX27 (f), UCLAHX92 (m)
Red Fox (*Vulpes vulpes*)	UCLA15180 (f), UCLA15267 (m)
Coyote (*Canis latrans*)	UCLA1225 (f), UCLA2739 (m)
Bat Eared Fox (*Otocyon megalotis*)	USNM429132 (f), USNM429129 (m)
Ethiopian Wolf (*Canis simensis*)	AMNH81001 (u)
African Wild Dog (*Lycaon pictus*)	USNM368443 (f), USNM368441 (m)
Bush Dog (*Speothos venaticus*)	MVZ184054 (m)
Maned Wolf (*Chrysocyon brachyurus*)	USNM ????
Crab Eating Fox (*Cerdocyon thous*)	USNM ????
Gray Fox (*Urocyon cinereoargenteus*)	UCLA E2 2000 (f), UCLA6928 (m)
Raccoon Dog (*Nyctereutes procyonoides*)	USNM254641 (f), USNM255530 (m)
Hyaenidae	
Spotted Hyena (*Crocuta crocuta*)	USNM164506 (f), USNM181527 (m)
Brown Hyena (*Parahyena brunnea*)	FMNH34584 (m), USNM181527 (u)
Striped Hyena (*Hyaena hyaena*)	USNM182034 (m)
Aardwolf (*Proteles cristatus*)	USNM368497 (f)

Los Angeles County Museum of Natural Hisotry = LACM, UCLA Donald R. Dickey Collection = UCLA, Chicago Field Museum = FMNH, American Museum of Natural History = AMNH, Berkeley Museum of Vertebrate Zoology = MVZ, USNM = National Museum of Natural History.

Table S1-2. Summary statistics for OLS and PGLS regressions of frontal sinus volume against skull and frontal bone size.

Log_{10} (TSV) vs.	Group	Method	N	b ± SE	a ± SE	r^2	p
Log_{10} (SK)	All Families	OLS	27	3.16 ± 0.42	-3.66 ± 1.01	0.69	<< 0.0001
		PGLS		3.30 ± 0.41	-4.01 ± 0.99	0.72	<< 0.0001
	Canidae	OLS	8	4.17 ± 0.82	-6.34 ± 1.96	0.81	< 0.01
		PGLS		3.77 ± 0.83	-5.45 ± 1.95	0.78	< 0.01
	Hyaenidae	OLS	4	7.14 ± 0.60	-13.37 ± 1.48	0.99	< 0.01
		PGLS		7.14 ± 0.60	-13.37 ± 1.48	0.99	< 0.01
	Felidae	OLS	15	2.61 ± 0.39	-2.29 ± 0.91	0.77	<< 0.0001
		PGLS		2.61 ± 0.39	-2.29 ± 0.91	0.77	<< 0.0001
Log_{10} (FR)	All Families	OLS	27	4.05 ± 0.38	-3.84 ± 0.73	0.82	< 0.0001
		PGLS		4.05 ± 0.38	-3.84 ± 0.73	0.82	< 0.0001
	Canidae	OLS	8	4.73 ± 0.91	-5.17 ± 1.71	0.82	< 0.0001
		PGLS		4.35 ± 0.86	-4.53 ± 1.58	0.81	0.001
	Hyaenidae	OLS	4	6.93 ± 0.62	-9.52 ± 1.25	0.98	< 0.01
		PGLS		6.90 ± 0.60	-9.50 ± 1.20	0.99	< 0.01
	Felidae	OLS	15	3.22 ± 0.41	-2.28 ± 0.76	0.83	< 0.0001
		PGLS		3.22 ± 0.41	-2.28 ± 0.76	0.83	< 0.0001

Regressions used log_{10} transformed data. TSV, total sinus volume; FR, frontal bone centroid size; SK, skull centroid size. N= sample size, a = y-intercept, b = slope, 95% SE = standard error, r^2 = correlation coefficient.

Table S1-3. Summary statistics for OLS and PGLS regressions of frontal sinus surface area against frontal sinus volume.

Log_{10} (TSA) vs. Log_{10} TSV						
Group	Method	N	b ± SE	a ± SE	r^2	p
All Families	GLS	27	0.69 ± 0.02	0.90 ± 0.07	0.98	< 0.0001
	PGLS		0.69 ± 0.02	0.90 ± 0.07	0.98	< 0.0001
Canidae	GLS	8	0.62 ± 0.04	1.17 ± 0.13	0.98	< 0.0001
	PGLS		0.62 ± 0.04	1.17 ± 0.13	0.98	< 0.0001
Hyaenidae	GLS	4	0.72 ± 0.01*	0.81 ± 0.05	1	< 0.001
	PGLS		0.72 ± 0.01*	0.82 ± 0.05	1	< 0.001
Felidae	GLS	15	0.68 ± 0.03	0.94 ± 0.10	0.98	< 0.0001
	PGLS		0.68 ± 0.04	0.92 ± 0.11	0.98	< 0.0001

Abbreviations as in Table S1-2.

LITERATURE CITED

Adler D, Murdoch D. 2013. rgl: 3D visualization device system (OpenGL). R package version 0.93.932. http://CRAN.R-project.org/package=rgl.

Cave AJE. 1967. Observations on the platyrrine nasal fossa. Am J Phys Anthropol 26:277-288.

Covey DSG, Greaves WS. 1994. Jaw dimensions and torsion resistance during canine biting in the Carnivora. Can J Zool 72:1055-1060.

Currey JD. 2002. Bones: Structure and Mechanics. Princeton NJ: Princeton University Press. 436 p.

Edinger T. 1950. Frontal sinus evolution particularly in the Equidae. Bull Mus Comp Zool at Harvard 103:409-496.

Ewer RF. 1973. The Carnivores. Ithaca NY: Cornell University Press. 500 p.

Farke AA. 2007. Morphology, constraints, and scaling of frontal sinuses in the hartebeest, *Alcelaphus buselaphus* (Mammalia: Artiodactyla, Bovidae). J Morphol 268:243-253.

Farke AA. 2008. Frontal sinuses and head-butting in goats: a finite element analysis. J Exp Biol 211:3085-3094.

Farke AA. 2010. Evolution and functional morphology of the frontal sinuses in Bovidae (Mammalia: Artiodactyla), and implications for the evolution of cranial pneumaticity. Zool J Linnean Soc 159:988-1014.

Ferretti MP. 2007. Evolution of bone-cracking adaptations in hyaenids (Mammalia, Carnivora). Swiss J Geosci 100:41-52.

Hallgrímsson B. 1998. Fluctuating asymmetry in the mammalian skeleton. Evol Biol 30; 187-251.

Hildebrand T, Laib A, Müller R, Dequeker J, Rüegsegger P. 1999. Direct three-dimensional morphometric analysis of human cancellous bone: microstructural data from spine, femur, iliac crest, and calcaneus. J Bone Mineral Res 14: 1167-1174.

Hildebrand T, Rüegsegger P. 1997. A new method for the model-independent assessment of thickness in three-dimensional images. J Microscopy 185: 67-75.

Huxley TH. 1880. On the cranial and dental characteristics of the Canidae. Proc Zool Soc London 48:238-288.

Joeckel RM. 1998. Unique frontal sinuses in fossil and living Hyaenidae (Mammalia,

Carnivora): description and interpretation. J Vertebr Paleontol 18:627-639.

Klingenberg CP. 2011. MORPHOJ: an integrated software package for geometric morphometrics. Molec Ecol Res 11:353-356.

Maier W. 2000. Ontogeny of the nasal capsule in cercopithecoids: a contribution to the comparative and evolutionary morphology of catarrhines. In: Whitehead PF, Jolly CJ, editors. Old World monkeys. Cambridge: Cambridge University Press. p 99-132.

Márquez S, Laitman JT. 2008. Climatic effects on the nasal complex: a CT imaging, comparative anatomical, and morphometric investigation of *Macaca mulatta* and *Macaca fascicularis*. Anat Rec 291:1420-1445.

Martins EP, Hansen TF. 1997. Phylogenies and the comparative method: a general approach to incorporating phylogenetic information into the analysis of interspecific data. American Naturalist 149:646-667.

McPeek MA, Shen L, Farid H. 2009. The correlated evolution of three-dimensional reproductive structures between male and female damselflies. Evolution 63:73-83.

McPeek MA, Symes LB, Zong DM, McPeek CL. 2011. Species recognition and patterns of population variation in the reproductive structures of a damselfly genus. Evolution 65:419-428.

Orme D. 2012. The Caper package: comparative analysis of phylogenetics and evolution in R. http://cran.r-project.org/web/packages/caper/vignettes/caper.pdf.

Paulli S. 1900a. Über die pneumaticität bei den säugerthieren. Ein morphologische studie. II. Über die Morphologie des siebbens und die der pneumaticität bei den ungulaten und prosbosciden. Gegenbaurs Morphol Jahrb 28:179-251.

Paulli S. 1900b. Über die pneumaticität bei den säugerthieren. Ein morphologische studie. III. Über die Morphologie des siebbens und die der pneumaticität bei den insectivoren, hyracoideen, chiropteren, carnivoren, pinnipedien, edentaten, rodentiern, prosimiern und primaten. Gegenbaurs Morphol Jahrb 28:483-564.

Radinsky LB. 1981a. Evolution of skull shape in carnivores: 1. Representative modern carnivores. Biol J Linnean Soc 15:369-388.

Radinsky LB. 1981b. Evolution of skull shape in carnivores: 1. Additional modern carnivores. Biol J Linnean Soc 16:337-355.

Rae TC, Koppe T. 2008. Independence of biomechanical forces and craniofacial pneumatization in *Cebus*. Anat Rec 291:1414-1419.

Rae TC, Koppe T, Spoor F, Benefit B, McCrossin M. 2002. Ancestral loss of the maxillary sinus

in Old World monkeys and independent acquisition in *Macaca*. Am J Phys Anthropol 117:293-296.

Rohlf JF, Corti M. 2000. Use of two-block partial least-squares to study covariation in shape. Syst Biol 49:740-753.

Salles LO. 1992. Felid phylogenetics: extant taxa and skull morphology (Felidae, Aeluroidea). Am Mus Novit 3047:1-67.

Schaller GB, Hu J, Pan W. 1985. The giant pandas of Wolong. Chicago: Chicago University Press. 298 p.

Schaller GB, Qitao T, Johnson KG, Xiaoming W, Heming S, Jinchu H. 1989. The feeding ecology of giant pandas and Asiatic black bears in the Tangjiahe Reserve, China. In: Gittleman JL, editor. Carnivore Behavior, Ecology, and Evolution: Part II. Ithaca NY: Cornell University Press. p 212-241.

Sharp NJ, McEntee M, Gilson S, Thrall D. 1991. Nasal cavity and frontal sinuses. Prob Vet Med 3:170-87.

Shen L, Farid H, McPeek MA. 2009. Modeling three-dimensional morphological structures using spherical harmonics. Evolution 63:1003-1016.

Shen L, Makedon F. 2006. Spherical mapping for processing of 3D closed surfaces. Image Vision Comput 24:743-761.

Slater GJ, Dumont ER, Van Valkenburgh B. 2009. Implications of predatory specialization for cranial form and function in canids. J Zool 278:181-188.

Slater GJ, Harmon LJ, Alfaro ME. 2012. Integrating fossils with molecular phylogenies improves inference of trait evolution. Evolution 66:3931-3944.

Slater GJ, Van Valkenburgh B. 2008. Long in the tooth: evolution of sabertooth cat cranial shape. Paleobiology 34:403-419.

Slater GJ, Van Valkenburgh B. 2009. Allometry and performance: the evolution of skull form and function in felids. J Evol Biol 22:2278-2287.

Smith RJ. 2009. Use and misuse of the reduced major axis for line-fitting. Am J Phys Anthropol 140:476-486.

Smith TD, Rossie JB, Cooper GM, Mooney MP, Siegel MI. 2005. Secondary pneumatization of the maxillary sinus in callitrichid primates: insights from immunohistochemistry and bone cell distribution. Anat Rec Part A 285A:677-689.

Smith TD, Rossie JB, Docherty BA, Cooper GM, Bonar CJ, Silverio AL, Burrows AM. 2008.

Fate of the nasal capsular cartilages in prenatal and perinatal tamarins (*Saguinus geoffroyi*) and extent of secondary pneumatization of maxillary and frontal sinuses. Anat Rec 291:1397-1413.

Smith TD, Rossie JB, Cooper GM, Schmeig RM, Bonar CJ, Mooney MP, Siegel MI. 2011. Comparative micro CT and histological study of maxillary pneumatization in four species of New World monkeys: The Perinatal period. Am J Phys Anthropol 144:392-410.

Tanner JB, Dumont ER, Sakai ST, Lundrigan BL, Holekamp KE. 2008. Of arcs andvaults: the biomechanics of bone-cracking in spotted hyenas (*Crocuta crocuta).*Biol J Linnean Soc 95:246-255.

Tedford RH, Taylor BE, Wang X. 1995. Phylogeny of the Caninae (Carnivora, Canidae): the living taxa. Am Mus Novit 3146:1-37.

Tedford RH, Wang X, Taylor BE. 2009. Phylogenetic systematics of the North American fossil Caninae (Carnivora: Canidae). Bull Am Mus Nat Hist 325:1-218.

Tseng ZJ. 2011. Variations and implications of intra-dentition Hunter Schreger band pattern in fossil hyaenids and canids (Carnivora, Mammalia). J Vertebr Paleontol 31:1163-1167.

Tseng ZJ, Wang X. 2010. Cranial functional morphology of fossil dogs and adaptations for durophagy in *Borophagus* and *Epicyon* (Carnivora, Mammalia). J Morphol 271: 1386-1398.

Tseng ZJ, Wang X. 2011. Do convergent ecomorphs evolve through convergent morphological pathways? Cranial shape evolution in fossil hyaenids and borophagine canids (Carnivora, Mammalia). Paleobiology 37:470-489.

Van Valkenburgh B, Koepfli KP. 1993. Cranial and dental adaptations to predation in canids. Symp Zool Soc Lond 65:15-37.

Wang R-G, Jiang S-C, Gu R. 1994. The cartilaginous nasal capsule and embryonic development of human paranasal sinuses. J Otolaryngol 23:239-243.

Wang X. 1994. Phylogenetic systematics of the Hesperocyoninae (Carnivora: Canidae). Bull Am Mus Nat Hist 221:1-207.

Wang X, Tedford RH, Taylor BE. 1999. Phylogenetic systematics of the Borophaginae (Carnivora: Canidae). Bull Am Mus Nat Hist 243:1-391.

Warton, DI, Duursma RA, Falster DS, Taskinen S. 2012. Smatr 3 – an R package for estimation and inference about allometric lines. Methods Ecol Evol 3:257-259.

Warton DI, Wright IJ, Falster DS, Westoby M. 2006. Bivariate line-fitting methods for

allometry. Biological Reviews 81:259-291.

Werdelin L. 1989. Constraint and adaptation in the bone-cracking canid *Osteoborus* (Mammalia: Canidae). Paleobiology 15:387-401.

Witmer LM. 1997. The evolution of the antorbital cavity of archosaurs: A study in soft tissue reconstruction in the fossil record with an analysis of the function of pneumaticity. J Vertebr Paleontol 17:1-77.

Witmer LM. 1999. The phylogenetic history of paranasal air sinuses. In: Koppe R, Nagai H, Alt KW, editors. The Paranasal Sinuses of Higher Primates: Development, Function, and Evolution. Chicago: Quintesence. p 21-34.

Zelditch ML, Swiderski DL, Sheets HD, Fink WL. 2004. Geometric Morphometrics for Biologists: A Primer. New York: Elsevier Academic Press. 437 p.

Zollikofer CPE, Ponce de León MS, Schmitz RW, Stringer CB. 2008. New insights into Mid-Late Pleistocene fossil hominin paranasal sinus morphology. Anat Rec 291:1506-1516.

Zollikofer CPE, Weissmann JD. 2008. A morphogenetic model of cranial pneumatization based on the invasive tissue hypothesis. Anat Rec 291:1446-1454.

CHAPTER 2:

REPEATED LOSS OF FRONTAL SINUSES IN ARCTOID CARNIVORANS

Repeated Loss of Frontal Sinuses in Arctoid Carnivorans

Abigail A. Curtis,[1]* George Lai,[1] Fuwen Wei,[2] and Blaire Van Valkenburgh[1]

[1]*Department of Ecology and Evolutionary Biology, University of California, Los Angeles, California 90095-1606*
[2]*Key Lab of Animal Ecology and Conservation Biology, Institute of Zoology, Chinese Academy of Sciences, Beijing 100101, China*

ABSTRACT Many mammal skulls contain air spaces inside the bones surrounding the nasal chamber including the frontal, maxilla, ethmoid, and sphenoid, all of which are called paranasal sinuses. Within the Carnivora, frontal sinuses are usually present, but vary widely in size and shape. The causes of this variation are unclear, although there are some functional associations, such as a correlation between expanded frontal sinuses and a durophagous diet in some species (e.g., hyenas) or between absent sinuses and semiaquatic lifestyle (e.g., pinnipeds). To better understand disparity in frontal sinus morphology within Carnivora, we quantified frontal sinus size in relationship to skull size and shape in 23 species within Arctoidea, a clade that is ecologically diverse including three independent invasions of aquatic habitats, by bears, otters, and pinnipeds, respectively. Our sampled species range in behavior from terrestrial (rarely or never forage in water), to semiterrestrial (forage in water and on land), to semiaquatic (forage only in water). Results show that sinuses are either lost or reduced in both semiterrestrial and semiaquatic species, and that sinus size is related to skull size and shape. Among terrestrial species, frontal sinus size was positively allometric overall, but several terrestrial species completely lacked sinuses, including two fossorial badgers, the kinkajou (a nocturnal, arboreal frugivore), and several species with small body size, indicating that factors other than aquatic habits, such as space limitations due to constraints on skull size and shape, can limit sinus size and presence. J. Morphol. 000:000–000, 2014. © 2014 Wiley Periodicals, Inc.

KEY WORDS: paranasal sinuses; secondary aquatic adaptations; geometric morphometrics

INTRODUCTION

Paranasal sinuses are among the most variable, yet under-studied, features of mammal skulls. They form as mucosal-lined pneumatic spaces within the bones of most mammalian skulls and maintain a connection to the nasal chamber via ostia that vary in size (Cave, 1967). They develop during ontogeny if the cartilaginous nasal capsule breaks down, allowing the nasal epithelium and an accompanying vascular, osteoclastic lamina propria to invade surrounding bones including the frontal, maxilla, ethmoid, and sphenoid (Wang et al., 1994; Witmer, 1997; Smith et al., 2005, 2008). Within the order Carnivora, the frontal sinuses vary in size and shape, but are almost fully enclosed in bone with only small ostia connecting them to the nasal chamber, unlike the maxillary sinuses that retain a more open connection. Ethmoid and sphenoid sinuses are not present in most members of Carnivora (Paulli, 1900).

Several hypotheses have been proposed to explain the function of paranasal sinuses, and have been thoroughly summarized in reviews by Blanton and Biggs (1969), Blaney (1990), Witmer (1997), and more recently by Márquez (2008) and Keir (2009). All of these authors find it difficult to identify a single function, in part because sinuses have been gained and lost multiple times throughout Mammalia. This is especially true of the subject of this article, the frontal sinuses (e.g., Edinger, 1950; Witmer, 1997; Rossie, 2008; Farke, 2010). Moreover, sinuses can be co-opted for novel functions, such as removing bone in areas that result in enhancing the skull's efficiency at

Additional Supporting Information may be found in the online version of this article.

Contract grant sponsor: NSF; Grant number: IOB-0517748, IOS-1119768 (B.V.V.); Contract grant sponsor: DOE-P200A120027 (A.A.C.).

*Correspondence to: Abigail A. Curtis; Department of Ecology and Evolutionary Biology, University of California, Los Angeles, 610 Charles E. Young Dr. E., Los Angeles, CA 90095-1606.
E-mail: abigailacurtis@gmail.com

Author Contributions: A.C. was the primary author of this article. A.C. developed the study concept and design, as well as data analysis, and interpretation. G.L. and A.C. collected all frontal sinus volume and skull morphometric data and conducted all data analyses. WF provided the CT scans of the giant panda. B.V.V. was the secondary author, and involved in study design, data analysis and interpretation. All authors contributed to the writing of this article.

Received 21 October 2013; Revised 19 June 2014;
Accepted 1 July 2014.

Published online 00 Month 2014 in
Wiley Online Library (wileyonlinelibrary.com).
DOI 10.1002/jmor.20313

dissipating stress, as evidenced by frontal sinuses in some taxa (e.g., Werdelin, 1989; Joeckel, 1998; Tanner et al., 2008), making it unlikely that there is a single overarching explanation for their function.

The best-supported hypothesis for frontal sinus function is that they, along with other paranasal sinuses, opportunistically pneumatize areas during development where bone is not mechanically necessary, which consequentially reduces skull mass. This hypothesis, commonly referred to as the "epithelial hypothesis" (Witmer, 1997), is supported by observations that in many mammals, frontal sinus size and shape are best explained by skull size and shape (e.g., Farke, 2007, 2010; Zollikofer et al., 2008; Curtis and Van Valkenburgh, in press) rather than similarities in feeding ecology or head-butting behavior. This hypothesis is additionally supported by histological studies (Smith et al., 2005, 2008) and results from a model simulating frontal sinus growth as an opportunistic process (Zollikofer and Weissmann, 2008). However, as noted above, it also appears that frontal sinuses in some species do play an indirect biomechanical role by removing bone to better optimize dissipation of stress across the skull during feeding (Tanner et al., 2008) and combat (Farke, 2008). This function appears to be enhanced when the frontal bone is dorsally convex or domed, as seen in many extinct hypercarnivorous canids and extant bone-cracking hyaenids (Tanner et al., 2008, Tseng, 2009). In fact, the opportunistic epithelial hypothesis does not preclude the fact that frontal sinus shape and/or size might be correlated with particular functions, such as durophagy or head-butting. If the frontal bone becomes domed to dissipate stresses, then the simultaneous evolution of a frontal sinus allows this enlargement to occur without adding excessive mass.

Here, we conduct the first broad-scale quantitative study of frontal sinus morphology within the carnivoran superfamily Arctoidea, a group that includes bears, weasels, raccoons, and pinnipeds. Arctoids include the smallest and largest carnivorans, allowing us to test for allometric patterns in frontal sinus morphology. Arctoids also show marked disparity in skull shape related to size, diet, and ecology, providing us with the opportunity to explore associations between frontal sinus size and these variables.

Notably, arctoids underwent three independent invasions of aquatic habitats (pinnipeds, mustelids, ursids; Fig. 1) and range in behavior from terrestrial (rarely or never forage in water), to semiterrestrial (forage in water and on land), to semiaquatic (forage only in water). The skulls of secondarily aquatic mammals are generally characterized by the loss of paranasal sinuses, dorsally flattened skull profiles, and large, dorsally positioned eyes and nostrils (Paulli, 1900; Uhen, 2007; Reidenberg and Laitman, 2008). The lack of paranasal sinuses in fully aquatic species, such as cetaceans and sirenians, has been attributed to the need to mitigate buoyancy and/or the negative effects of having rigid gas-filled spaces within the skull that could collapse while diving due to extreme pressure increases with depth (Wall, 1983; Reidenberg and Laitman, 2008). However, a lack of pneumaticity is only described in obligate aquatic species, including cetaceans and sirenians, and did not explicitly explore frontal sinus size in semiaquatic and semiterrestrial mammals, such as are found within arctoids.

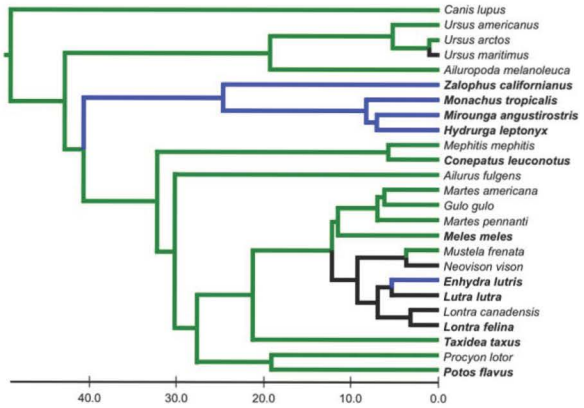

Fig. 1. Time-calibrated phylogeny of species included in this study with *Canis lupus* as the outgroup. Topology based on tree from Slater et al. (2012). Branch color represents ecology: green = terrestrial (rarely or never forage in water), black = semiterrestrial (forage in water and on land), blue = semiaquatic (forage only in water). Species highlighted in bold do not have sinuses.

Unlike maxillary sinuses, which are present in nearly all placental mammals (Paulli, 1900), frontal sinuses are much more variable in presence among species. For example, among arctoids, Paulli (1900) found that several mustelids (*Martes foina, Mustela putorius, Mustela erminea, Lutra lutra*, and *Taxidea taxus)* lacked frontal sinuses, as did two pinnipeds (*Phoca vitulina* and *Halichoerus grypus*) and two procyonids (*Nasua narica, Procyon cancrivorus*). Ursids, on the other hand, appear to have expansive frontal sinuses, as exemplified by brown bears (*Ursus arctos*; Paulli, 1900) and especially giant pandas (*Ailuropoda melaneuca*) in which the frontal sinuses extend caudally to completely overlie the braincase (Davis, 1964). Enlarged frontal sinuses, such as observed in the bamboo-feeding giant panda, have also been described for various bone-cracking carnivorans, including extant hyenas and extinct borophagine canids (Joeckel, 1998; Wang et al., 1999; Ferretti, 2007).

Here, we use a comparative approach to explore how frontal sinus morphology varies among

TABLE 1. Species included in this study with associated means for total sinus volume in mm^3 (TSV) and skull centroid size (CS)

Species	Family	*n*	Species code	Ecology	TSV	CS
Leopard seal (*Hydrurga leptonyx*)	Phocidae	2	HLE	SA[a]	0	478.12
Caribbean monk seal (*Monachus tropicalis*)	Phocidae	2	MTR	SA[a]	0	325.77
Northern elephant seal (*Mirounga angustirostris*)	Phocidae	1	MAN	SA[a]	0	349.03
California sea lion (*Zalophus californianus*)	Otariidae	2	ZCA	SA[a]	0	323.33
Kinkajou (*Potos flavus*)	Procyonidae	2	PFL	T[a]	0	122.24
Raccoon (*Procyon lotor*)	Procyonidae	2	PLO	T[a]	3386.9	164.08
Grizzly bear (*Ursus arctos*)	Ursidae	2	UAR	T[a]	152039.3	486.47
American black bear (*Ursus americanus*)	Ursidae	2	UAM	T[a]	39667.4	380.09
Polar bear (*Ursus maritimus*)	Ursidae	2	UMA	ST[a]	46310.6	554.73
Giant panda (*Ailuropoda melanoleuca*)	Ursidae	1	AME	T[b]	58210.6	380.05
Marine otter (*Lontra felina*)	Mustelidae	1	LFE	ST[b]	0	123.80
River otter (*Lutra lutra*)	Mustelidae	1	LLU	ST[b]	0	140.26
European badger (*Meles meles*)	Mustelidae	1	MME	T[b]	0	175.81
Long-tailed weasel (*Mustela frenata*)	Mustelidae	2	MFR	T[a]	2.8	61.28
Sea otter (*Enhydra lutris*)	Mustelidae	2	ELU	SA[a]	0	196.23
Wolverine (*Gulo gulo*)	Mustelidae	2	GGU	T[a]	4180.2	208.26
North American River Otter (*Lontra canadensis*)	Mustelidae	2	LCA	ST[a]	46.6	138.84
North American badger (*Taxidea taxus*)	Mustelidae	2	TTA	T[a]	0	155.99
Fisher (*Martes pennanti*)	Mustelidae	2	MPE	T[b]	604.2	158.03
American marten (*Martes americana*)	Mustelidae	2	MAM	T[b]	25.6	101.04
Striped skunk (*Mephitis mephitis*)	Mephitidae	2	MMT	T[a]	569.9	102.99
Hog nosed skunk (*Conepatus leuconotus*)	Mephitidae	1	CLE	T[b]	0	94.75
Red panda (*Ailurus fulgens*)	Ailuridae	1	AFU	T[b]	2188.0	154.94

Ecology indicated as terrestrial (T), semiterrestrial (ST), semiaquatic (SA). Species Codes are utilized in all subsequent figures
[a]Ecology obtained from sources used by Van Valkenburgh et al. (2010), however, "Aquatic" is changed to "Semiaquatic" in this article because these species show limited terrestrial behavior, unlike cetaceans, which are obligate aquatic organisms.
[b]Obtained from sources used by Samuels et al. (2013). Fossorial, scansorial, and arboreal species were designated as terrestrial for this study.

arctoid species that range in body size, ecology, and diet. If frontal sinuses form in areas where bone is not mechanically necessary, we expect to observe a strong relationship between frontal sinus size and skull size and shape. We expect to see proportionally larger frontal sinuses in species with domed frontal bones and proportionally smaller frontal sinuses in species with flat dorsal profiles. Based on this, reduced or absent frontal sinuses should characterize semiterrestrial and semiaquatic species, which, as previously mentioned, have flat skull roofs and large eyes that may limit space for pneumatization, relative to terrestrial species that often have more doming of the frontal.

We use CT-technology and specialized visualization software to visualize and quantify sinus morphology, and use three-dimensional landmark-based geometric morphometrics to quantify skull size and shape. CT-technology allows us to noninvasively examine skulls for the presence of frontal sinuses, and will allow us to apply our methods to fossil species in future studies. Three-dimensional geometric morphometrics was used rather than traditional linear morphometrics because the former highlights changes in the relative position of anatomical structures (Zelditch et al., 2004; Klingenberg, 2011). In addition, three-dimensional CT-data removes the need to correct for parallax encountered when using two-dimensional methods (Zelditch et al., 2004). We also explore the effect of nonindependence among species due to shared ancestry on the relationship between sinus morphology and skull morphology using phylogenetic generalized least squares (PGLS) (Martins and Hansen, 1997).

MATERIALS AND METHODS

Comparative Sample

The sample includes 39 skulls from 23 species representing six families of arctoid carnivorans and spans the range of body size and ecology observed in extant arctoids (Table 1 and Supporting Information Table S1). Whenever possible, we sampled one adult wild-caught male and female per species, with adult age determined by fusion of the basioccipital-basisphenoid suture. Although our intraspecific sampling is small and certainly does not encompass the full range of intraspecific variation, it should be sufficient for documenting interspecific differences in sinus morphology among terrestrial, semiterrestrial, and semiaquatic species. Sample size was mostly limited by the time required to process CT-scans, build volumetric models, and quantify size and shape. Species were classified as terrestrial, semiterrestrial, or semiaquatic as defined above based on the literature (Table 1). Skulls were scanned at the University of Texas High-Resolution CT-scanning facilities (http://www.ctlab.geo.utexas.edu/), the UCLA Crump Preclinical Imaging Technology Center (http://www.crump.ucla.edu/tech.aspx), or at the UCLA School of Dentistry with slice numbers ranging from 292 to 1,200 slices per skull. All scans done at the University of Texas facilities are freely available at http://www.digimorph.org, and all scans done at the UCLA Crump Center are available through A. Curtis.

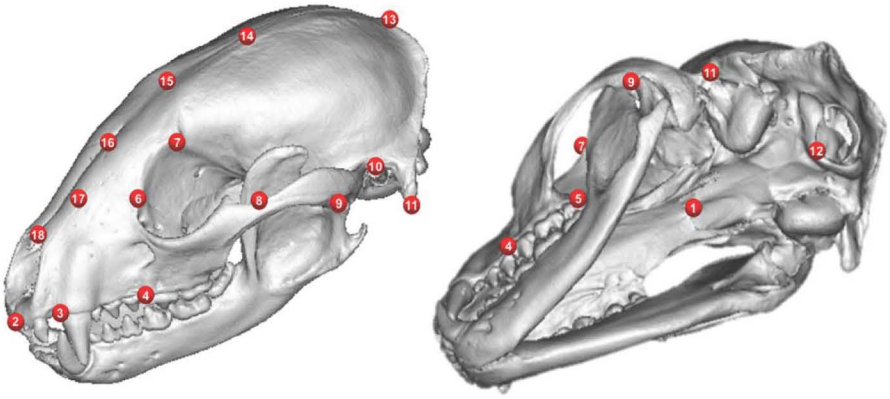

Fig. 2. Landmarks used to calculate skull size and for the 3-dimensional geometric morphometric analysis. Descriptions of landmarks given in Table 2.

Unknown prior to scanning, all individuals in our sample of skunk species (*Mephitis mephitis, Conepatus leuconotus*) showed evidence of nematode infection. The external shape of their skull did not appear to be strongly affected by this pathology, so these specimens are included in our analyses with caution.

Morphometrics

CT-scans for each skull were examined for the presence of frontal sinuses. Frontal sinuses were identified as any pneumatization between the outer and inner tables of the frontal bone with an ostium connecting to the nasal chamber posterior to the turbinal bones. For species with frontal sinuses, we used Amira (Visage Imaging) and Mimics (Materialise) visualization software to generate volumetric models of frontal sinuses and estimate total sinus volume, that is, the summed volume of left and right sinuses (Table 1). Despite using two different visualization software packages, measurement error between programs was similar to measurement error using only one program (less than 0.35%).

To quantify skull size and shape, we selected 18 landmarks (Fig. 2 and Table 2) that best distinguish shape variation among arctoids related to body size, diet and ecology [e.g., proportions of the rostrum and braincase, dorsal profile, position and size of ears, eyes, and nares [apertura nasi ossea]; Uhen, 2007; Reidenberg, 2007) and used MorphoJ to conduct a three-dimensional geometric morphometric analysis of skull shape (Klingenberg, 2011). Landmarks were placed on the left side of each skull. Specimens were scaled, rotated and aligned by their centroids using a Procrustes fit, and centroid size was calculated as a proxy for skull size (Zelditch et al., 2004). Species means were computed for Procrustes coordinates and centroid size for use in subsequent analyses (Klingenberg, 2011). All morphometric data were collected by Lai with an estimated measurement error of less than 0.35%, which was estimated by reconstructing the left sinus of *Ailurus fulgens* five times *de novo* and computing percentage error for volume.

Statistical Analyses

To quantify variation in skull shape among arctoids, a principle components analysis (PCA) was performed on the covariance matrix generated from Procrustes-fitted landmark data (Klingenberg, 2011). Because pinnipeds are highly specialized for semiaquatic behavior, we conducted a second PCA excluding pinnipeds to better visualize how skull shape relates to sinus morphology among the less-derived, more terrestrial species in our sample. We regressed significant PC's against skull centroid size to test for relationships between skull shape and skull size.

To examine the relationship between frontal sinus size, skull size, and ecology, Log_{10}-transformed values of sinus volume were plotted against Log_{10}-transformed values of skull centroid size. To account for phylogenetic nonindependence among species, we constructed a phylogeny (Fig. 1) by trimming taxa from a previously published arctoid phylogeny (Slater et al., 2012). Using this phylogenetic framework for our analyses, we then applied PGLS regression using the caper package in R (R Core Team, 2012). Because semiterrestrial and semiaquatic behavior are derived conditions in our sample, we conducted a regression analysis for our terrestrial sample only to establish the hypothesized ancestral relationship between frontal sinus size and skull size against which we could compare relative sinus size in our aquatic sample. All regression analyses were conducted using R (R Core Team, 2012).

TABLE 2. Descriptions of landmarks used to calculate skull shape and centroid size

Landmark	Description
1	Posterior margin of palatine along midsagittal line
2	Anterior margin of incisive along midsagittal line
3	Anterior border of canine alveolus
4	Anterior border or carnassial alveolus
5	Posterolateral border of the last cheek tooth
6	Intersection of frontal, lacrimal, and maxilla
7	Postorbital process of the frontal
8	Anterior extension of the squamosal on the zygomatic arch
9	Posterior most point of the jugal on the zygomatic arch
10	Dorsal border of the external auditory meatus
11	Ventral most extension of the mastoid process
12	Ventral midsagittal border of the foramen magnum
13	Most posterior point on the sagittal crest
14	Frontoparietal suture on skull midline
15	Midpoint between landmarks 14 and 15
16	Most posterior extension of nasal along midsagittal line
17	Intersection of nasal, incisive and maxilla
18	Anterior most extension of the nasals along the midsagittal line

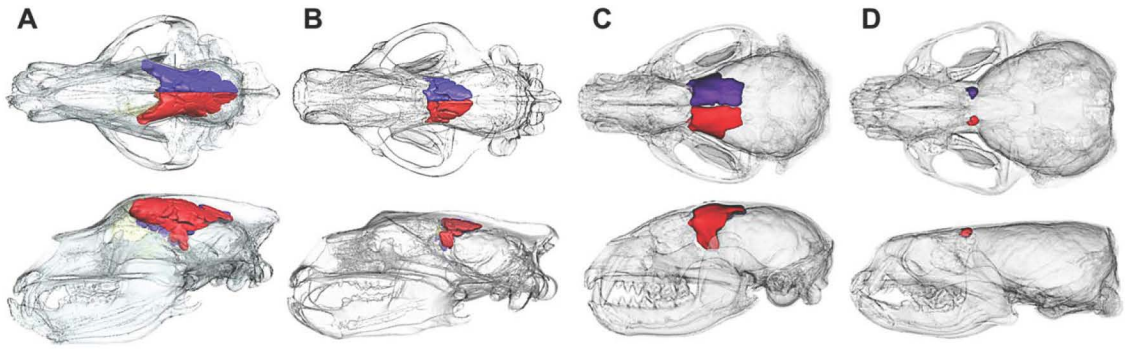

Fig. 3. Frontal sinus variation among arctoid species showing the large, posteriorly extended sinuses typical of terrestrial ursids (**A**: *Ursus arctos*) versus the reduced sinuses in the semi-terrestrial polar bear (**B**: *Ursus maritimus*), typical sinus shape for medium-sized arctoids (**C**: *Procyon lotor*), and reduced sinuses typical of semiterrestrial mustelids and the smallest species in our sample (**D**: *Lontra canadensis*). Left sinuses colored red, right sinuses colored purple.

RESULTS

Sinus Size and Skull Size

There was considerable variation in the size and presence of frontal sinuses in our sample that was not well explained by phylogeny (Fig. 3). In terrestrial species with frontal sinuses, frontal sinus size was significantly related to skull centroid size and scaled with positive allometry for both our analysis on raw data and our PGLS analysis (Fig. 4 and Table 3), indicating that larger species have proportionally larger than predicted frontal sinuses given a null expectation of isometry (slope = 3). This suggests that frontal sinus volume is related to space available for pneumatization in species where frontal sinuses can form. The fact that the smaller terrestrial species in our sample, the long-tailed weasel (*Mustela frenata*) and American marten (*Martes americana*) had relatively reduced frontal sinuses for their size suggests that there may be a lower limit on the size of a skull in which frontal sinuses can form for a given skull shape.

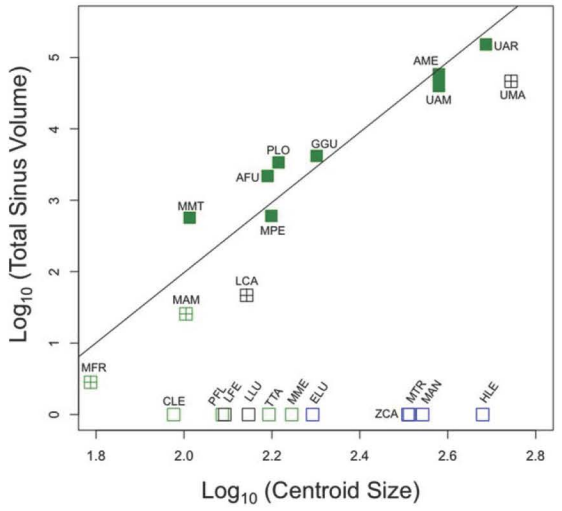

Fig. 4. Plot of species means for Log_{10} total frontal sinus volume (TSV) against Log_{10} skull centroid size (CS) showing regression line for terrestrial species. Species without sinuses plotted at zero to illustrate the range of skull sizes that lack sinuses. Ecology represented by color: terrestrial (green), semiterrestrial (black), semiaquatic (blue). Sinus morphology shown as: present (■), reduced (+), absent (□). Species abbreviated as in Table 1. Regression statistics given in Table 3.

Sinus Size and Ecology

As expected, based on the observations of Paulli (1900), none of the four semiaquatic species (three pinnipeds, one mustelid) had frontal sinuses. In addition, four semiterrestrial species (one ursid, three mustelids) had absent or reduced frontal sinuses relative to the frontal sinuses in similarly sized terrestrial species. Among the 14 terrestrial species, 10 (one procyonid, one ailurid, one mephitid, three ursids, four mustelids) had frontal sinuses and four did not (one procyonid, one mephitid, and two mustelids). We observed a convergent lack of frontal sinuses in fossorial American and European badgers, and a loss of frontal sinuses in the arboreal and nocturnal kinkajou (*Potos flavus*).

Patterns in Skull Shape Variation

The first five principle components (PCs) from the PCA including all samples accounted for 73.5% of total skull shape variation among species

TABLE 3. Summary statistics for Log_{10}/Log_{10} GLS and PGLS regressions of species means for total sinus volume against skull centroid size, where b = slope, and a = y-intercept, SE_b = standard error of the slope, SE_a = standard error of the y-intercept, r^2 = correlation coefficient

Analysis	DF	$b \pm SE_b$	$a \pm SE_a$	r^2	P
GSL	8	4.91 ± 0.52	−7.84 ± 1.19	0.92	<0.0001
PGLS	8	5.83 ± 0.52	−9.80 ± 1.23	0.94	<0.0001

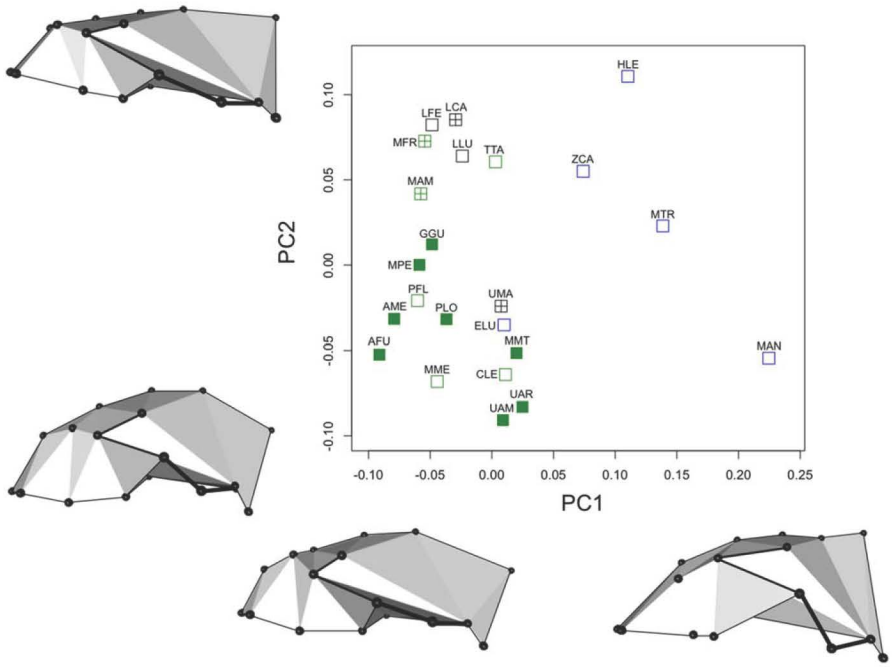

Fig. 5. PCA of arctoid skull shape with wireframe representations of shape variation along each axis. PC1 explains 25.84% and PC2 explains 16.67% of the variation in skull shape. PC1 is positively correlated with skull size and snout length (Supporting Information Fig. S1); PC2 is positively correlated with dorsal flattening. Species coded as in Table 1. Ecology and sinus size coded as in Figure 1.

(the remaining PCs each accounted for less than 5%). We chose to focus on PC1 and PC2, which together accounted for 43.5% of total shape variation, because they best explained disparity in skull shape associated with skull size and ecological groups. Variation along PC1 (25.8% of total shape variation) separated highly derived pinnipeds from the rest of our sample (Fig. 5). It was also positively related to skull size ($r^2 = 0.29$, $P < 0.01$), but this relationship is driven by large pinnipeds plotting positively along PC1 and was not significant when phylogenetic nonindependence was taken into account (Supporting Information Fig. S1A). PC2 (16.7% of total variation in skull shape) separated mostly terrestrial species with domed profiles (negative PC2 values) from semiterrestrial and semiaquatic species, except the sea otter, with large, dorsally positioned orbits, posterodorsally positioned external nares and flattened skull roofs (positive PC2 values; Fig. 5), and was not correlated with skull size (Supporting Information Fig. S1B). Notably, three of the four terrestrial species with reduced or absent frontal sinuses (*Taxidea taxus, Mustela frenata*, and *Martes americana*) had somewhat positive values on PC2 and were clustered with the semiaquatic and semiterrestrial species (Fig. 5).

Results from our PCA that excluded pinnipeds distinguished species with reduced or absent frontal sinuses from species with unreduced frontal sinuses (Fig. 6). PC1, which accounted for 25.9% of total shape variation, was negatively related to skull size, an association that was significant even after accounting for phylogenetic nonindependence (see Supporting Information Fig. S1C). Species with dorsally shifted orbits, flat skull roofs, and short snouts that are slightly upturned relative to the basicranium plotted positively and species with domed skull roofs and longer, more downturned snouts plotted negatively along PC1. Species with reduced or absent frontal sinuses had slightly more positive values along this axis. PC2 (19.7% of total shape variation) differentiated species with large external nares, flattened dorsal profiles, and short snouts (positive values) from species with smaller nares, domed skull profiles, and long snouts (negative values), and was not related to skull size (Supporting Information Fig. S1D). This PC distinguished the bamboo-feeding giant and lesser pandas, both with quite negative values, from the rest of the arctoids. However, species with reduced or absent frontal sinuses had more positive values along PC2 than other arctoids in our sample. The remaining PCs were not

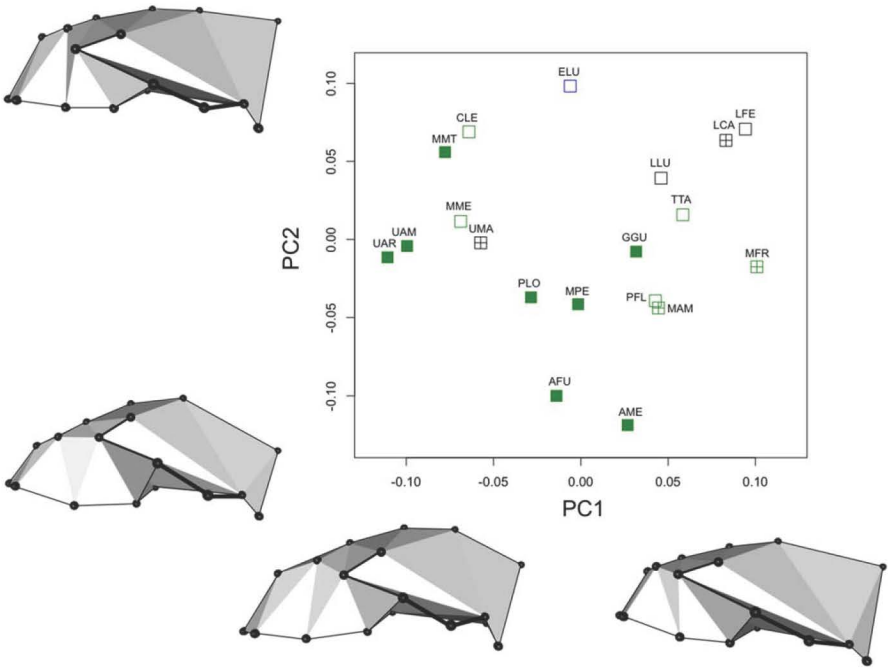

Fig. 6. PCA of arctoid skull shape with pinnipeds omitted. PC1 explains 25.89% and PC2 explains 19.70% of the variation in skull shape. Species coded as in Table 1. Ecology and sinus size coded as in Figure 1.

informative concerning disparity in skull shape related to ecology or frontal sinus morphology.

DISCUSSION

In Arctoidea, skull shape disparity is related to skull size, ecology, and diet, all of which are also related to frontal sinus morphology. Species with the largest skulls tended to have the largest frontal sinuses. In our terrestrial sample, larger skulls tended to exhibit greater doming of the frontal bone, whereas smaller species were characterized by flatter skull roofs. This allometry in skull shape may explain the positive allometry of frontal sinus size with skull size. Doming the frontal increases its relative size, and thus provides a larger space for pneumatization. In addition, a domed frontal is intrinsically stronger than a flat skull roof (Tseng and Wang, 2010), which may make it possible for a proportionally greater amount of bone to be removed in larger species.

Among the largest terrestrial species in our sample, the giant panda (*Ailuropoda melanoleuca*) had frontal sinuses that were similar in size to those of the grizzly bear (*Ursus arctos*), but those of the giant panda were confined closer to the midsagittal plane, creating a sagittal crest that is triangular in cross section, similar to that of bone cracking hyenas (*Crocuta crocuta, Parahyaena brunnea, Hyaena hyaena*; Fig. 7). Previous studies have highlighted the convergence in skull shape between durophagous herbivores (giant panda and red panda) and durophagous carnivores (extinct borophagine canids and all bone-cracking hyaenids; Figueirido et al., 2013). In hyenas, caudally elongated frontal sinuses are associated with enlarged bone cracking premolars, and facilitate more even dissipation of stress across the skull. Green bamboo is a very hard substance, similar in material properties to bone (Figueirido et al., 2013), so it appears that caudally elongated and medially positioned frontal sinuses in combination with a domed frontal bone are also an adaptation for herbivorous durophagy. We did not observe the same caudal elongation of the frontal sinuses in the lesser panda, which is a much smaller animal than the giant panda.

Interestingly, the giant panda's left and right frontal sinuses were relatively symmetrical in size and shape, whereas those of bone cracking hyenas were found to be asymmetrical. Curtis and Van Valkenburgh (in press) observed that in spotted, brown, and striped hyenas, the left frontal sinus is larger and pneumatizes farther posterior in the skull relative to the right, but the overall space pneumatized within the skull was symmetrical in shape.

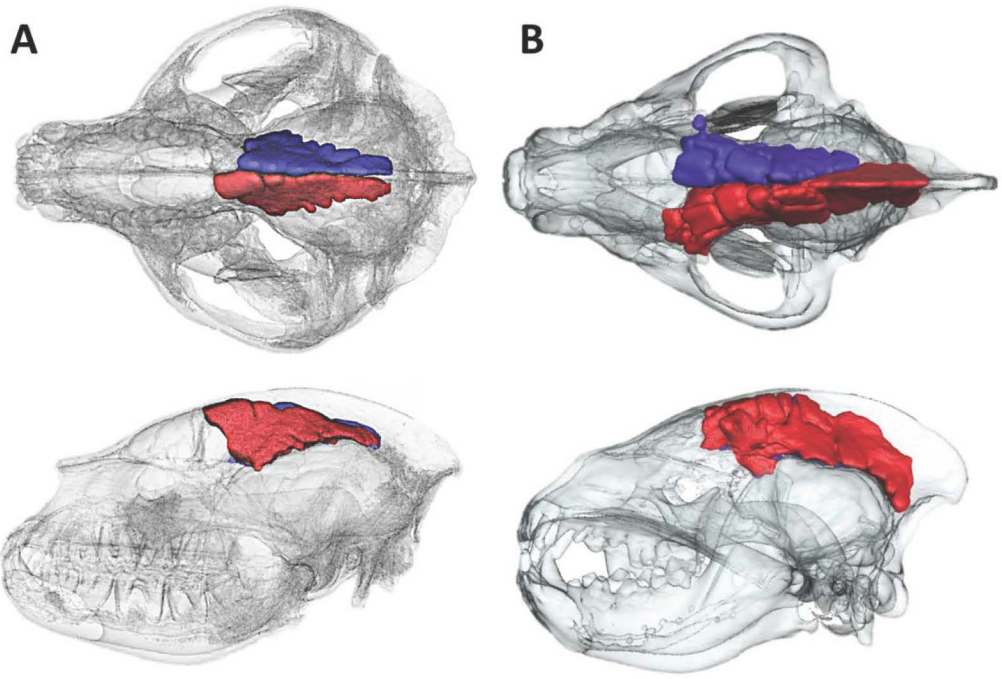

Fig. 7. Dorsal and lateral views of frontal sinus morphology in *Ailuropoda melanoleuca* (**A**) and the similarity with the sinuses of bone-cracking hyaenas as represented by *Crocuta crocuta* (**B**). Left sinuses in red, right sinuses in purple. Note the asymmetry in how far posterior the left versus right frontal sinuse of *C. crocuta* pneumatizes versus the left and right sinuses of *A. melanoleuca*, which pneumatizes a similar distance posteriorly.

The association between large skull size and an expanded frontal sinus is not apparent within our sample of semiterrestrial and semiaquatic arctoids that range in size from river otter to elephant seal. All 10 of these species have either reduced or absent frontal sinuses relative to terrestrial species with frontal sinuses. Notably, terrestrial mammals evolved some degree of secondarily aquatic behavior at least seven times in different lineages including cetaceans, desmostylians, sirenians, pinnipeds, ursids, mustelids, and even a group of extinct ground sloths (nothrotheres; Uhen, 2007). The shift from a terrestrial to an aquatic existence selects for a number of common physiological and morphological adaptations that relate to issues such as underwater sensory perception, buoyancy, increasing and variable atmospheric pressure, and streamlining, especially for more derived species. Our study of semiaquatic and semiterrestrial carnivorans suggests that frontal sinus reduction is one of these adaptations. However, it is not clear that this is due to the need to mitigate the negative effects of pressure when diving, as has been suggested for highly aquatic, deep-diving species (Reidenberg and Laitman, 2008). There is considerable variation among our 10 species in their typical and maximum dive depths (Table 4), ranging from relatively shallow divers including polar bears that often dive under sea ice (Stirling, 2011) to pinnipeds that reach extreme depths such as *Mirounga angustirostris* (Debey, 2013). *Lontra canadensis* can dive to a maximum of around 20 m and is the deepest diving species that still retains frontal sinuses. However, we do not know what the actual threshold of atmospheric pressure is that would result in the fracture of a bone containing a sinus, so we do not interpret these data as reflecting this limit. An alternative explanation for the reduction in frontal sinus size in these more shallow divers might be changes in skull shape that enhance underwater foraging and/or surface foraging, such as enlarged eyes, dorsally positioned nose and ears, and a flattened dorsal profile.

For example, polar bears have reduced frontal sinuses relative to their terrestrial sister taxon, brown bears, and differ markedly from the latter in cranial shape. Polar bears have a flattened dorsal profile as opposed to the much more domed profile of brown bears, and the orbits of polar bears have a more dorsal position (Slater et al., 2010). As a result of the flat dorsal profile and elevated orbits, which are presumably advantageous for a surreptitious aquatic approach on prey (Stirling, 2011), the frontal presents minimal space for frontal sinus development. Fossorial species also show flattened dorsal profiles, which is an adaptation for digging with the snout and ease of

TABLE 4. Maximum diving depths for semiterrestrial and semiaquatic species in our sample obtained from the literature, where + indicates presence of frontal sinuses and − indicates absence of frontal sinuses

Species	Max Diving Depth (m)	Sinus	Source
Ursus maritimus	<10	+	Stirling (2011)[a]
Lutra lutra	14	−	Nolet and Kruuk (1989)
Lontra canadensis	<20	+	Lariviére and Walton (1998)
Lontra felina	30–40	−	Castilla and Bahamondes (1979)
Enhydra lutra	<100	−	Debey (2013)
Hudrurga leptonyx	424.5	−	Sources in Debey (2013)
Zalophus californianus	482	−	Sources in Debey (2013)
Monachus schauinslandi	500	−	Sources in Debey (2013)
Mirounga angustirostris	1389.5	−	Sources in Debey (2013)

[a]Based on estimates of sea ice depth.

locomotion within burrows (Samuels and Van Valkenburgh, 2009). In our sample, the fossorial American and European badgers, exhibited a dorsal flattening of the skull, and both these species independently lost their frontal sinuses, suggesting, again, that a flattened dorsal profile limits space where pneumatization can occur.

Two other species in our sample lacked frontal sinuses, the kinkajou (*Potos flavus)* and the hog-nosed skunk (*Conepatus leuconotus*), and neither is semiterrestrial or semiaquatic. In the case of the kinkajou, it appears that an unusual skull shape may explain the absence of frontal sinuses. In this case, it is not a flat skull but instead one that has been highly modified for nocturnal foraging for fruits, including the hard drupes of palm trees (Kays, 1999). Kinkajous are convergent with primates in having very large, forward facing eyes that, in combination with adaptations for herbivory, such as a brachycephalic snout, robust and anteriorly oriented zygomatic arches, and short neurocranium, may limit the space available for frontal sinuses to form (Ford and Hoffmann, 1988; Figueirido et al., 2010). The absent frontal sinuses of the hog-nosed skunk are not as easily explained. Their skulls are similar in size and shape to that of the striped skunk, a species that has well-developed frontal sinuses. Exceptions such as this make it clear that there are other factors affecting frontal sinus form that we have yet to discover.

All individuals from both species of skunk in our sample showed evidence of infection by nematodes in their nasal cavities that caused perforations in the dorsal side of the frontal bone. Given the size and shape of hog-nosed skunk skulls and the juxtaposition of the fronto/ethmoturbinals relative to the braincase, noninfected individuals probably do not have frontal sinuses, or may have very reduced frontal sinuses like the long-tailed weasel. The frontal sinuses of the striped skunk did not appear to be greatly affected by the nematodes, as they were comparable in size to the frontal sinuses of other similarly sized terrestrial species (Fig. 4).

Although we found evidence that water pressure is not the only factor that selects against maintenance of frontal sinuses, it may explain why semiaquatic species, such as sea otters and pinnipeds have a significant amount of spongy bone occupying the space between the inner and outer tables of the frontal bone, which was observed grossly in CT-scans. Terrestrial species that lack frontal sinuses, such as the American and European badgers have frontal bones with very little space between the outer and inner tables that is filled with a minimal amount of spongy bone. In studies of terrestrial species, spongy bone between the outer and inner tables of the frontal bone is what is removed by the pneumatic epithelium as a sinus develops (Cave, 1967). Perhaps the presence of spongy bone between the outer and inner tables of the frontal in semiaquatic arctoids does enhance rigidity and is an adaptation for mitigating increased pressures due to deep diving. Filling the frontal bone with cancellous bone, which is less dense and presumably less costly to maintain than compact bone, might be an efficient way to avoid having hollow air spaces, especially for species that dive the deepest. In addition, it might increase skull density and be a response to overall selection for a heavier skeleton such as been found in the postcranial skeletons of some semiaquatic and aquatic mammals (Wall, 1983). In these species, a greater density is achieved by having cancellous bone fill the marrow cavities of their long bones (Wall, 1983).

Our study suggests that skull shape changes associated with aquatic habits may be the initial factor that limits frontal sinus development in aquatic arctoid species. Having reduced or absent frontal sinuses as a consequence of a more flattened dorsal profile that allows only the eyes to protrude above the water surface may be an exaptation for deeper diving. It is also clear that a durophagous diet can result in expanded frontal sinuses as was demonstrated by the giant panda in our sample, and the hyenas and borophagine canids in previous work. Our data also suggest that among terrestrial species, frontal sinus size is likely to increase positively with overall skull size. Moreover, frontal sinus size may be constrained at

TABLE 5. Factors associated with frontal size in Carnivora

	Frontal sinus present at moderate to large size	Frontal sinus reduced or absent
Skull size	Large	Very small
Skull shape	Domed	Flattened
Orbit size and orientation	Small or average, frontolaterally positioned	Enlarged, dorsally or frontally positioned
Habitat	Terrestrial	Semiaquatic, semiterrestrial, fossorial
Diet	Durophagous	Not durophagous

Note that the association between skull size and frontal sinus size is not consistent across the order, and is highly dependent on ecology-related changes in skull shape

very small skull sizes as suggested here by the long-tailed weasel. However, exceptions are apparent (e.g., striped skunk, which has sinuses, versus spotted skunk that does not have sinuses, despite being similar in size) and make it difficult to readily predict the relative size and shape of frontal sinuses in smaller species, especially because frontal sinus morphology appears to be dependent on factors other than skull size and shape in some cases [e.g., patterns of skull development and ossification, as may be the case in some canid species (Curtis and Van Valkenburgh, in press)].

Overall, our results support the hypothesis that when present, frontal sinuses fill space where bone is not mechanically necessary, and that their morphology can be modified to aid in skull function, which we summarize in Table 5. They tend to be relatively larger in large-bodied terrestrial carnivorans, suggesting that they evolved as a response to selection for mass reduction, and become extremely large in species with domed skulls that are modified for a durophagous diet. However, frontal sinuses are reduced or absent among semiaquatic and semiterrestrial carnivorans, whether large or small, and this may reflect multiple factors, such as the presence of enlarged orbits in association with a flattened dorsal profile and in some cases, selection for reduced buoyancy and/or enhanced cranial strength due to diving. Among terrestrial carnivorans, enlarged orbits are also associated with frontal sinus reduction, as are skulls with dorsally flattened profiles. Thus it appears that skull shape plays a major role in carnivoran frontal sinus size and it will be interesting to extend our analysis of frontal sinus to other morphologically and behaviorally diverse groups of mammals, such as bats and rodents.

ACKNOWLEDGMENTS

The authors thank M. Colbert, R. Ketcham, and J. Maisano of the University of Texas HRCT Digital Morphology group, W. Ladno at the UCLA Crump Preclinical Imaging Technology Center, and S. Tetradis in the UCLA School of Dentistry for their dedication and skills in producing the CT scans, and the multiple curators and collection managers that allowed us to borrow skulls for scanning. The authors are grateful to D. Bird, A.R. Friscia, M. Balisi, and J. Wolf for helpful discussions and comments on the manuscript, and the paper was much improved by the comments of two anonymous reviewers.

LITERATURE CITED

Blaney SPA. 1990. Why paranasal sinuses? J Laryngol Otolog 104:690–693.

Blanton PL, Biggs NL. 1969. Eighteen hundred years of controversy: The paranasal sinuses. Am J Anat 124:135–147.

Castilla JC, Bahamondes I. 1979. Observaciones conductuales y ecológias sobre *Lutra felina* (Molina) 1792 (Carnivora: Mustelidae) en las zonas central y contro-norte de Chile. Arch Biol Med Exp (Santiago) 12:119–132.

Cave AJ. 1967. Observations on the platyrrhine nasal fossa. Am J Phys Anthropol 26:277–288.

Curtis A, Van Valkenburgh B. 2014. Beyond the sniffer: frontal sinuses in Carnivora. Anat Rec 297.

Davis DD. 1964. The giant panda: a morphological study of evolutionary mechanisms. Fieldiana 3:1–339.

Debey LB. 2013. Osteological correlates and phylogenetic analysis of deep diving in living and extinct pinnipeds: What good are big eyes? Mar Mamm Sci 29:48–83.

Edinger T. 1950. Frontal sinus evolution particularly in the Equidae. Bull Mus Comp Zool, Harvard 103:409–496.

Farke AA. 2007. Morphology, constraints, and scaling of frontal sinuses in the hartebeest, *Alcelaphus buselaphus* (Mammalia: Artiodactyla, Bovidae). J Morphol 268:243–253.

Farke AA. 2008. Frontal sinuses and head-butting in goats: a finite element analysis. J Exp Biol 211:3085–3094.

Farke AA. 2010. Evolution and functional morphology of the frontal sinuses in Bovidae (Mammalia: Artiodactyla), and implications for the evolution of cranial pneumaticity. Zool J Linnean Soc 159:988–1014.

Ferretti MP. 2007. Evolution of bone-cracking adaptations in hyaenids (Mammalia, Carnivora). Swiss J Geosci 100:41–52.

Figueirido B, Tseng ZJ, Martín-Serra A. 2013. Skull shape evolution in durophagous carnivorans. Evolution 67:1975–1993.

Figueirido B, Serrano-Alarcón FJ, Slater GJ, Palmqvist P. 2010. Shape at the cross-roads: homoplasy and history in the evolution of the carnivoran skull towards herbivory. J Evol Biol 23:2579–2594.

Ford LS, Hoffmann RS. 1988. Potos flavus. Mamm Species 321: 1–9.

Joeckel RM. 1998. Unique frontal sinuses in fossil and living Hyaenidae (Mammalia, Carnivora): description and interpretation. J Vertebr Paleontol 18:627–639.

Kays RW. 1999. Food preferences of kinkajous (*Potos flavus*): A frugivorous carnivore. J Mamal 80:589–599.

Keir J. 2009. Why do we have paranasal sinuses? J Laryngol Otol 123:4–8.

Klingenberg CP. 2011. MORPHOJ: an integrated software package for geometric morphometrics. Molec Ecol Res 11:353–356.

Larivière, S. and L.R. Walton. 1998. *Lontra canadensis*. Mamm Species 587:1–8.

Márquez S. 2008. The paranasal sinuses: The last frontier in craniofacial biology. Anat Rec 291:1350–1361.

Martins EP, Hansen TF. 1997. Phylogenies and the comparative method: A general approach to incorporating phylogenetic information into the analysis of interspecific data. Am Nat 149:646–667.

Nolet BA, Kruuk H. 1989. Grooming and resting of otters *Lutra lutra* in a marine habitat. J Zool 218:433–440.

Paulli S. 1900. Über die pneumaticität bei den säugerthieren. Ein morphologische studie. III. Über die Morphologie des siebbens ud die der pneumaticität bei den Insectivoren, Hyracoideen, Chiropteren, Carnivoren, Pinnipedien, Edentaten, Rodentiern, Prosimiern und Primaten. Gegenbaurs Morphol Jahrb 28:179–251.

R Core Team. 2012. R: A language and environment for statistical computing, Vienna, Austria: R Foundation for Statistical Computing.

Reidenberg JS. 2007. Anatomical adaptations of aquatic mammals. Anat Rec 290:507–513.

Reindenberg J, Laitman JT. 2008. Sisters of the sinuses: cetacean air sacs. Anat Rec 291:1389–1396.

Rossie JB. 2008. The phylogenetic significance of anthropoid paranasal sinuses. Anat Rec 291:1485–1498.

Samuels JX, Van Valkenburgh B. 2009. Craniodental adaptations for digging in extinct burrowing beavers. J Vertebr Paleontol 29:254–268.

Samuels JX, Meachen JA, Sakai SA. 2013. Postcranial morphology and the locomotor habits of living and extinct carnivores. J Morphol 274:121–146.

Slater GJ, Harmon LJ, Alfaro ME. 2012. Integrating fossils with molecular phlyogenies improves inference of trait evolution. Evolution 66:3931–3944.

Slater GJ, B, Louis L, Yang P, Van Valkenburgh B. 2010. Biomechanical consequences of rapid evolution in the polar bear lineage. PLoS ONE 11:e13870, doi: 10.1371/journal.pone.0013870.

Smith TD, Rossie JB, Cooper GM, Mooney MP, Siegel MI. 2005. Secondary Pneumatization of the maxillary sinus in callitrichid primates: Insights from immunohistochemistry and bone cell distribution. Anat Rec A 285A:677–689.

Smith TD, Rossie JB, Docherty BA, Cooper GM, Bonar CJ, Silverio AL, Burrows AM. 2008. Fate of the nasal capsular cartilages in prenatal and perinatal tamarins (*Saguinus geoffroyi*) and extent of secondary pneumatization of maxillary and frontal sinuses. Anat Rec 291:1397–1413.

Stirling I. 2011. Polar Bears: The Natural History of a Threatened Species. Brighton: Fitzhenry and Whiteside. 334 p.

Tanner JB, Dumont ER, Sakai ST, Lundrigan BL, Holekamp KE. 2008. Of arcs and vaults: the biomechanics of bone-cracking in spotted hyenas (*Crocuta crocuta*). Biol J Linnean Soc 95:246–255.

Tseng ZJ. 2009. Cranial function in a late Miocene *Dinocrocuta gigantea* (Mammalia: Carnivora) revealed by comparative finite element analysis. Biol J Linnean Soc 96:51–67.

Tseng ZJ, Wang X. 2010. Cranial functional morphology of fossil dogs and adaptation for durophagy in *Borophagus* and *Epicyon* (Carnivora, Mammalia). J Morphol 271:1386–1398.

Uhen MD. 2007. Evolution of marine mammals: Back to the sea after 300 million years. Anat Rec 290:514–522.

Van Valkenburgh B, Curtis A, Samuels JX, Bird D, Fulkerson B, Meachen-Samuels J, Slater GJ. 2010. Aquatic adaptations in the nose of carnivorans: evidence from the turbinates. J Anat 218:298–310.

Wall WP. 1983. The correlation between high limb-bone density and aquatic habits in recent mammals. J Paleontol B:197–207.

Wang RG, Jiang SC, Gu R. 1994. The cartilaginous nasal capsule and embryonic development of human paranasal sinuses. Journal of otolaryngology. 23:239–243.

Wang X, Tedford RH, Taylor BE. 1999. Phylogenetic systematics of the Borophaginae (Carnivora, Canidae). Bull Am Mus Nat Hist 243:1–391.

Werdelin L. 1989. Constraint and adaptation in the bone-cracking canid *Osteoborus* (Mammalia: Canidae). Paleobiology 15:387–401.

Witmer LM. 1997. The evolution of the antorbital cavity of archosaurs: A study in soft-tissue reconstruction in the fossil record with an analysis of the function of pneumaticity. J Vertebr Paleontol 17:1–77.

Zelditch ML, Swiderski DL, Sheets HD, Fink WL. 2004. Geometric Morphometrics for Biologists: A Primer. New York: Elsevier Academic Press. 437 p.

Zollikofer CPE, Ponce de León MS, Schmitz RW, Stringer CB. 2008. New insights into Mid-Late Pleistocene fossil hominin paranasal sinus morphology. Anat Rec 291:1506–1516.

Zollikofer CPE, Weissmann JD. 2008. A morphogenetic model of cranial pneumatization based on the invasive tissue hypothesis. Anat Rec 291:1446–1454.

Supporting Information

Figure S2-1. A: PC1 from figure 5 plotted against Log_{10} centroid size (OLS: $r^2 = 0.26$, P = 0.01, PGLS: Not significant), B: PC2 from figure 5 plotted against Log_{10} centroid size (OLS: Not significant, PGLS: Not significant). C: PC1 from figure 6 plotted against Log_{10} centroid size (OLS: $r^2 = 0.28$, P < 0.05, PGLS: $r^2 = 0.54$, P = 0.01), D: PC2 from figure 6 plotted against Log_{10} centroid size (r^2 = Not significant, PGLS: Not significant).

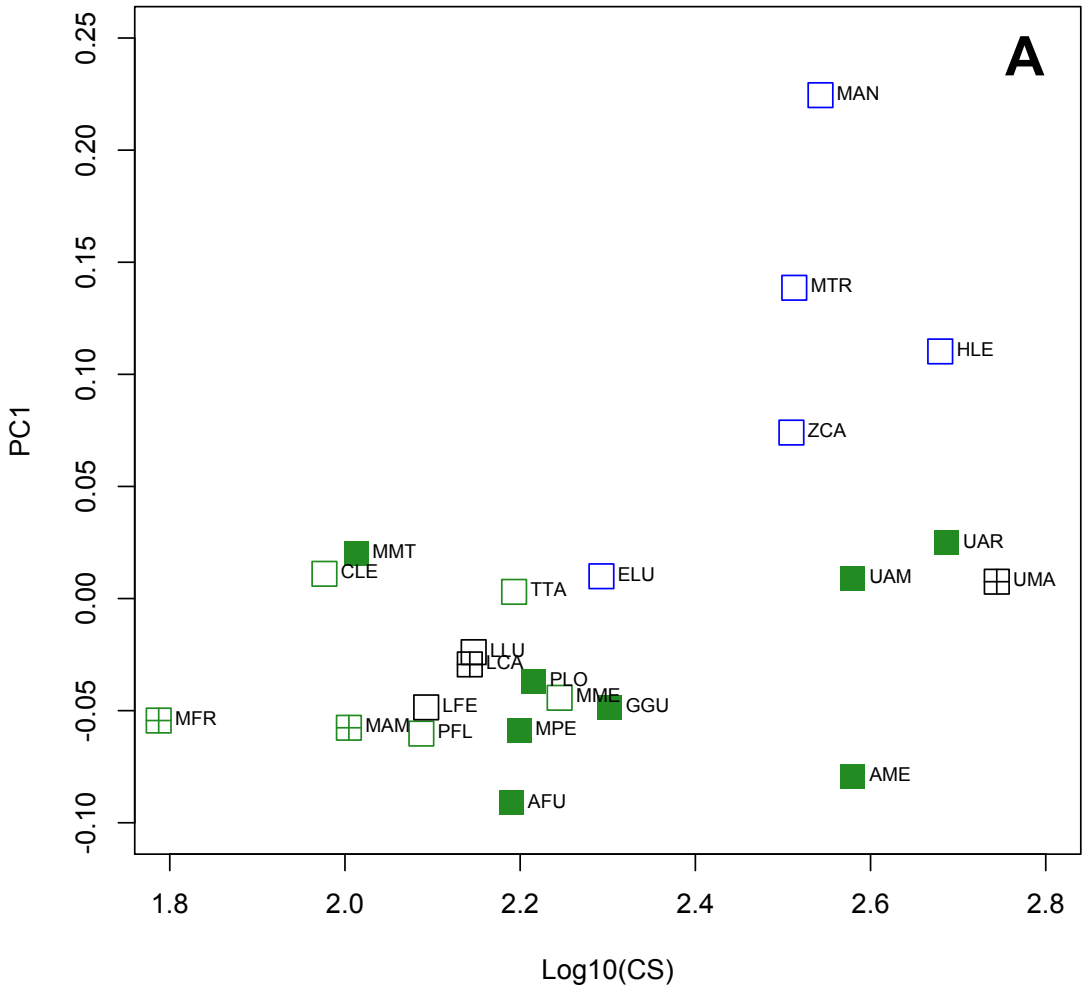

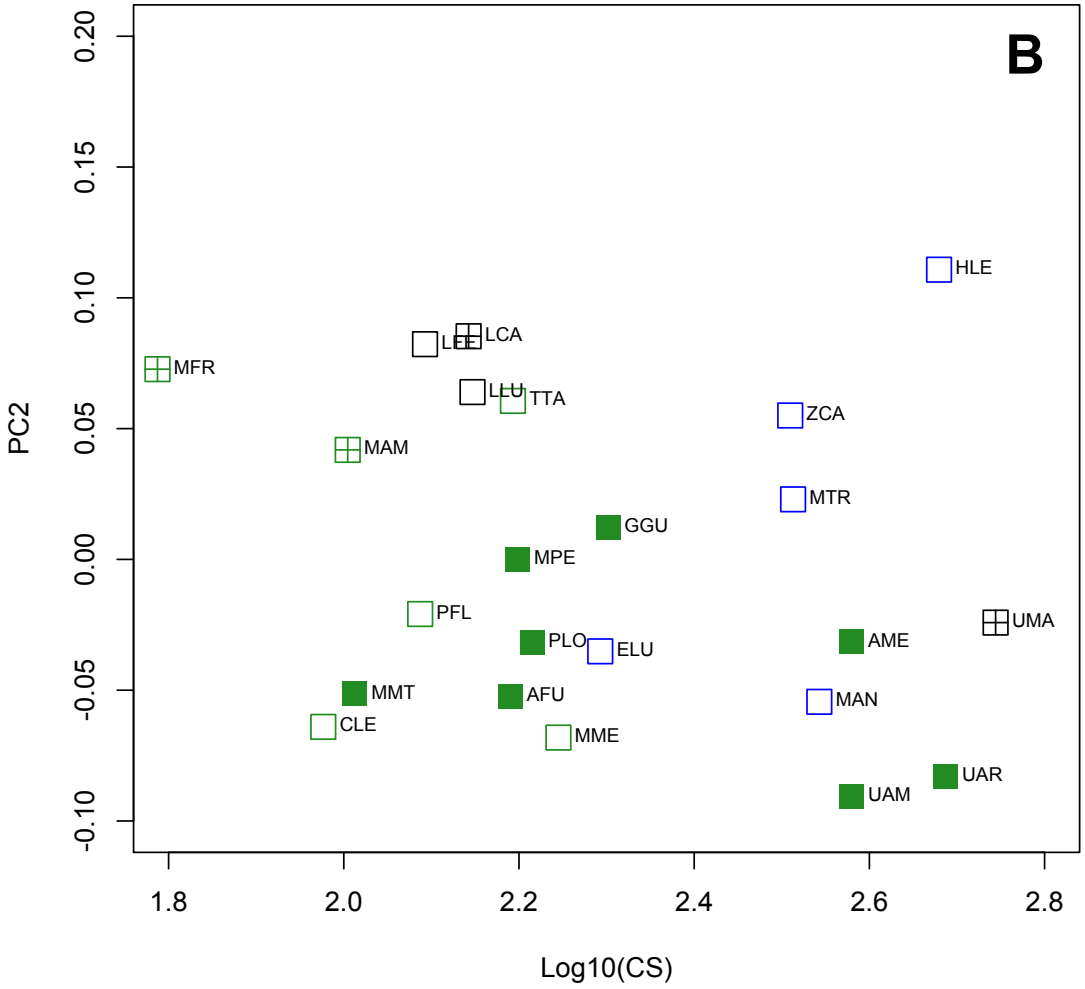
B
PC2
0.20
0.15
0.10
0.05
0.00
-0.05
-0.10
1.8
2.0
2.2
2.4
2.6
2.8
Log10(CS)
HLE
LCA
MFR
LLU
TTA
ZCA
MAM
MTR
GGU
MPE
PFL
UMA
PLO
ELU
AME
MMT
AFU
MAN
CLE
MME
UAR
UAM

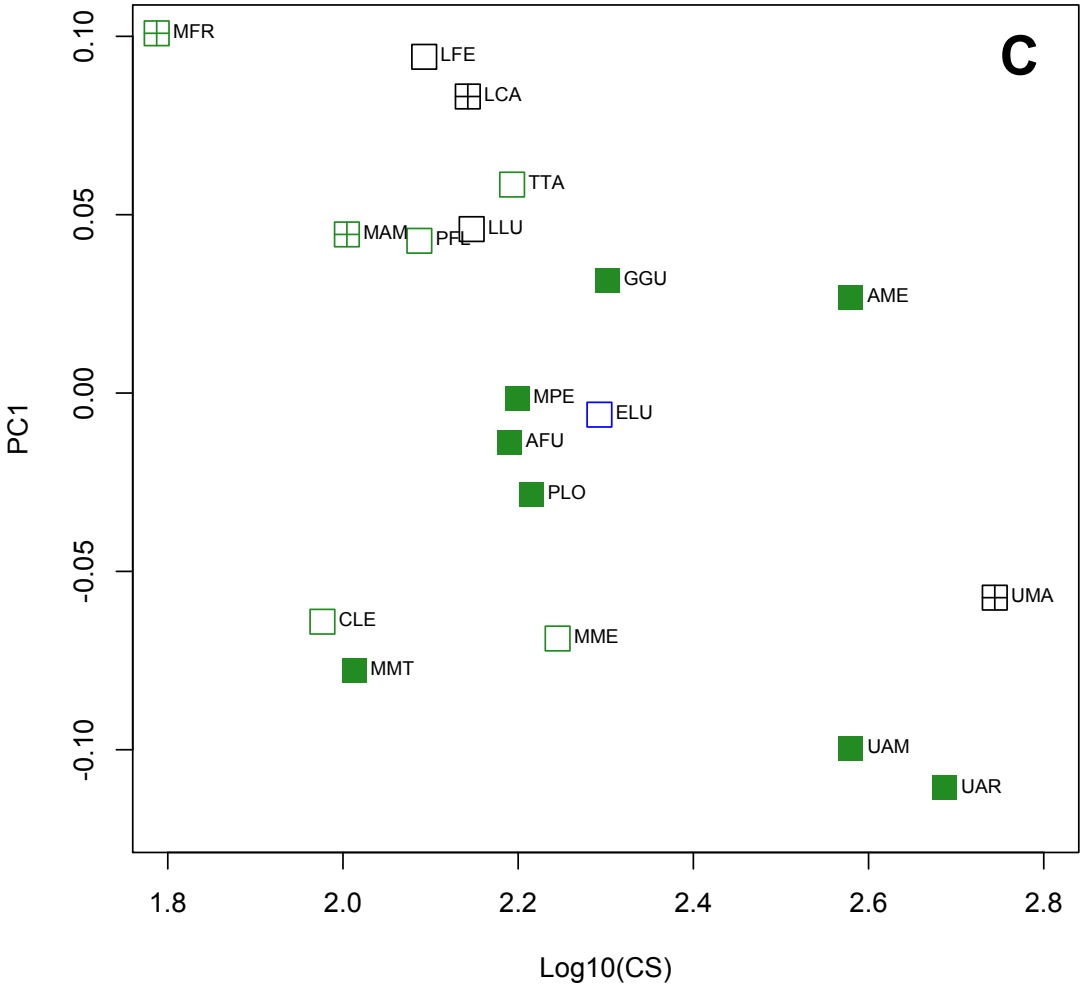
C
MFR
LFE
LCA
TTA
MAM
PFL
LLU
GGU
AME
MPE
ELU
AFU
PLO
UMA
CLE
MME
MMT
UAM
UAR
PC1
0.10
0.05
0.00
-0.05
-0.10
1.8
2.0
2.2
2.4
2.6
2.8
Log10(CS)

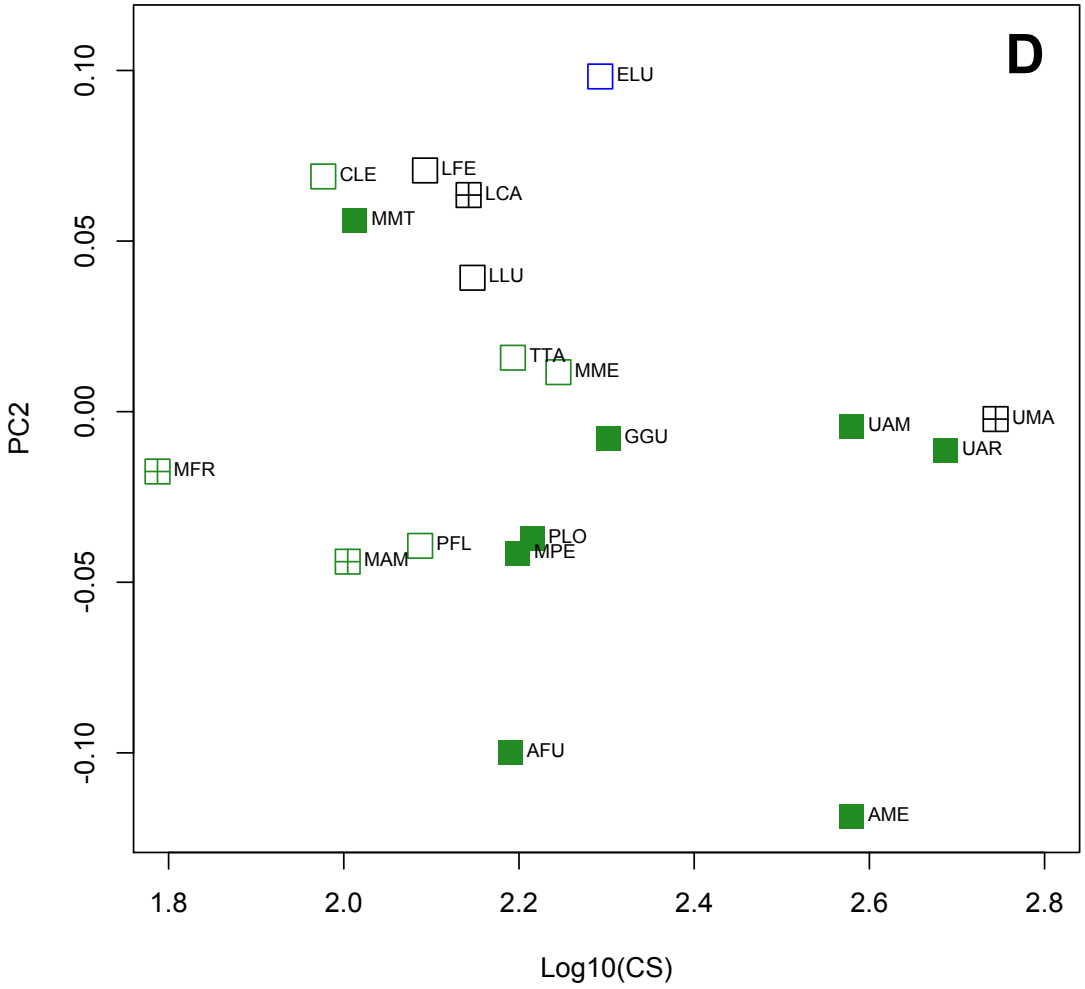
D
ELU
CLE
LFE
LCA
MMT
LLU
TTA
MME
GGU
UAM
UMA
UAR
MFR
PFL
PLO
MAM
MPE
AFU
AME
0.10
0.05
0.00
-0.05
-0.10
PC2
1.8
2.0
2.2
2.4
2.6
2.8
Log10(CS)

Table S2-1: Species and specimen list. USNM, United States National Museum of Natural History. UCLA, D.R. Dickey Collection of the University of California, Los Angeles. LACM, Los Angeles County Museum of Natural History. ISM, Illinois State Museum, IZCA, Institute of Zoology of the Chinese Academy of Sciences. Sex: F, female; M, male; U, unknown. Specimens available through DIGIMORPH.org denoted with an asterisk. All other specimens available through A. Curtis upon request.

Binomial	Specimen Number	sex
Ailuropoda melanoleuca	IZCAS6072	U
Ailurus fulgens	UCLA1989	U
Conepatus leuconotus	UCLA6844	M
Enhydra lutris	SO2853-97*	F
	SO2951-98*	M
Gulo gulo	USNM157327*	F
	USNM314885*	M
Hydrurga leptonyx	USNM269533*	F
	USNM270326*	U
Lontra canadensis	UCLA18958*	F
	UCLA15275*	M
Lontra felina	UCLA141632	M
Lutra lutra	FMNH99384	M
Martes pennanti	UCLA14915	F
	UCLA14987	M
Martes americana	UCLA1003	F
	UCLA15804	F
Meles meles	FMNH47418	M
Mephitis mephitis	USNM147523*	F
	USNM147553*	M
Mirounga angustirostris	MVZ184140*	F
Monachus tropicalis	USNM102527*	F
	USNM100358*	M
Mustela frenata	USNM95054*	F
	USNM52702*	M
Potos flavus	USNM337630*	F
	USNM291066*	M
Procyon lotor	LACM07241	F
	LACM52261	M
Taxidea taxus	LACM45012*	F
	UCLA14841*	M
Ursus americanus	USNM211387*	F
	USNM22070*	M

Ursus arctos	USNM82003*	M
	USNM98062*	F
Ursus maritimus	ISM H 001-05*	M
	USNM2750272*	U
Zalophus californianus	LACM95730*	F
	UCLA252*	M

LITERATURE CITED

Blaney SPA. 1990. Why paranasal sinuses? J Laryngol Otolog 104:690-693.

Blanton PL, Biggs NL. 1969. Eighteen hundred years of controversy: The paranasal sinuses. Am J Anat 124:135-147.

Castilla JC, Bahamondes I. 1979. Observaciones conductuales y ecológias sobre *Lutra felina* (Molina) 1792 (Carnivora: Mustelidae) en las zonas central y contro-norte de Chile. Arch Biol Med Exp (Santiago) 12:119-132.

Cave AJ. 1967. Observations on the platyrrhine nasal fossa. Am J Phys Anthropol 26:277-288.

Curtis A, Van Valkenburgh B. 2014. Beyond the sniffer: frontal sinuses in Carnivora. Anat Rec.

Davis DD. 1964. The giant panda: a morphological study of evolutionary mechanisms. Fieldiana 3:1-339.

Debey LB. 2013. Osteological correlates and phylogenetic analysis of deep diving in living and extinct pinnipeds: What good are big eyes? Mar Mamm Sci 29:48-83.

Edinger T. 1950. Frontal sinus evolution particularly in the Equidae. Bull Mus Comp Zool at Harvard 103:409-496.

Farke AA. 2007. Morphology, constraints, and scaling of frontal sinuses in the hartebeest, *Alcelaphus buselaphus* (Mammalia: Artiodactyla, Bovidae). J Morphol 268:243-253.

Farke AA. 2008. Frontal sinuses and head-butting in goats: a finite element analysis. J Exp Biol 211:3085-3094.

Farke AA. 2010. Evolution and functional morphology of the frontal sinuses in Bovidae (Mammalia: Artiodactyla), and implications for the evolution of cranial pneumaticity. Zool J Linnean Soc 159:988-1014.

Ferretti MP. 2007. Evolution of bone-cracking adaptations in hyaenids (Mammalia, Carnivora). Swiss J Geosci 100:41-52.

Figueirido B, Serrano-Alarcón FJ, Slater GJ, Palmqvist P. 2010. Shape at the cross-roads: homoplasy and history in the evolution of the carnivoran skull towards herbivory. J Evolution Biol 23:2579-2594.

Figueirido B, Tseng ZJ, Martín-Serra A. 2013. Skull shape evolution in durophagous carnivorans. Evolution 67:1975-1993.

Ford LS, Hoffmann RS. 1988. *Potos flavus*. Mammalian Species 321:1-9.

Joeckel RM. 1998. Unique frontal sinuses in fossil and living Hyaenidae (Mammalia, Carnivora): description and interpretation. J Vertebr Paleontol 18:627-639.

Kays RW. 1999. Food preferences of kinkajous (*Potos flavus*): A frugivorous carnivore. J Mamal 80:589-599.

Keir J. 2009. Why do we have paranasal sinuses? J Laryngol Otol 123:4-8.

Klingenberg CP. 2011. MORPHOJ: an integrated software package for geometric morphometrics. Molec Ecol Res 11:353-356.

Larivière, S. and L.R. Walton. 1998. *Lontra canadensis*. Mammalian Species 587:1-8.

Márquez S. 2008. The paranasal sinuses: The last frontier in craniofacial biology. Anat Rec 291:1350-1361.

Martins EP, Hansen TF. 1997. Phylogenies and the comparative method: A general approach to incorporating phylogenetic information into the analysis of interspecific data. Amer Nat 149:646-667.

Nolet BA, Kruuk H. 1989. Grooming and resting of otters *Lutra lutra* in a marine habitat. J Zool 218:433-440.

Paulli S. 1900. Über die pneumaticität bei den säugerthieren. Ein morphologische studie. III. Über die Morphologie des siebbens ud die der pneumaticität bei den Insectivoren, Hyracoideen, Chiropteren, Carnivoren, Pinnipedien, Edentaten, Rodentiern, Prosimiern und Primaten. Gegenbaurs Morphol Jahrb 28:179-251.

R Core Team. 2012. R: A language and environment for statistical computing. R Foundation for Statistical Computing, Vienna, Austria.

Reidenberg JS. 2007. Anatomical adaptations of aquatic mammals. Anat Rec 290:507-513.

Reindenberg J, Laitman JT. 2008. Sisters of the sinuses: cetacean air sacs. Anat Rec 291:1389-1396.

Rossie JB. 2008. The phylogenetic significance of anthropoid paranasal sinuses. Anat Rec 291:1485-1498.

Samuels JX, Meachen JA, Sakai SA. 2013. Postcranial morphology and the locomotor habits of living and extinct carnivores. J Morphol 274:121-146.

Samuels JX, Van Valkenburgh B. 2009. Craniodental adaptations for digging in extinct burrowing beavers. J Vertebr Paleontol 29:254-268.

Slater GJ, Figueirido B, Louis L, Yang P, Van Valkenburgh B. 2010. Biomechanical consequences of rapid evolution in the polar bear lineage. PLoS ONE 11(5):e13870, doi:10.1371/journal.pone.0013870.

Slater GJ, Harmon LJ, Alfaro ME. 2012. Integrating fossils with molecular phlyogenies improves inference of trait evolution. Evolution 66:3931-3944.

Smith TD, Rossie JB, Cooper GM, Mooney MP, Siegel MI. 2005. Secondary Pneumatization of the maxillary sinus in callitrichid primates: Insights from immunohistochemistry and bone cell distribution. Anat Rec Part A 285A:677-689.

Smith TD, Rossie JB, Docherty BA, Cooper GM, Bonar CJ, Silverio AL, Burrows AM. 2008. Fate of the nasal capsular cartilages in prenatal and perinatal tamarins (*Saguinus geoffroyi*) and extent of secondary pneumatization of maxillary and frontal sinuses. Anat Rec 291:1397-1413.

Stirling I. 2011. Polar Bears: The Natural History of a Threatened Species. Brighton: Fitzhenry and Whiteside. 334 p.

Tanner JB, Dumont ER, Sakai ST, Lundrigan BL, Holekamp KE. 2008. Of arcs and vaults: the biomechanics of bone-cracking in spotted hyenas (*Crocuta crocuta*). Biol J Linnean Soc 95:246-255.

Tseng ZJ. 2009. Cranial function in a late Miocene *Dinocrocuta gigantea* (Mammalia: Carnivora) revealed by comparative finite element analysis. Biol J Linnean Soc 96:51-67.

Tseng ZJ, Wang X. 2010. Cranial functional morphology of fossil dogs and adaptation for durophagy in *Borophagus* and *Epicyon* (Carnivora, Mammalia). J Morphol 271:1386-1398.

Uhen MD. 2007. Evolution of marine mammals: Back to the sea after 300 million years. Anat Rec 290:514-522.

Van Valkenburgh B, Curtis A, Samuels JX, Bird D, Fulkerson B, Meachen-Samuels J, Slater GJ. 2010. Aquatic adaptations in the nose of carnivorans: evidence from the turbinates. J Anat 218:298-310.

Wall WP. 1983. The correlation between high limb-bone density and aquatic habits in recent mammals. J Paleontol B:197-207.

Wang RG, Jiang SC, Gu R. 1994. The cartilaginous nasal capsule and embryonic development of human paranasal sinuses. Journal of otolaryngology. 23:239-243.

Wang X, Tedford RH, Taylor BE. 1999. Phylogenetic systematics of the Borophaginae (Carnivora, Canidae). Bull Am Mus Nat Hist 243:1-391.

Werdelin L. 1989. Constraint and adaptation in the bone-cracking canid *Osteoborus* (Mammalia: Canidae). Paleobiology 15:387-401.

Witmer LM. 1997. The evolution of the antorbital cavity of archosaurs: A study in soft-tissue reconstruction in the fossil record with an analysis of the function of pneumaticity. J Vertebr Paleontol 17:1-77.

Witmer LM. 1999. The phylogenetic history of paranasal air sinuses. In: Koppe R, Nagai H, Alt KW, editors. The Paranasal Sinuses of Higher Primates: Development, Function, and Evolution. Chicago: Quintesence. p 21-34.

Zelditch ML, Swiderski DL, Sheets HD, Fink WL. 2004. Geometric Morphometrics for Biologists: A Primer. New York: Elsevier Academic Press. 437 p.

Zollikofer CPE, Ponce de León MS, Schmitz RW, Stringer CB. 2008. New insights into Mid-Late Pleistocene fossil hominin paranasal sinus morphology. Anat Rec 291:1506-1516.

Zollikofer CPE, Weissmann JD. 2008. A morphogenetic model of cranial pneumatization based on the invasive tissue hypothesis. Anat Rec 291:1446-1454.

CHAPTER 3:

INTRASPECIFIC DISPARITY IN FRONTAL SINUS AND CRANIAL MORPHOLOGY IN RELATION TO DIET-RELATED SKULL USE AND AGE IN COYOTES (*Canis* latrans)

INTRODUCTION

Bone is a highly plastic tissue that is remodeled throughout an organism's life in response to how it is loaded. This results in skeletons seemingly optimized to meet the mechanical demands of diet, locomotion, and support (Wolff, 1892). In mammal skulls, pneumatic cavities called paranasal sinuses are commonly found in the bones surrounding the nasal chamber including the frontal, maxilla, ethmoid, and sphenoid. Theses sinuses appear to develop in areas where bone is mechanically unnecessary, and, thus, aid in economizing skull function (Witmer, 1995, 1997,1999; Farke, 2007; Farke, 2010). In Carnivora, the morphology of the frontal bone and its associated sinus are correlated with diet and ecology, and appear to develop where bone is not mechanically necessary (Curtis and Van Valkenburgh, 2014; Curtis et al., 2014). However, whether or not this pattern holds true within as well as between species remains unclear and is the subject of this study.

Witmer (1997) hypothesized that the development and maintenance of pneumatic cavities, including frontal sinuses, is a compromise between pneumatic epithelia that opportunistically resorb bone, and bone deposition in response to biomechanical loading of a bone. If this is the case, then similarity in sinus form within a species should be due to similarities in how individuals use their skulls, and the fact that this places similar loading regimes on the skull.

To better understand the causes of variation in frontal sinus form and size, I investigated intraspecific variation in frontal sinus morphology within a single species, the coyote (*Canis latrans*), using a unique sample of captive individuals of known age and diet. These individuals were raised under controlled conditions and fed a soft diet for a study of cranial growth and development (La Croix, 2011a,b). The size and shape of the frontal sinus in these captive coyotes

were compared with a known aged sample of wild coyotes previously studied by Blood et al. (1985). The diet of the wild coyotes (largely lagomorphs and rodents) is expected to have demanded higher bite forces on average than the soft diet given to the captive coyotes. This should reveal whether frontal sinus morphology (size, shape, complexity) varies in response to diet-related skull loading within a species, as well as whether or not frontal sinus morphology is plastic throughout an individual's life.

Skull shape differences between captive and wild conspecifics have been shown to relate to differences in relation to diet-related skull utility in many mammal species and other vertebrates (see review by O'Regan and Kitchener [2005]). In lions, captive individuals show lesser development of the zygomatic arches, sagittal and lamboidal crests, and occipital and mastoid regions, reflecting the reduced size of the jaw closing and neck muscles involved in subduing and consuming prey in wild individuals (Hollister, 1917; O'Regan, 2001; O'Regan and Turner, 2004; Zuccareli, 2004). Similar differences were also observed in captive versus wild leopards (O'Regan, 2001; O'Regan and Turner, 2004). Captive cheetahs were shown to suffer from malocclusion of the teeth, due to perforation and infection of the palate that resulted from minimal use and consequent atrophy of the masticatory muscles (Fitch and Fagan, 1982). Adult captive hyenas reportedly retain many cub-like features, versus their highly durophagous wild counterparts that have domed frontal bones, large sagittal crests filled with a caudally elongated frontal sinus, and well-developed zygomatic arches (See caption for Fig. 3.3 in West-Eberhard, 2003). Thus, I expected to find differences in external cranial morphology between captive and wild coyotes, and thus possible differences in frontal sinus morphology. Skull function in captive coyotes, especially those fed on a soft diet, is presumably less constrained and mechanically demanding than it is in wild coyotes. As a result, skull shape is expected to be more variable in

captive coyotes and should exhibit lesser development of attachment sites for the feeding musculature, as seen in similar comparisons within other taxa. If skull shape is more variable in captive coyotes and sinuses are opportunistically invading space where bone deposition is limited, frontal sinus shape should also be more variable within this group.

Results from Curtis and Van Valkenburgh (2014) suggest that sinus morphology can be affected by how an individual skull is loaded. For example, the skull of a captive bush dog (*Speothos venaticus*) had no frontal sinuses, despite the fact that Huxley (1880) described this species as having frontal sinuses. Bush dogs are adapted for hunting and subduing relatively large prey (Van Valkenburgh and Koepfli, 1993), and a softer diet may have affected development of the feeding musculature resulting in a lack of space for a frontal sinus to develop in that particular specimen. In addition, the male raccoon dog (*Nyctereutes procyonoides*) examined by Curtis and Van Valkenburgh (2014) showed small sinuses while the female lacked sinuses. The skull of the male showed greater development of muscle attachment sites related to feeding than did the female.

A few authors have previously examined intraspecific variation in frontal sinus morphology. Farke (2007) found that in the hartebeest (*Alcelaphus buselaphus*), frontal sinus volume was strongly correlated with frontal bone size and that frontal sinus shape was similar among individuals and appears to conform largely to the shape of the frontal bone within which it resides. In addition, the number of bony struts subdividing the frontal sinuses differed between males and females, with males showing a greater number of struts than females, and males having absolutely larger frontal sinuses than females. Relative sinus size was similar between the sexes, however. Humans appear to show some of the most extreme disparity in frontal sinus morphology, so much so that frontal sinus shape can be used to successfully identify individuals

(Christensen, 2005). Some of this variation is related to age, as frontal sinuses are known to increase in volume in elderly humans in response to decreased bone deposition (Fatu et al., 2006). Given this and the fact that La Croix et al. (2011a,b) showed that skull performance (bite force) increased with age in the captive coyotes, despite no change in skull size and little change in shape, I expected to see changes in frontal sinus morphology with age. Moreover, based on the results of Farke (2007), I expected to find a strong correlation between frontal sinus morphology and the morphology of the frontal bone. The latter has also been observed at higher taxonomic levels (e.g. Carnivora [Curtis and Van Valkenburgh, 2014], Bovidae [Farke, 2010]).

It is not well understood how differences in skull loading affect sinus morphology. Based on Witmer's (1997) hypothesis, it might be expected that species or individuals that subject their skulls to greater loads (e.g. eat tough foods that require higher bite forces) might have proportionally smaller paranasal sinuses because the strain incurred during feeding would induce bone deposition to maintain skull strength. A study comparing the relative volume of maxillary sinuses between two closely related species of New World monkeys in the genus *Cebus* that differed in dietary hardness showed no significant differences in maxillary sinus size between these species (Rae and Koppe, 2008). However, several species of New World monkeys in Pitheciinae that are hard-object feeders lack maxillary sinuses, while sister taxa with softer diets have maxillary sinuses (Martin et al., 2003; Nishimura et al., 2005; Rossie, 2006). Thus, the influence of biomechanical loading on sinus morphology remains unclear. This is the first study to document changes in sinus size and shape in response to differences in skull loading within a species, and the first to look at the impact of age on sinus morphology in a non-human species.

In addition to documenting variation in frontal sinus size and shape within these two populations of coyotes, I also compared the two in terms of frontal sinus complexity. More

complex sinuses are characterized by relatively high surface to volume ratios that result from having a somewhat furrowed surface with many internal struts (Chapter 1, Curtis and Van Valkenburgh, 2014). In Chapter 1, I showed that, within the Carnivora, larger frontal sinuses have proportionally greater surface area than smaller sinuses, and this reflects the greater number of bony struts subdividing larger sinuses. The largest sinuses with the greatest number of struts typically belonged to hypercarnivorous canids and durophagous hyaenids, thus making it difficult to determine whether sinus complexity is simply a byproduct of large size and consequent rapid pneumatization, or if additional bony struts within a sinus aid in skull function. By comparing the relationship between sinus surface area and volume between two populations with known dietary differences, I can test for differences in the amount of strutting in relation to skull use. If wild coyotes show a proportionally greater number of struts for a given volume, it would favor the hypothesis that struts play a role in skull function.

MATERIALS AND METHODS

Specimens

Specimens were sampled from two populations: wild-caught and captive-reared *Canis latrans* (Table 3-1). The wild-caught population consisted of twelve skulls of male *Canis latrans* collected in Kern County, CA between the years 1969-1973, that were aged by counts of cementum annuli (Blood et al. 1985). All specimens chosen for inclusion were those that Blood et al. (1985) rated as having negligible error in age estimation. The diet of this population consisted predominantly of lagomorphs and rodents, with some livestock supplementation, (Cypher et al., 1994). The captive-reared sample consisted of twelve skulls of male *Canis latrans* drawn from a captive population maintained at the Logan Field Station in Millville, Utah (La

Croix et al., 2011a,b). This population was established using wild coyotes trapped as pups in Idaho and Utah, where their natural diet is largely lagomorphs and rodents (Johnson, 1978; Bartel, 2003). The diet of the captive-reared sample consisted of commercially produced wet food for fur bearing mammals, and never included bones, other foods, or chew toys (La Croix et al., 2011a,b). Specimens ranged in age from six months (by which time skull size and shape have matured [La Croix et al., 2011]) to 13 years. The captive and wild samples for this study were age-matched as closely as possible, and did not differ significantly in age (paired t-test, $t = 1.19$, $df = 10$, $p > 0.05$). Only one sex was included (males) because male and female coyotes mature at different rates, and are sexually dimorphic (La Croix et al., 2011a,b; Blood et al., 1985).

One specimen (MSU 36583) in the captive sample was found to be an outlier in sinus size, shape and skull size, and, thus was excluded from all quantitative analyses, but was considered with respect to qualitative differences between captive versus wild coyotes in the results section.

CT scanning

Skulls were CT scanned in the UCLA School of Dentistry by S. Tetradis using a dental Cone-Beam CT scanner, and were exported as DICOM files with slice thickness of 0.03mm for all scans. I segmented skulls from CT scans by manually thresholding bone from air using Mimics Version 17 (http://biomedical.materialise.com/mimics) specialized imaging software, and volumetric models of skulls were generated in preparation for placement of landmarks for skull size and shape analyses. Copies of all CT data are stored with the Los Angeles County Museum of Natural History and the Michigan State University Museum of Natural History and are available to other researchers.

Tooth Wear and Tooth Fracture

Tooth wear and tooth fracture are both indicators of food texture in mammalian carnivores (Van Valkenburgh, 1988, 2009). Consequently, as an additional preliminary test of dietary differences between my samples, I assessed tooth wear for the upper dentition by binning specimens into one of five categories: slight, slight-moderate, moderate, moderate-severe, and severe (Van Valkenburgh, 1988, 2009). I also quantified tooth wear stage for different tooth types (incisors, canines, premolars (P1-P3), carnassials (P4)) to test for variation in tooth wear that might relate to differences in age and/or tooth use between wild and captive coyotes.

Tooth fracture frequency was assessed by counting the number of teeth broken in life per individual, as well as by quantifying the frequency of tooth breakage for incisors, canines, premolars, carnassials and molars. A tooth was counted as broken if it showed wear on the broken surface, thus indicating the fracture occurred antemortem. Due to the fact that several specimens had missing teeth, I analyzed raw data for tooth fracture and standardized tooth fracture counts by dividing the number of teeth broken by the total number of teeth present.

I expected to observe significantly greater amounts of tooth wear and tooth fracture in wild coyotes than in captive coyotes, which would also reflect dietary differences and thus differences in skull loading in each group. I also expected to see tooth wear and tooth fracture to increase at a greater rate with age in wild than in captive coyotes. Pairwise Wilcoxon signed rank tests were used to test for differences in tooth wear and tooth fracture. To test how tooth wear and tooth fracture vary with age, I used ordinary least squares regressions to estimate the relationship between these variables and age and test the strength of the relationships.

Skull Size and Shape

To capture skull and frontal bone shape, 20 landmarks were placed on crania using the MedCAD module in Mimics Version 17 (http://biomedical.materialise.com/mimics). Landmarks were divided into two datasets, the first including landmarks that describe frontal bone dimensions and the second that describe overall skull shape minus the frontal bone (Table 3-2). The landmarks were divided into these two sets because preliminary results indicated that frontal sinus size and shape disparity were not related to frontal bone morphology, but instead were related to the shape of the rest of the skull. Thus, analyses using all landmarks, including those for the frontal bone, obscured significant correlations between frontal sinus morphology and skull shape.

MorphoJ geometric morphometric software was used to perform a Procrustes fit to align, rotate, and scale landmark configurations to a common centroid size (Klingenberg, 2011). Centroid size was also computed for the frontal bone and skull of each specimen during the Procrustes fit, which was then used as a proxy for skull and frontal bone size in subsequent analyses. To test for differences in size between captive and wild coyotes, a paired t-test was used on centroid sizes for the frontal bone and the skull.

To test for differences in shape between captive and wild coyotes, a principle components analysis (PCA) was performed on the covariance matrix generated from Procrustes-fitted landmark data from the entire skull and frontal bone (Klingenberg, 2011). Wild coyotes were expected to show less skull shape disparity than captive coyotes due to the need to meet the functional demands of a harder diet. Wild coyotes were also expected to show greater development of attachment sites for the feeding musculature, such as the zygomatic arches, sagittal crest, and more doming of the frontal bone.

Sinus Size, Complexity, and Shape

Left and right frontal sinuses were segmented from each CT scan and their total surface area and volume were estimated as proxies for sinus size using Mimics. Paired t-tests were used to test for significant differences in sinus size between populations. Because wild coyote skulls are subjected to more diet-related loading than captive coyotes, I expected to find smaller sinuses in wild coyotes, which would reflect greater bone deposition in the frontal region to strengthen the skull.

In addition to absolute size, the size of frontal sinuses relative to the size of the frontal bone may also differ. Relative frontal sinus size was quantified by dividing total frontal sinus volume by frontal bone centroid size for each individual and using a paired t-test to test for significant differences between groups. If greater loading of the skull results in increased bone deposition within the frontal, I expected wild coyotes to have relatively smaller frontal sinuses than captive coyotes.

To test whether frontal sinus size changes with age or tooth wear, the cube root of total frontal sinus surface volume was plotted against each of these variables, respectively, and the relationships were fit with three separate regression models (linear, quadratic with a linear term, and quadratic without a linear term) due to the fact that the data appeared to covary in a non-linear fashion. AIC scores were then used to evaluate which model best fit the data for both captive and wild coyotes, with the lowest score representing the model that best fit the data. The relationship with both age and tooth wear were examined because, despite the fact that they covary, sinus morphology may be influenced more by one than the other. As previously

mentioned, in humans a decrease in bone deposition in elderly individuals appears to facilitate an increase in sinus volume, so I expected to observe a similar trend in both coyote samples.

I tested for differences in frontal sinus complexity between captive and wild specimens using reduced major axis (RMA) regression to regress $\log_{10}$ transformed values of total frontal sinus surface area (mm^2) against total frontal sinus volume (mm^3). RMA regressions were accomplished using the smatr package in R (Warton et al., 2012; R Core Team, 2012). RMA regression analysis is preferred over OLS when both variables are measured with error, and the allometric relationship between two variables is the desired outcome rather than the ability to predict one variable from another (Warton et al., 2006; Smith, 2009). If bony struts within frontal sinuses aid to strengthen the skull, I expected to see a larger scaling coefficient (slope) for wild coyotes than for captive coyotes.

Frontal sinus shape was quantified using spherical harmonics (SPHARM) (http://www.enallagma.com/SPHARM.php; Shen and Makedon, 2006; Shen et al., 2009) following Curtis et al. (2014). To explore the influence of age and diet on sinus shape, as well as to document the amount of shape variation within each population, I performed a PCA on sinus SPHARM coefficients. Again, due to the fact that wild coyotes have greater functional demands on skull performance, frontal sinus shape was expected to show less variation within wild coyotes than in captive coyotes.

Covariation Between Sinus Morphology and Skull Morphology

The relationship between sinus size and skull size (entire skull and frontal bone) was examined the two samples separately using reduced major axis (RMA) regressions of the log-transformed values of total sinus volume against skull centroid size and frontal bone centroid

size, respectively. Frontal sinus size was expected to be more strongly correlated with frontal bone size than the size of the rest of the skull due to the fact that the frontal sinus is constrained by the size of the frontal bone in most species. In addition, scaling coefficients may differ between wild and captive coyotes, and may reveal if the scaling of sinus size is related to skull utility.

Based on prior work, individuals with domed frontal bones and large jaw muscle attachment sites were expected to have the largest sinuses. To test for covariation between frontal sinus size and frontal bone size or skull shape, respectively, and sinus shape and skull shape or skull size, respectively, I used two block partial least squares (2B-PLS) analysis (Rohlf and Corti, 2000). I $\log_{10}$-transformed values of total sinus volume, skull, and frontal bone centroid size, and multivariate data consisted of frontal sinus SPHARM coefficients (frontal sinus shape), and Procrustes coordinates obtained from skull and frontal bone landmark configurations using functions in MorphoJ (Klingenberg, 2011).

2B-PLS analysis provides a measure of covariation between multivariate datasets (Rohlf and Corti, 2000). A 2B-PLS maximizes covariation between two multivariate datasets and provides an RV coefficient, which is a measure of the strength of covariation between the two blocks of data, and is analogous to r^2 in linear regression (Rohlf and Corti, 2000). Statistical significance of the covariation between two blocks is evaluated using permutation tests that test against a null expectation of no covariation between the blocks (Rohlf and Corti, 2000). I ran separate analyses for wild and captive coyotes for all comparisons. All permutation tests were set to perform 10,000 runs.

RESULTS

Tooth Wear, Tooth Fracture, and Age. As expected, comparisons of tooth wear and tooth fracture differed between wild and captive coyotes, supporting the fact that these groups differed in diet-related skull loading. Total tooth wear was similar between wild and captive coyotes, but wild coyotes did have significantly greater wear for all tooth types ($p < 0.05$), except the incisors (Table 3-3). Total and adjusted counts of tooth fracture were significantly higher in wild coyotes ($p < 0.05$), and the carnassials were found to have significantly greater wear in wild than captive coyotes ($p < 0.05$) in comparisons of individual tooth types (Table 3-2).

Tooth wear (Fig. 1-3A, Table 3-4, $R^2 = 0.93$, $p < 0.0001$) and tooth fracture (Fig. 1-3B, Table 3-4, $R^2 = 0.64$, $p < 0.05$) were both correlated with age within wild coyotes. In my sample of captive coyotes, tooth wear was positively correlated with age, but not as strongly as seen in wild coyotes (Fig. 3-1A, Table 3-4, $R^2 = 72$, $p < 0.001$), and tooth fracture was not correlated with age in captive coyotes (Table 3-4). Wild coyotes also showed a greater rate of tooth wear and tooth fracture accumulation with age than did captive coyotes, showing higher slopes in regressions of tooth wear and tooth fracture against age (Table 3-4).

I also observed that the pulp cavities of the teeth in the oldest individuals from our wild sample that also showed the greatest amount of tooth wear and tooth fracture, were almost completely filled with secondary dentin, but in the captive sample, pulp cavities were still clearly visible in CT scans (Fig. 3-2).

Skull Size and Shape Differences. Paired t-tests revealed no significant difference in skull ($t = 1.13$, $df = 10$, $p > 0.05$) or frontal bone centroid size ($t = 2.09$, $df = 10$, $p > 0.05$) between captive and wild coyotes. Neither skull size (wild: $r^2 = 0.01$, $p > 0.05$; captive: $R^2 = 0.00$, $p > 0.05$) nor frontal bone size (wild: $R^2 = 0.07$, $p > 0.05$; captive: $r^2 = 0.30$, $p > 0.05$) were correlated with age in either group.

A PCA on the covariance matrix generated using Procrustes coordinates for skull shape excluding the frontal bone revealed that captive and wild coyotes share similar shape space (Fig 3-3a). PC1 (19.6% of total skull shape variation) contrasted individuals with dorsoventrally shallow, mediolaterally slender, and downturned rostra, slender zygomatic arches, poorly developed sagittal crests and small mastoid processes, which plotted positively, from individuals with deep, broad upturned rostra, broad zygomatic arches, well developed sagittal crests and large mastoid processes, which plotted negatively, and was not significantly correlated with skull size ($r^2 = 0.07$, $p > 0.05$). PC2 (16.31% of total skull shape variation) contrasted individuals with proportionally short and dorsoventrally deep rostra, broad zygomatic arches and a well developed sagittal crest (positive scores) from individuals with proportionally long, dorsoventrally shallow rostra and poorly developed sagittal crests (negative values), and was correlated with skull size ($r^2 = 0.32$, $p < 0.01$).

However, a PCA on a covariance matrix generated using Procrustes coordinates for frontal bone shape alone showed that wild coyotes exhibit much less disparity in frontal bone shape than do captive coyotes (Fig 3-3b). PC1 (36.8% of total frontal bone shape variation) distinguished frontal bones with slender postorbital processes, that were dorsoventrally shallow with flat dorsal profiles (positive scores) from those with wide postorbital processes that were dorsoventrally deep with more domed profiles (negative values), and was not significantly related to frontal bone size ($r^2 = 0.00$, $p > 0.05$). PC2 (24% of total frontal bone shape variation) distinguished frontal bone with wider postorbital processes that were dorsally convex (positive scores), from those with slender postorbital processes that were dorsally flat (negative scores), and was correlated with frontal bone size ($r^2 = 0.25$, $p < 0.05$). Despite falling within the same

shape space as captive coyotes, wild coyote frontal bone shape tended to plot more positively along PC2.

Sinus Size and Shape Differences. Qualitatively, frontal sinus morphology was broadly similar among all specimens examined (Fig. 3-4a,b; Fig 3-5a,b). In general, the frontal sinuses were centered at the postorbital processes, and never reached the margin of the fronto-parietal suture as is seen in larger hypercarnivorous canids such as the gray wolf (*Canis lupus*). However, in the wild-caught coyotes, the frontal sinuses tended to pneumatize farther posteriorly toward the fronto-parietal suture than those of the captives. In both groups, the posterior margin of the frontal sinuses on each side of the midline typically showed what appear to be three lobes of pneumatization separated by two small bony struts, but the number of lobes and struts appeared to be more variable in the captive than wild coyotes. Anteriorly, the frontal sinuses on each side of the midline usually had two lobes that differed little within or between captive and wild coyotes; a medial lobe where the sinus is connected to the nasal chamber via an ostium located posterior to frontoturbinal 2 (sensu Paulli, 1900), and a lateral lobe that expands anteriorly from the postorbital process.

Absolute frontal sinus volume was not significantly different between captive and wild populations (paired t-test, $t = -0.42$, $df = 10$, $p > 0.05$), nor was relative frontal sinus volume (paired t-test, $t = -0.77$, $df = 10$, $p > 0.05$), which was calculated as (total sinus volume/frontal bone centroid size). Frontal sinus volume was not correlated with skull centroid size (wild: $r^2 = 0.16$, $p > 0.05$; captive: $r^2 = 0.04$, $p > 0.05$) or frontal bone centroid size (wild: $r^2 = 0.06$, $p > 0.05$; captive: $r^2 = 0.09$, $p > 0.05$) in both wild and captive coyotes.

A PCA on SPHARM coefficients that describe frontal sinus shape revealed that sinus shape shows slightly greater variation in captive coyotes than in wild coyotes, but both groups

overlapped widely in morphospace (Fig. 3-6). PC1 (21.2% of total frontal sinus shape variation) contrasted individuals with dorsoventrally deep, dorsally convex frontal sinuses with a greater number of bony struts (positive values) from those with dorsoventrally shallow, less dorsally convex, and less complex sinuses (negative values), and showed a weak, but significant relationship with frontal sinus volume ($r^2 = 0.30$, $p < 0.01$). PC 2 accounted for 13.9% of total frontal sinus shape variation, and again separated individuals based on dorsoventral depth and complexity, and also showed a weak, but significant correlation with frontal sinus volume ($r^2 = 0.2$, $p < 0.05$). In this case, sinuses that plotted negatively were dorsoventrally deep, had bony struts, and pneumatized farther posteriorly across the braincase. Wild coyotes tended to plot more positively along PC1 and negatively along PC2 than captive coyotes, supporting qualitative observations that although the frontal sinuses of the wild sample are largely similar in overall shape to those of the captives, they do show slight differences in that they pneumatize farther posteriorly, have more bony struts, and are deeper dorsoventrally and more convex dorsally.

Sinus Morphology, Age, and Tooth Wear. Frontal sinus volume increased with age and tooth wear until about eight years of age and moderate tooth wear (stage 3), and decreased thereafter. This relationship was best modeled as a quadratic function including a linear term (Fig 3-7, Table 3-5), and was significant with tooth wear but not age. When each sample was analyzed separately, there was no significant relationship with age or tooth wear in captive coyotes, but both remained significant for the wild sample.

Sinus Volume and Skull Shape. Frontal sinus volume was not correlated with the shape of the frontal bone or entire skull in either group. However, contrary to what was observed in Chapter 1 among canids, felids, and hyaenids, as well as within Canidae (See Chapter 1, Table 1-4), frontal sinus volume in wild coyotes showed a weak, but significant correlation with the

shape of the skull without the frontal bone (Fig. 3-8, RV = 0.40, $p < 0.05$). This was not true of the captive sample. In the wild coyotes, larger sinuses were associated with skulls that had dorsoventrally deep, mediolaterally broad rostra, wide zygomatic arches, well-developed sagittal crests, and large mastoid processes. Smaller sinuses were associated with skulls that had dorsoventrally shallow, mediolaterally slender rostra, slender zygomatic arches, poorly developed sagittal crests, and small mastoid processes.

Sinus Shape versus Skull Shape and Skull Size. Frontal sinus shape was not correlated with either skull shape or frontal bone shape in captive and wild coyotes. In addition, frontal sinus shape was not significantly correlated with frontal bone size in either group. However, as was the case for frontal sinus volume, frontal sinus shape was significantly correlated with the size of the skull without the frontal bone in wild but not captive coyotes (Fig. 3-9, RV = 0.40, $p < 0.05$). Frontal sinuses that pneumatized farther laterally into the postorbital processes, showed a greater number of bony struts, and the lateral lobe that pneumatizes anteriorly from the postorbital process was positioned farther anteriorly than the medial lobe in individuals with larger skulls. Frontal sinuses that were more mediolaterally restricted, less complex, and with the two anterior lobes pneumatizing the same distance anteriorly were seen in smaller skulls.

Frontal Sinus Surface Complexity. As seen across Carnivora (Curtis and Van Valkenburgh, 2014), frontal sinus surface area and volume are strongly correlated in both wild and captive coyotes ($R^2 = 0.95$, $R^2 = 0.98$, respectively). In both groups, the relationship between frontal sinus surface area and volume did not differ significantly from isometry (slope = 0.66) (Fig. 3-10, Table 3-6). Although this relationship differs from that observed at the ordinal level in Chapter 1 (Chapter 1, Table 1-5: slope = 0.70 (0.67 – 0.73)), it is not different from the relationship observed within Canidae (Chapter 1, Table 1-5, slope = 0.66 (0.54 – 0.72)).

DISCUSSION

This study was the first to compare the effect of variation in diet-related skull utility on frontal sinus morphology within a single species, as well as the first to examine how frontal sinus morphology varies among adult individuals of known age in a non-human sample. Overall, results support the hypothesis that frontal sinuses develop where bone is mechanically unnecessary, which is consistent with previous studies on frontal sinus morphology (e.g. Farke, 2010; Curtis et al., 2014; Curtis and Van Valkenburgh, 2014). Frontal sinus morphology is related to the size and shape of the skull, varies with skull use, and is not static throughout an organism's lifetime.

The assumption that captive and wild coyotes do load their skulls differently was confirmed by the greater degree of tooth wear and tooth fracture frequency seen in wild coyotes than in captive coyotes. In particular, the carnassials, and molars, which are used by canids to pull skin, and chew muscle plus bone and bone (Van Valkenburgh, 1996), showed much greater wear and were more likely to be fractured in wild coyotes. A greater amount of secondary dentin filling the pulp cavities (sometimes completely) in wild coyotes reflects repeated trauma to the teeth, which induces deposition of secondary dentin by odontoblasts along the periphery of the tooth pulp cavity (Klugh, 2010).

Similar to previous studies comparing skull morphology between captive and wild conspecifics (e.g. O'Regan, 2001; O'Regan and Turner, 2004; Zuccareli, 2004), I found no significant differences in size (skull or frontal bone) between captive and wild coyotes. However, there were differences in cranial shape between captive and wild coyotes. As expected, wild

coyote skulls were less variable in frontal bone shape, with dorsally convex frontal bones, compared with captive coyotes that often showed flatter dorsal profiles. This is consistent with the hypothesis that skull morphology is more constrained in wild individuals due to the functional demands of a harder diet, however the shape differences were fairly subtle as wild and captive individuals overlap in shape space. Skulls with dorsally convex frontal bones are stronger than skulls that are dorsally flat during feeding related behaviors and are seen in large, hypercarnivorous canids and hyaenids (Tseng and Wang, 2010).

Although I expected to observe either absolutely or proportionally smaller frontal sinuses in wild coyotes than in captive coyotes, I did not observe any significant differences in sinus size (relative or absolute) between these groups. The lack of significant differences in absolute and relative sinus size between captive and wild coyotes was similar to Rae and Koppe's (2008) observations concerning maxillary sinus size in two closely related species of New World monkeys that also differed in dietary hardness. However, there were slight differences in frontal sinus shape between the coyote samples, suggesting that, in response to differences in diet-related loading of the skull, patterns of bone deposition and removal may differ spatially without resulting in major differences in sinus size. It would be interesting to examine disparity in skull and frontal sinus morphology among a greater sample of coyote populations, especially sampling from populations that frequently subdue prey larger than lagomorphs, such as in areas where they seasonally hunt and kill white-tailed deer (Lingle, 2002).

The coyote data also suggest that frontal sinus morphology is plastic over an individual lifespan and can change in response to changes in skull loading. The decrease in frontal sinus volume associated with the acquisition of heavier tooth wear in the wild coyotes may reflect a need to produce sufficient bite forces to apprehend prey and/or process food with blunted and/or

missing teeth. Assuming that bite force is increased by enlarging the jaw closing musculature, this could result in greater strain within the skulls of individuals with heavy tooth wear, and thereby induce bone deposition and remodeling of the frontal region, thus resulting in the observed decrease in sinus volume. This hypothesis is supported by the fact that sagittal crest size was largest in the oldest wild individuals, and the enlarged crest reflects greater development of the temporalis muscle (the primary jaw closing muscle in carnivores). Interestingly, captive coyotes did not show a similar increase in the development of the sagittal crest with the accumulation of greater tooth wear (Fig. 11), and the frontal sinuses of the oldest individuals in our captive sample appear to be proportionally larger than those of our wild sample. Thus, although the captive coyotes did not show an increase in sinus volume with age as is seen in humans, they did not exhibit as much of a decrease in volume as the wild coyotes, suggesting that bone strains were less on average in the captive sample.

In Farke's (2007) study of frontal sinus variation within hartebeest, he found evidence for a stronger relationship between frontal sinus size and frontal bone size, than with the size of the snout and braincase. In Canidae, the family to which coyotes belong, Curtis and Van Valkenburgh (2014) found significant covariation between frontal sinus size and skull and frontal bone size, respectively, as well as between frontal sinus shape and skull and frontal bone size, respectively. Results from this study differ from observations made by previous authors on the relationship between frontal sinus morphology and skull morphology. In contrast to Farke (2007), and in contrast with expectations, no significant relationship was observed between frontal sinus size and skull size or frontal bone size in my sample. In addition, also contrary to expectations, within the wild coyotes, frontal sinus size was only correlated with the shape of the skull excluding the frontal bone, and frontal sinus size was only correlated with the size of the

skull excluding the frontal bone. Thus, frontal sinus morphology was only correlated with the morphology of the snout and braincase, but not the frontal bone. Perhaps if the frontal bone is relatively constrained in form among individuals within a species, in comparison to the rest of the skull, then regions left unloaded, and, thus, available for pneumatization would be more strongly related to the size and configuration of the rostrum and braincase, rather than the frontal bone itself. Similar to results in Curtis and Van Valkenburgh (2014), the largest sinuses that pneumatized farther posteriorly and were dorsoventrally deep were found in wild specimens that showed greater development of muscle attachment sites for the feeding musculature and deeper snouts, which are characteristics often seen in carnivores that are more durophagous and/or subdue large prey (Van Valkenburgh and Koepfli, 1993; Tseng and Wang, 2010, 2011; Curtis and Van Valkenburgh, 2014).

Previous authors suggested that the number of bony struts within the frontal sinuses is not related to skull loading, but, rather, a byproduct of rapid pneumatization that leaves struts of bone behind (Zollikofer and Weissmann, 2008; Farke, 2010; Curtis and Van Valkenburgh, 2014). However, other studies have suggested that struts may play a limited, biomechanical role (e.g. Farke, 2008). Based on the observation that frontal sinus surface complexity scales isometrically with sinus size in both captive and wild coyotes, it does not appear that a harder diet results in a proportionally greater quantity of struts within larger sinuses, nor does sinus complexity appear to differ in relation to skull loading, which does not support the hypothesis that struts within the sinus aid in skull function. Qualitative observations do suggest that there is a greater consistency in the number and orientation of struts along the posterior border of the frontal sinuses in wild coyotes relative to those of captive coyotes, so perhaps this could be quantified, or perhaps there would be a measureable difference in a species with greater

mechanical demands on its skull, such as the durophagous spotted hyena (*Crocuta crocuta*). It also still remains unclear if struts reorient throughout an organism's lifetime to better meet the demands of skull use.

This study shows the importance of examining both relative size and shape of pneumatic spaces to better understand how frontal sinus morphology is affected by diet-related skull loading. A lack of difference in the size of pneumatic cavities in relation to biomechanical loading doesn't necessarily indicate that the process of pneumaticity is equivalent across differing loading regimes. It is also clear that age related changes in frontal sinus morphology may differ among species. For example. the frontal sinuses of humans often increase in volume in elderly individuals (Fatu et al., 2006) whereas they decreased in our study. Further studies examining patterns of bone deposition and bone removal from a histological perspective among individuals that differ in diet may reveal how skull loading can affect frontal sinus remodeling. These differences also suggest that there may be a certain level of strain required to maintain the form of a sinus and its enclosing bone, which could have implications for human health, as the relative enlargement of the frontal sinus that sometimes occurs in elderly patients can lead to complications during medical procedures (Natsis, 2004).

TABLES

Table 3-1. List of specimens included in this study paired by age with associated skull size and sinus size data.

Captive-Reared Coyotes						Wild-Caught Coyotes					
Specimen Number	**Age**	**FCS**	**SKCS**	**TSA**	**TSV**	**Specimen Number**	**Age**	**FCS**	**SKCS**	**TSA**	**TSV**
MSU 37104	0.5	60.73	232.85	1656.37	2835.29	LACM 43378	0.5	62.64	234.29	1839.27	3322.79
MSU 37107	1.2	63.60	242.93	2954.89	6632.26	LACM 43320	1	63.96	243.13	3275.83	7657.52
MSU 36584	1.4	63.35	245.47	3005.41	5818.61	LACM 33335	1	55.44	228.36	2324.79	4798.70
MSU 37147	1.5	58.62	240.55	2520.40	5243.23	LACM 43294	2	58.42	235.39	2301.06	4903.52
MSU 37117	3.9	61.96	234.94	2874.63	6012.54	LACM 43325	4	56.90	238.44	3081.07	6244.94
MSU 37120	4.4	61.39	239.81	1926.55	3246.49	LACM 43326	5	62.22	241.06	2842.12	5750.17
MSU 37121	6.8	62.19	245.73	3518.18	7736.33	LACM 43292	7	60.78	230.94	3236.78	7829.60
MSU 37123	7.51	62.14	238.07	2660.36	5750.16	LACM 43306	7	63.15	242.85	3735.31	8529.39
MSU 36587	10.3	66.87	250.62	2740.78	5684.83	LACM 43324	10	62.40	246.86	2682.61	5531.92
MSU 36590	12.3	64.57	241.09	2481.59	4829.73	LACM 33332	11	59.79	240.47	3057.11	6451.14
MSU 36583	13.3	NA	NA	5083.97	14523.24	LACM 43391	13	63.27	232.77	2723.24	6399.90
MSU 36591	13.3	62.76	231.51	3501.20	8501.66	LACM 43293	13	60.65	234.40	2203.36	4023.50

MSU = Michigan State University Museum of Natural History, LACM = Los Angeles County Museum of Natural History. Age is listed in years. Ages for captive-reared specimens obtained from La Croix, et al. (2011) and were based on known dates of birth and death. Ages for wild-caught specimens obtained from Blood, et al. (1985) based on cementum annuli analysis. Frontal bone centroid size (FCS), skull centroid size (SKCS), total sinus surface area (TSA) in mm^2, and total frontal sinus volume (TSV) in mm^3.

Table 3-2. Descriptions of landmarks used for geometric morphometric analysis of skull shape.

Landmark	Region	Description
1	SK	Posteromedial most point on the palatine
2	SK	Anteromedial most point on the incisive
3	SK	Anterior border of the C1 alveolus
4	SK	Posterior border of the C1 alveolus
5	SK	Anterior border of the P4 alveolus
6	SK	Posterior border of the alveolus of the last upper cheek tooth
7	FR	Intersection of the frontal, maxilla, and lacrimal
8	FR	Post-orbital process of the frontal
9	SK	Anterior extension of the squamosal on the zygomatic arch
10	SK	Posterior extension of the jugal on the zygomatic arch
11	SK	Superior border of the external auditory meatus
12	SK	Ventral most point on the mastoid process
13	SK	Medial point on the ventral border of the foramen magnum
14	SK	Posterior most point on the sagittal crest
15	FR	Midsagittal point of the frontoparietal suture
16	FR	Mid-point between landmarks 15 and 17
17	FR	Midsagittal point of the frontonasal suture.
18[a]	SK	Anteromedial most point on the nasal
19[a]	FR	Midpoint between landmarks 16 and 8
20[a]	FR	Intersection of the frontal, lacrimal, and palatine

SK, skull, FR, frontal bone. See Chapter 1, Figure 2 for illustration of landmarks on a skull. [a] Landmarks 18, 19, and 20 in this study correspond with landmarks 19, 20, and 22, respectively, in Chapter 1 (Table 2, Fig. 2).

Table 3-3. Summary statistics from paired Wilcoxon Signed Rank Tests comparing tooth fracture frequency and tooth wear stage in captive versus wild coyotes.

Tooth Fracture	**Captive mean**	**Wild mean**	**p**
Total	2.09	4.18	<0.05
% Broken	0.10	0.24	<0.01
incisors	0.27	0.55	NS
canines	0.91	1.09	NS
premolars	0.55	1.18	NS
carnassials	0.18	0.73	<0.05
molars	0.18	0.64	NS
Tooth Wear	**Captive mean**	**Wild mean**	**p**
Total	2.36	2.82	NS
incisors	2.45	2.91	NS
canines	2.36	3.00	<0.05
premolars	2.36	3.00	<0.05
carnassials	2.18	2.82	<0.05
molars	2.18	2.82	<0.05

For tooth fracture: Total = mean raw number of broken teeth, % Broken = mean (number of broken teeth/total teeth present).

Table 3-4. Regression statistics for total tooth wear against age and total tooth fracture against age.

Tooth Wear vs. Age	slope	y-intercept	R^2	p
Captive	0.19 (0.10 - 0.28)	1.28 (0.65 - 1.92)	0.72	<0.001
Wild	0.27 (0.22 - 0.33)	1.31 (0.91 - 1.70)	0.93	<0.0001
Tooth Fracture vs. Age	**slope**	**y-intercept**	**R^2**	**p**
Captive	0.22 (-0.05 - 0.05)	0.85 (-1.08 - 2.79)	0.27	NS
Wild	0.67 (0.32 - 1.03)	0.85 (-1.78 – 3.64)	0.64	<0.05

Tooth Fracture represents total number of broken teeth. 95% confidence intervals given for slope and y-intercept.

Table 3-5. Comparison of regression models of frontal sinus volume against tooth wear and age.

TSV vs Tooth Wear	R^2	p	AIC Score
quadratic with linear term	0.51	<0.05	44.36
quadrating without linear term	0	NS	50.79
OLS	0.04	NS	50.31
TSV vs Age	**R^2**	**p**	**AIC Score**
quadratic with linear term	0.42	NS	46.36
quadrating without linear term	0	NS	50.82
OLS	0.03	NS	50.48

Lowest AIC Score represents the model that best fits the data.

Table 3-6. Regression statistics for Log_{10}/Log_{10} RMA regression of total frontal sinus surface area (TSA) against total frontal sinus volume (TSV).

TSA vs. TSV	slope	y-intercept	R^2	p
MSU	0.67 (0.62 - 0.74)	0.89 (0.67 - 1.11)	0.98	<0.0001
LACM	0.72 (0.62 - 0.85)	0.71 (0.28 - 1.14)	0.95	<0.0001

95% confidence intervals given for slope and y-intercept.

FIGURE LEGENDS

Figure 3-1. Regression of A: tooth wear stage against age and B: raw number of broken teeth against age. Wild coyotes = green, captive coyotes = orange. Regression statistics given in Table 4.

Figure 3-2. Comparison of pulp cavity of the first upper molar (M1) taken at the paracone between captive and wild coyotes showing that the pulp cavities of the oldest wild coyotes in our samples are filled almost completely with secondary dentin in comparison to captive coyotes, which still have visible pulp cavities even at similar age and tooth wear stage.

Figure 3-3. PCA on A: Procrustes coordinates for skull shape. PC 1 accounted for 19.60% of total shape variation, and PC 2 accounted for 16.31% of total shape variation, B: Procrustes coordinates for frontal bone shape. PC 1 accounted for 36.77% of total shape variation, and PC 2 accounted for 23.96% of total shape variation. Wild and captive coyotes colored as in Fig. 1.

Figure 3-4. Dorsal views of sinuses within the skulls of A: wild coyotes, and B: captive coyotes. LACM 43391 is only shown with a right frontal sinus because the left frontal bone had a gun shot wound.

Figure 3-5. Lateral views of frontal sinuses within the skulls of A: wild coyotes, and B: captive coyotes.

Figure 3-6. PCA on SPHARM coefficients. PC 1 accounted for 21.22% of total shape variation, and PC 2 accounted for 13.93% of total shape variation. Dorsal and medial views of skulls showing sinus shapes at the extremes for each PC along each axis. Wild and captive coyotes colored as in Fig. 1.

Figure 3-7. Plot of (total frontal sinus volume)$^{1/3}$ against A: Age, B: tooth wear stage. Regression line shown for wild coyotes only as the relationship between sinus size and tooth wear was not significant in captive coyotes. Regression statistics given in Table 5. Wild and captive coyotes colored as in Fig. 1.

Figure 3-8. Partial least squares plot of $\log_{10}$ (total sinus volume) (TSV) against Procrustes coordinates for skull shape in wild coyotes. Wild and captive coyotes colored as in Fig. 1.

Figure 3-9. Partial least squares plot of sinus shape against skull centroid size. Wild and captive coyotes colored as in Fig. 1.

Figure 3-10. Log_{10}/Log10 RMA regression of frontal sinus surface area against frontal sinus volume. Wild and captive coyotes colored as in Fig. 1.

Figure 3-11. Differences in the development of the sagittal crest in captive versus wild coyotes. A: dorsal view. Red bracket denotes the length of the sagittal crest, and curve extending to the postorbital process delimits the temporal line. B: lateral view with red line delimiting the base of

the sagittal crest. Note the greater development of the sagittal crest in the wild coyote in both views.

FIGURE 3-1

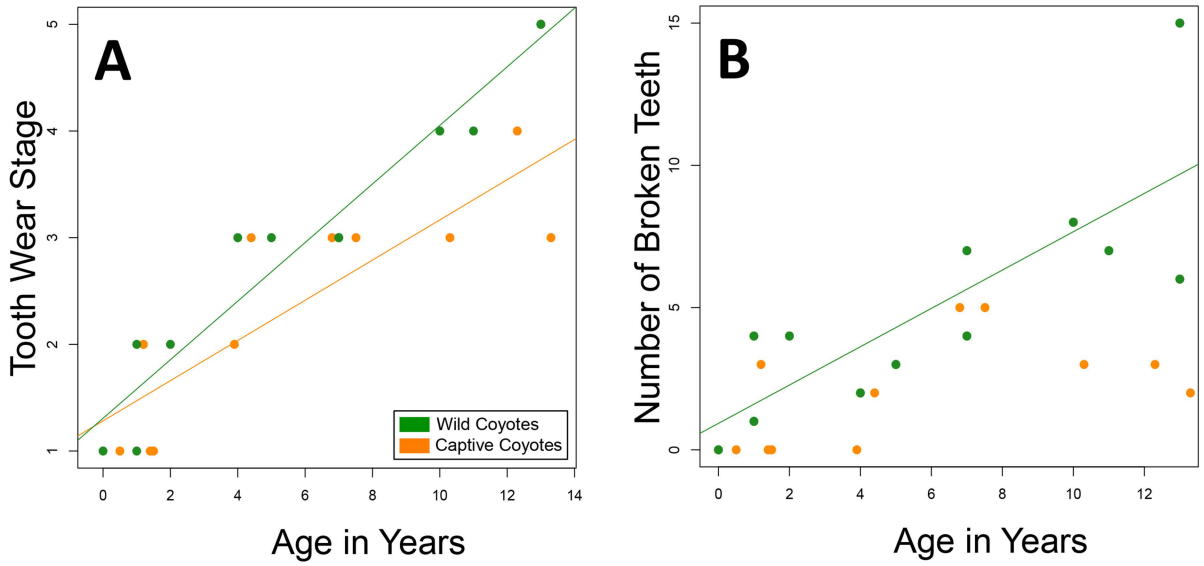
A
Tooth Wear Stage
Age in Years
Wild Coyotes
Captive Coyotes
B
Number of Broken Teeth
Age in Years

FIGURE 3-2

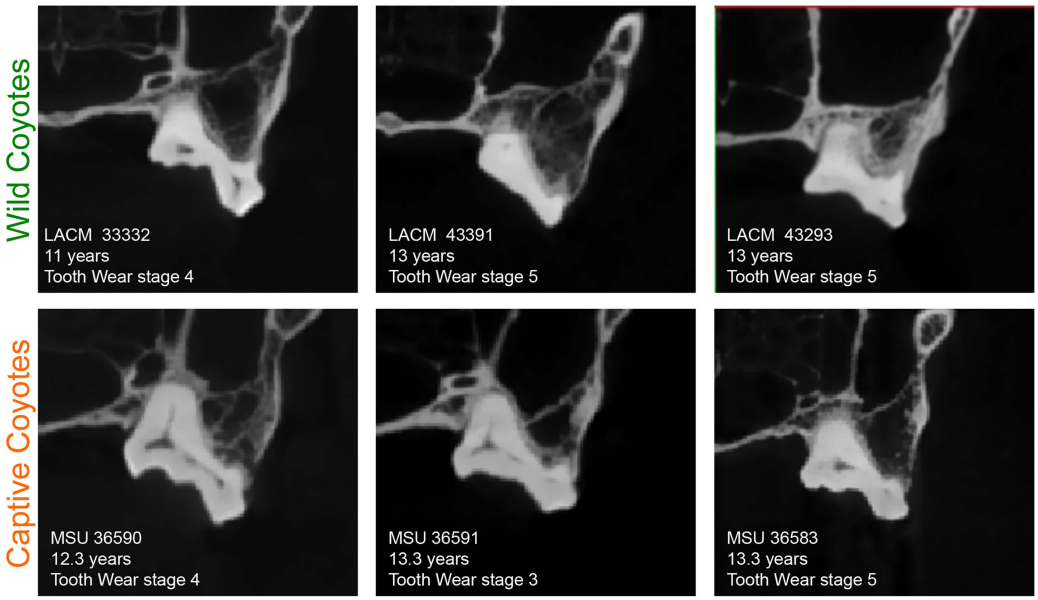
Wild Coyotes
LACM 33332
11 years
Tooth Wear stage 4
LACM 43391
13 years
Tooth Wear stage 5
LACM 43293
13 years
Tooth Wear stage 5
Captive Coyotes
MSU 36590
12.3 years
Tooth Wear stage 4
MSU 36591
13.3 years
Tooth Wear stage 3
MSU 36583
13.3 years
Tooth Wear stage 5

FIGURE 3-3

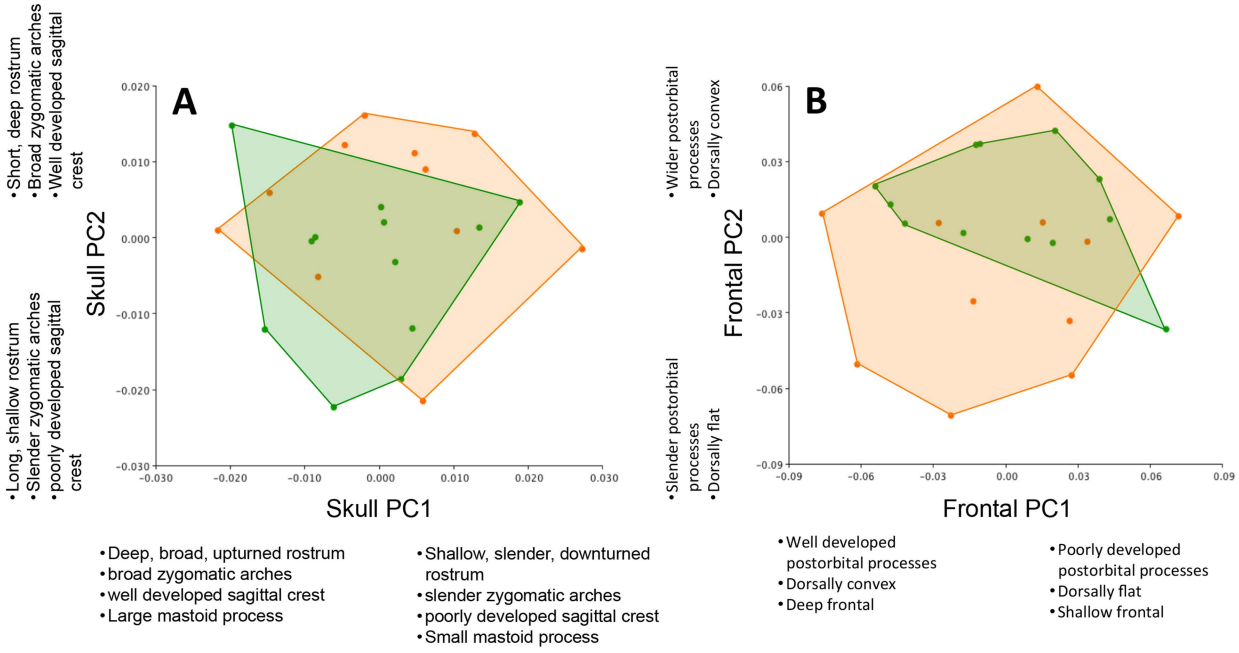

- Deep, broad, upturned rostrum
- broad zygomatic arches
- well developed sagittal crest
- Large mastoid process

- Shallow, slender, downturned rostrum
- slender zygomatic arches
- poorly developed sagittal crest
- Small mastoid process

- Well developed postorbital processes
- Dorsally convex
- Deep frontal

- Poorly developed postorbital processes
- Dorsally flat
- Shallow frontal

FIGURE 3-4

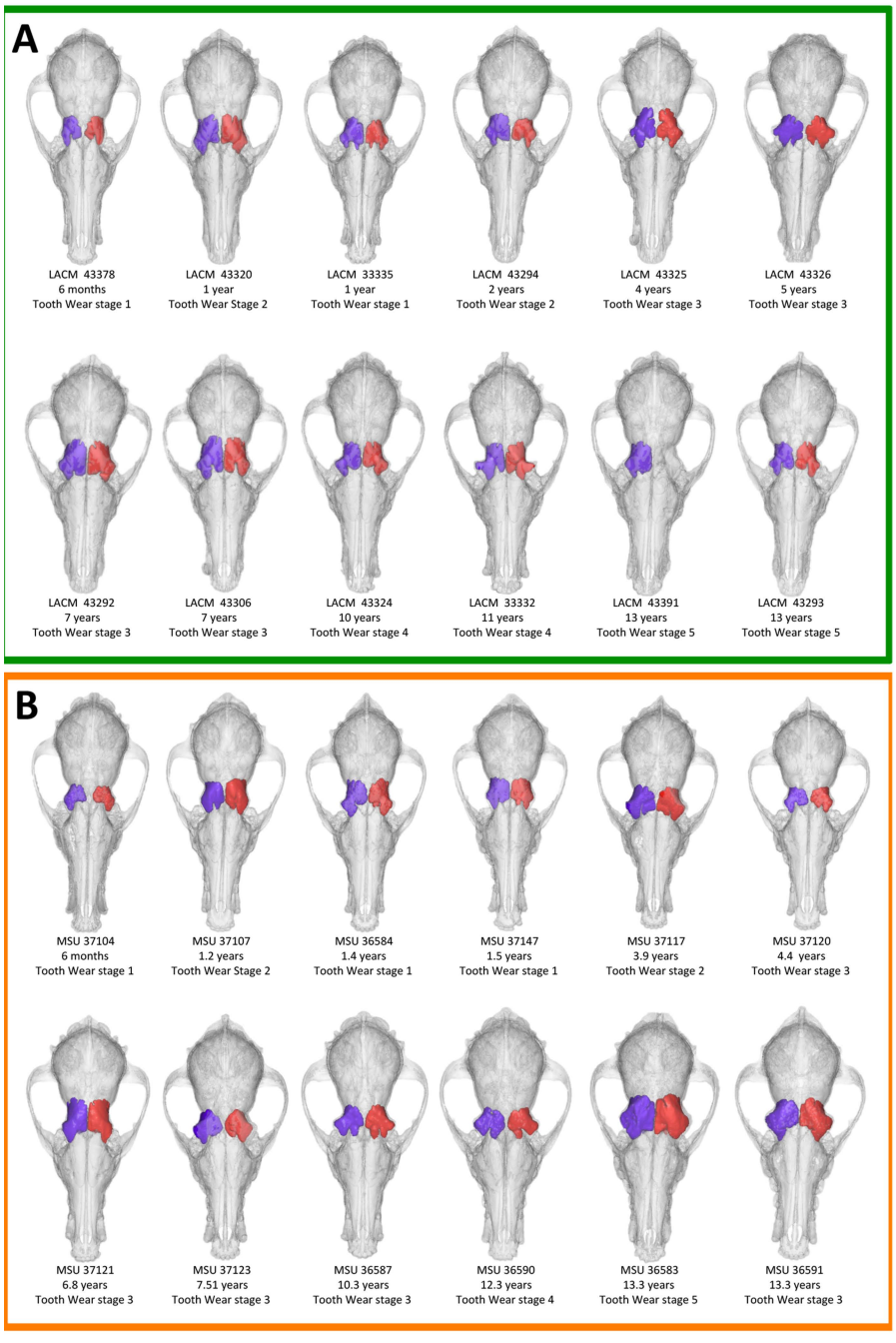
A
LACM 43378
6 months
Tooth Wear stage 1
LACM 43320
1 year
Tooth Wear Stage 2
LACM 33335
1 year
Tooth Wear stage 1
LACM 43294
2 years
Tooth Wear stage 2
LACM 43325
4 years
Tooth Wear stage 3
LACM 43326
5 years
Tooth Wear stage 3
LACM 43292
7 years
Tooth Wear stage 3
LACM 43306
7 years
Tooth Wear stage 3
LACM 43324
10 years
Tooth Wear stage 4
LACM 33332
11 years
Tooth Wear stage 4
LACM 43391
13 years
Tooth Wear stage 5
LACM 43293
13 years
Tooth Wear stage 5
B
MSU 37104
6 months
Tooth Wear stage 1
MSU 37107
1.2 years
Tooth Wear Stage 2
MSU 36584
1.4 years
Tooth Wear stage 1
MSU 37147
1.5 years
Tooth Wear stage 1
MSU 37117
3.9 years
Tooth Wear stage 2
MSU 37120
4.4 years
Tooth Wear stage 3
MSU 37121
6.8 years
Tooth Wear stage 3
MSU 37123
7.51 years
Tooth Wear stage 3
MSU 36587
10.3 years
Tooth Wear stage 3
MSU 36590
12.3 years
Tooth Wear stage 4
MSU 36583
13.3 years
Tooth Wear stage 5
MSU 36591
13.3 years
Tooth Wear stage 3

FIGURE 3-5

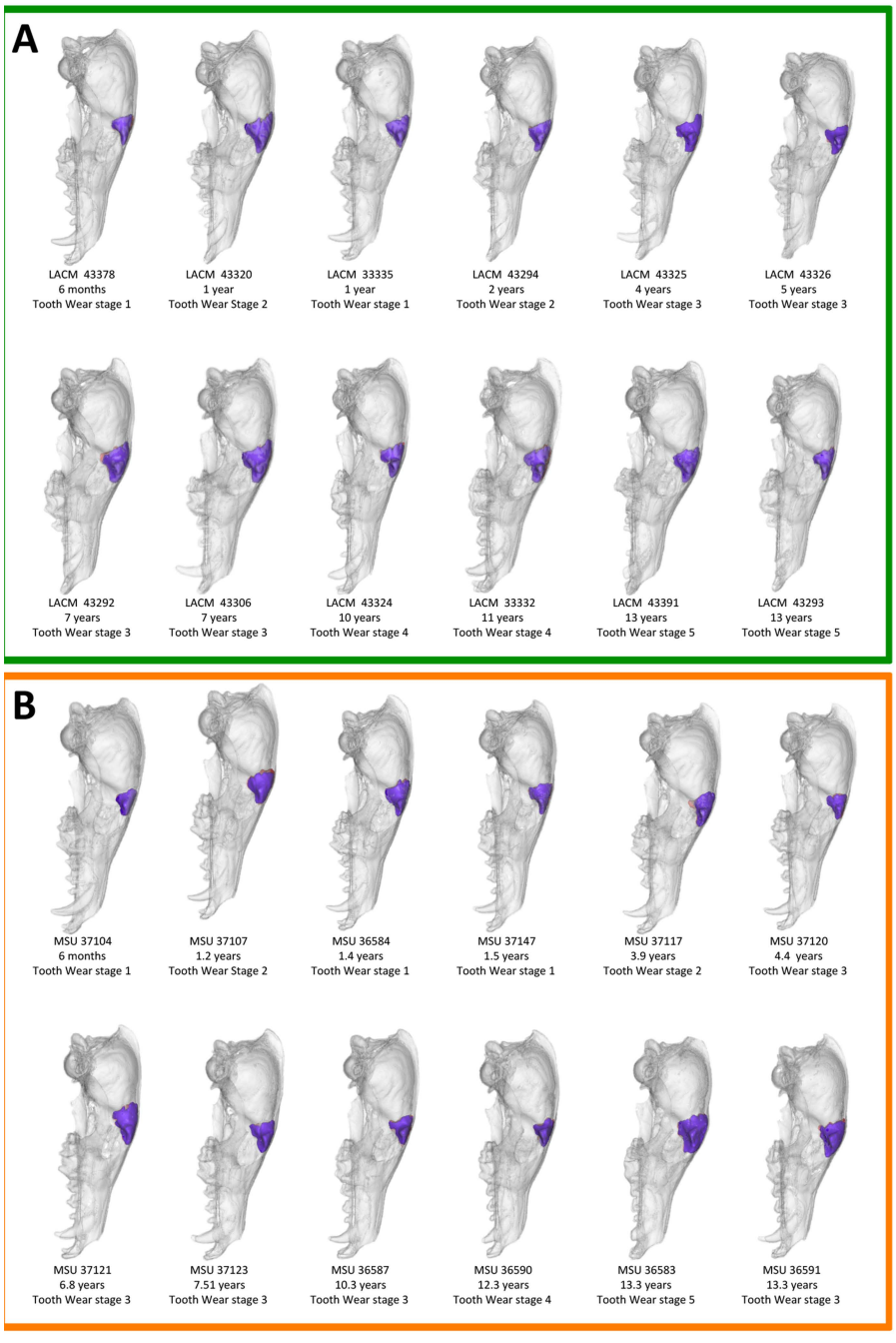
A
LACM 43378
6 months
Tooth Wear stage 1
LACM 43320
1 year
Tooth Wear Stage 2
LACM 33335
1 year
Tooth Wear stage 1
LACM 43294
2 years
Tooth Wear stage 2
LACM 43325
4 years
Tooth Wear stage 3
LACM 43326
5 years
Tooth Wear stage 3
LACM 43292
7 years
Tooth Wear stage 3
LACM 43306
7 years
Tooth Wear stage 3
LACM 43324
10 years
Tooth Wear stage 4
LACM 33332
11 years
Tooth Wear stage 4
LACM 43391
13 years
Tooth Wear stage 5
LACM 43293
13 years
Tooth Wear stage 5
B
MSU 37104
6 months
Tooth Wear stage 1
MSU 37107
1.2 years
Tooth Wear Stage 2
MSU 36584
1.4 years
Tooth Wear stage 1
MSU 37147
1.5 years
Tooth Wear stage 1
MSU 37117
3.9 years
Tooth Wear stage 2
MSU 37120
4.4 years
Tooth Wear stage 3
MSU 37121
6.8 years
Tooth Wear stage 3
MSU 37123
7.51 years
Tooth Wear stage 3
MSU 36587
10.3 years
Tooth Wear stage 3
MSU 36590
12.3 years
Tooth Wear stage 4
MSU 36583
13.3 years
Tooth Wear stage 5
MSU 36591
13.3 years
Tooth Wear stage 3

FIGURE 3-6

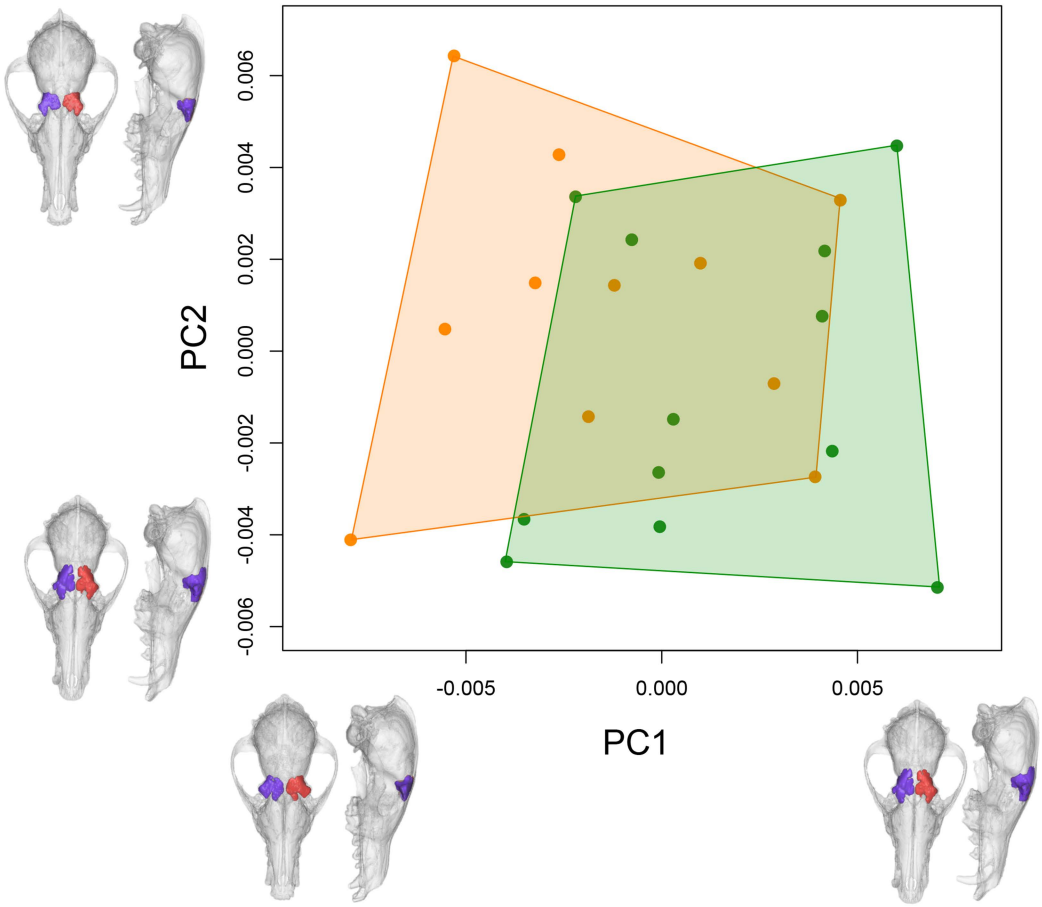

FIGURE 3-7

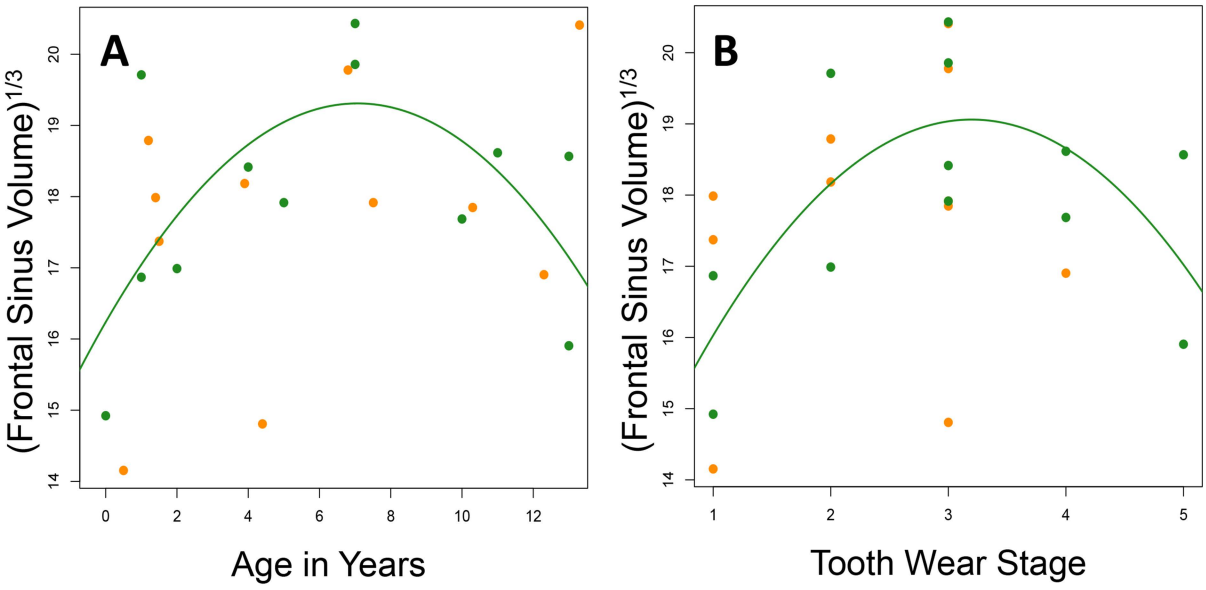
A
B
(Frontal Sinus Volume)^1/3
Age in Years
Tooth Wear Stage
14
15
16
17
18
19
20
0
2
4
6
8
10
12
1
2
3
4
5

FIGURE 3-8

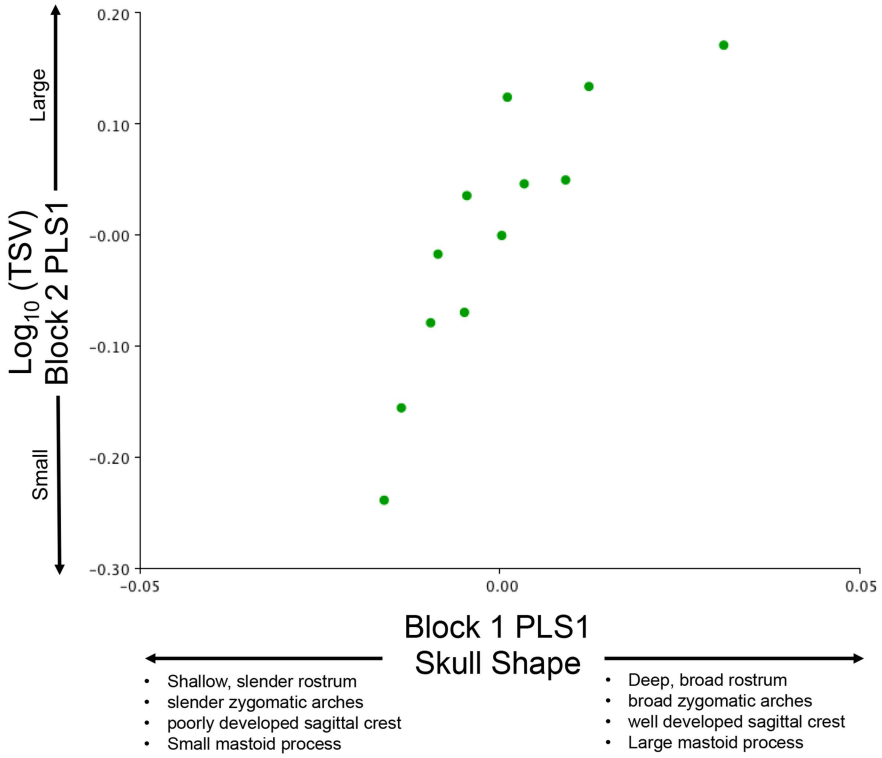
Large
Small
Log10 (TSV)
Block 2 PLS1
0.20
0.10
-0.00
-0.10
-0.20
-0.30
-0.05
0.00
0.05
Block 1 PLS1
Skull Shape
• Shallow, slender rostrum
• slender zygomatic arches
• poorly developed sagittal crest
• Small mastoid process
• Deep, broad rostrum
• broad zygomatic arches
• well developed sagittal crest
• Large mastoid process

FIGURE 3-9

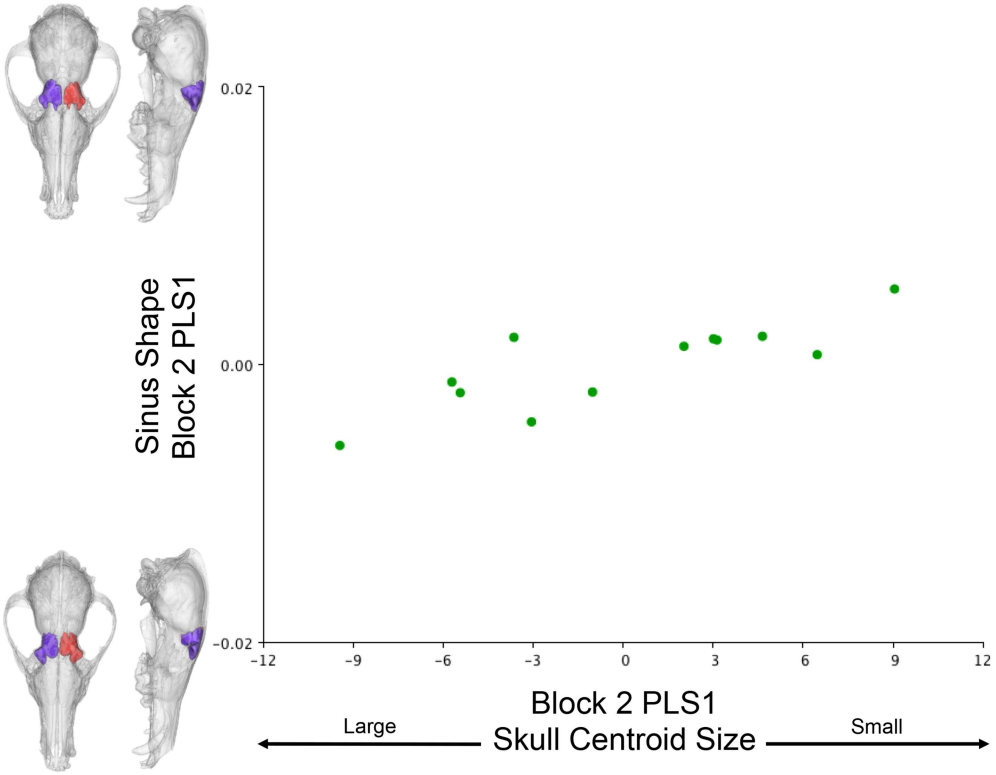
0.02
0.00
-0.02
Sinus Shape
Block 2 PLS1
-12
-9
-6
-3
0
3
6
9
12
Block 2 PLS1
Skull Centroid Size
Large
Small

FIGURE 3-10

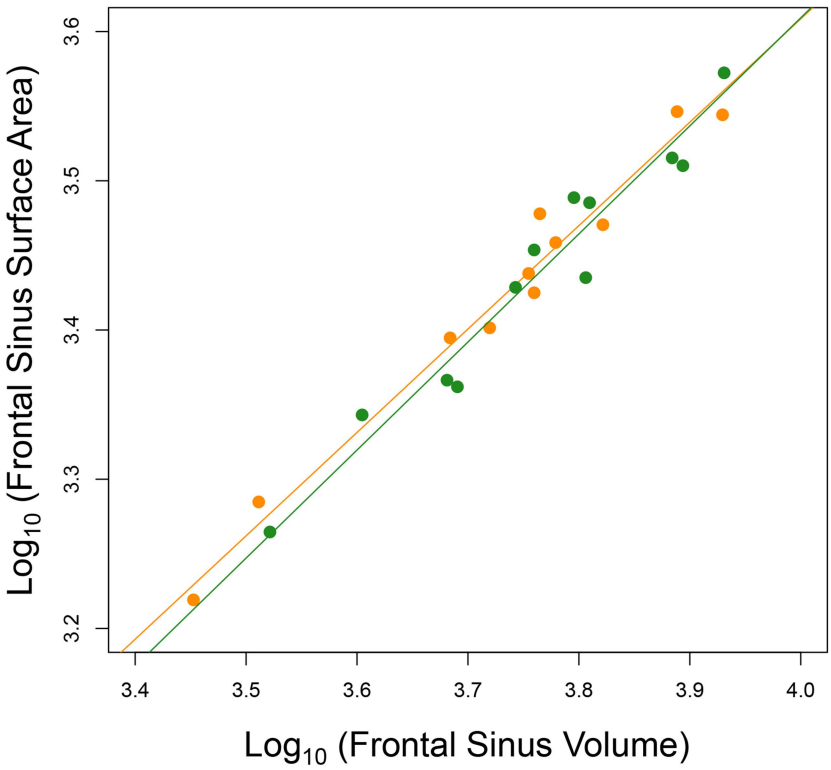
Log10 (Frontal Sinus Surface Area)
3.2
3.3
3.4
3.5
3.6
3.4
3.5
3.6
3.7
3.8
3.9
4.0
Log10 (Frontal Sinus Volume)

FIGURE 3-11

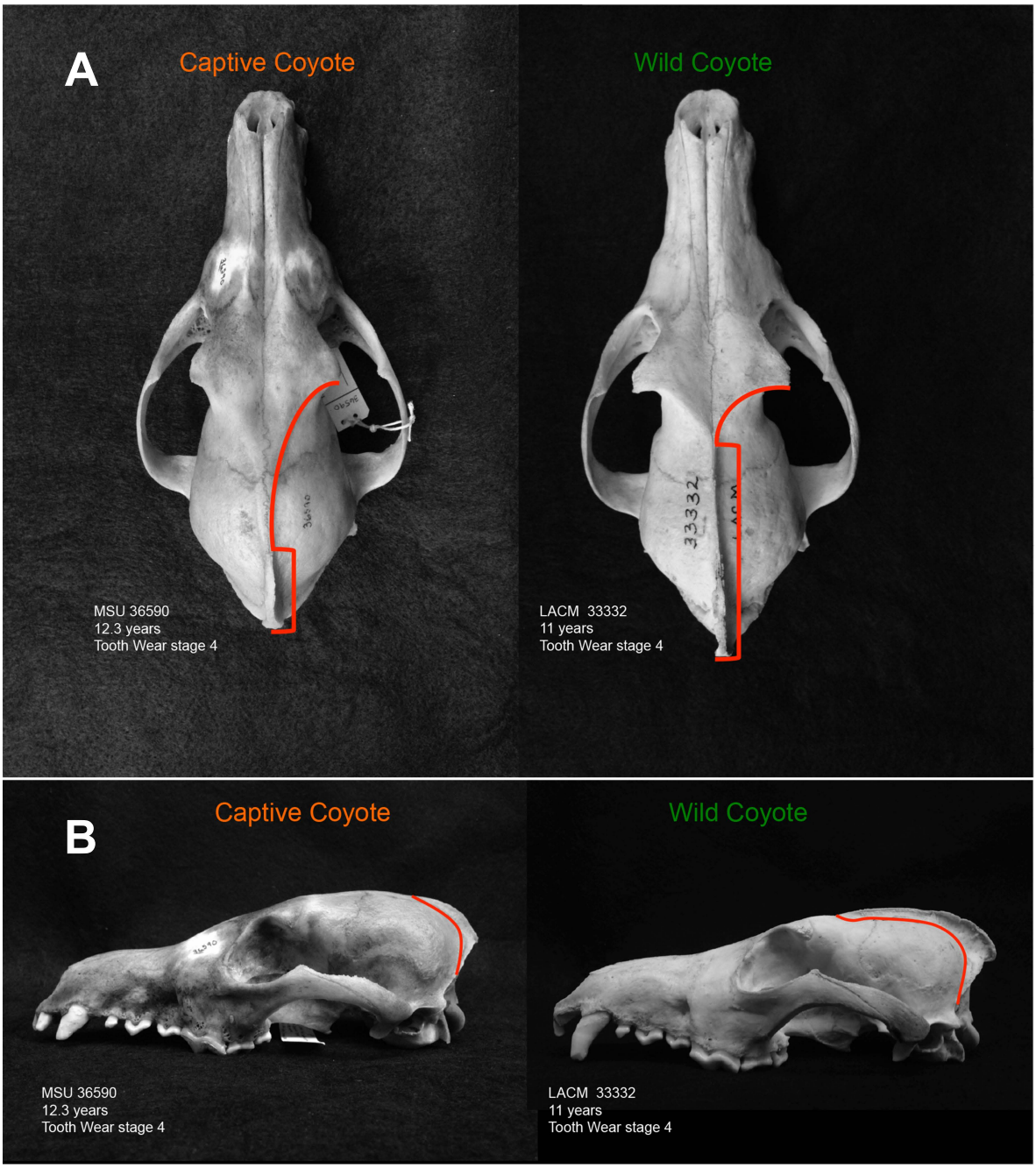
A
Captive Coyote
Wild Coyote
MSU 36590
12.3 years
Tooth Wear stage 4
LACM 33332
11 years
Tooth Wear stage 4
B
Captive Coyote
Wild Coyote
MSU 36590
12.3 years
Tooth Wear stage 4
LACM 33332
11 years
Tooth Wear stage 4

LITERATURE CITED

Bartel RA, Knowlton FF. 2005. Functional feeding responses of coyotes, *Canis latrans*, to fluctuating prey abundance in the Curlew Valley, Utah, 1977-1993. Can J Zool 83:569-578.

Blood BR, Matson JO, Patten DR. 1985. Multivariate analysis of allometry in a single population of coyotes (Canidae: *Canis latrans* Say). Aust Mammal 8:221-231.

Christensen AM. 2005. Assessing the variation in individual frontal sinus outlines. Am J Phys Anthropol 127:291-295.

Curtis AA, Lai G, Wei F, Van Valkenburgh B. 2014. Repeated loss of frontal sinuses in arctoid carnivorans. J Morphol DOI: 10.1002/jmor.20313

Curtis AA, Van Valkenburgh B. 2014. Beyond the sniffer: frontal sinuses in Carnivora. Anat Rec.

Cypher BL, Spencer KA, Scrivner JH. 1994. Food-item use by coyotes at the Naval Petroleum Reserves in California. Southwest Nat 39:91-95.

Farke AA. 2007. Morphology, constraints, and scaling of frontal sinuses in the hartebeest, *Alcelaphus buselaphus* (Mammalia: Artiodactyla, Bovidae). J Morphol 268:243-253.

Farke AA. 2008. Frontal sinuses and head-butting in goats: a finite element analysis. J Exp Biol 211:3085-3094.

Farke AA. 2010. Evolution and functional morphology of the frontal sinuses in Bovidae (Mammalia: Artiodactyla), and implications for the evolution of cranial pneumaticity. Zool J Linnean Soc 159:988-1014.

Fatu C, Puisoru M, Rotaru M, Truta AM. 2006. Morphometric evaluation of the frontal sinus in relation to age. Ann Anat 188:275-280.

Fitch HM, Fagan DA. 1982. Focal palatine erosion associated with dental malocclusion in captive cheetahs. Zoo Biol. 1:295-310.

Hollister N. 1917. Some effects of environment and habit on captive lions. Proc U S Nat Mus 53:177-193.

Johnson MK. 1978. Food habits of coyotes in south central Idaho. (Doctoral dissertation, Colorado State University).

Klugh DO. 2010. Principles of Equine Dentistry. Manson Publishing, London, UK.

La Croix S, Holekamp KE, Shivik JA, Lundrigan BL, Zelditch ML. 2011a. Ontogenetic

relationships between cranium and mandible in coyotes and hyenas. J Morphol 272:662-674.

La Croix S, Zelditch ML, Shivik JA, Lundrigan BL, Holekamp KE. 2011b. Ontogeny of feeding performance and biomechanics in coyotes. J Zool 285:301-315.

Lingle S. 2002. Coyote predation and habitat segregation of white-tailed deer and mule deer. Ecology 87:2037-2048.

Martin LB, Olejniczak AJ, Maas MC. 2003. Enamel thickness and microstructure in pitheciin primates, with comments on dietary adaptations of the middle Miocene hominoid *Kenyapithecus*. J Hum Evol 45:351-367.

Natsis K, Karabatakis V, Tsikaras P, Chazibalis T, Stangos N. 2004. Frontal sinus anatomical variations with potential consequences for the orbit. Study on cadavers. Morphologie 88:35-38.

Nishimura TD, Takai M, Tsubamoto T, Egi N, Shigehara N. 2005. Variation in maxillary sinus anatomy among platyrrine monkeys. J Hum Evol 49:370-389.

O'Regan HJ. 2001. Morphological effects of captivity in big cat skulls. In: Wehnelt S, Hudson C, editors. Proceedings of the 3rd Zoo Research Symposium. Chester Zoo, Chester. p. 18–22.

O'Regan HJ, Kitchener AC. 2005. The effects of captivity on the morphology of captive, domesticated and feral mammals. Mammal Rev 35:215-230.

O'Regan HJ, Turner A. 2004. The interface between conservation biology, palaeontology and archaeozoology: morphometrics and population viability analysis. In: Lauwerier RCGM, Plug I, editors. The Future from the Past: Archaeozoology in Wildlife Conservation and Heritage Management. Oxford: Oxbow Books. p 90–96.

Paulli S. 1900. Über die pneumaticität bei den säugerthieren. Ein morphologische studie. III. Über die Morphologie des siebbens und die der pneumaticität bie den insectivoren, hyracoidean, chiropteran, carnivoren, pinnipedien, edentaten, rodentiern, prosimiern und primate. Gegenbaurs Morphol Jahrb 28:483-564.

R Core Team. 2012. R: A language and environment for statistical computing. R Foundation for Statistical Computing, Vienna, Austria.

Rae TC, Koppe T. 2008. Independence of biomechanical forces and craniofacial pneumatization in *Cebus*. Anat Rec 291:1414-1419.

Rossie JB. 2006. Ontogeny and homology of the paranasal sinuses in Platyrrhini (Mammalia: Primates). J Morphol 267:1-40.

Shen L, Farid H, McPeek MA. 2009. Modeling three-dimensional morphological structures

using spherical harmonics. Evolution 63:1003-1016.

Shen L, Makedon F. 2006. Spherical mapping for processing of 3D closed surfaces. Image Vision Comput 24:743-761.

Tseng ZJ, Wang X. 2010. Cranial functional morphology of fossil dogs and adaptations for durophagy in *Borophagus* and *Epicyon* (Carnivora, Mammalia). J Morphol 271:1386-1398.

Tseng ZJ, Wang X. 2011. Do convergent ecomorphs evolve through convergent morphological pathways? Cranial shape evolution in fossil hyaenids and borophagine canids (Carnivora, Mammalia). Paleobiology 37:470-489.

Van Valkenburgh B. 1988. Incidence of tooth breakage among large, predatory mammals. The Am Nat 131:291-302.

Van Valkenburgh B. 1996. Feeding behavior in free-ranging, large African carnivores. J Mammal 77:240-254.

Van Valkenburgh B. 2009. Costs of carnivory: tooth fracture in Pleistocene and Recent carnivores. Biol J Linnean Soc 96:68-81.

Van Valkenburgh B, Koepfli K-P. 1993. Cranial and dental adaptations to predation in canids. Symp Zool Soc London 65:15-37.

West-Eberhard MJ. 2003. Developmental plasticity and evolution. Oxford University Press, New York.

Witmer LM. 1997. The evolution of the antorbital cavity of archosaurs: A study in soft tissue reconstruction in the fossil record with an analysis of the function of pneumaticity. J Vertebr Paleontol 17:1-77.

Witmer LM. 1999. The phylogenetic history of paranasal air sinuses. In: Koppe R, Nagai H, Alt KW, editors. The paranasal sinuses of higher primates: development, function, and evolution. Chicago: Quintesence. p 21-34.

Wolff JD. 1892. Das gesetz der transformation der knochen. Berlin, A. Hirschwald.

Zollikofer CPE, Weissmann JD. 2008. A morphogenetic model of cranial pneumatization based on the invasive tissue hypothesis. Anat Rec 291:1446-1454.